



universität
wien

DISSERTATION

Titel der Dissertation

Functionalized Liposomes as a Model to Reveal
Cell-Surface Associated Events
of the Human Rhinovirus Infection-Pathway

angestrebter akademischer Grad

Doktor der Naturwissenschaften (Dr. rer.nat.)

Verfasser:	Mag. Gerhard Bilek
Matrikel-Nummer:	a0003655
Dissertationsgebiet (lt. Studienblatt):	Genetik - Mikrobiologie
Betreuer:	Univ.-Prof. Mag. rer. nat. Dr. Ernst Kenndler Univ.-Prof. Dipl.-Ing. Dr. Dieter Blaas

Wien, im August 2009

Table of Contents

1	Abstract	3
2	Abbreviations	5
3	Introduction.....	6
3.1	Virology of Rhinoviruses.....	6
3.2	Biological Membranes	13
3.3	Model System: Lipofectosome	20
3.4	Liposomes in Capillary Electrophoresis	23
4	Materials and Methods	24
4.1	Liposome Preparation	24
4.2	Liposome Purification.....	25
4.3	Liposome Characterization.....	27
4.4	Genome Transfer / Monitoring of Pore Formation.....	28
5	Results and Discussion	33
5.1	Liposome Characterization.....	33
5.1.1	Determination of Lipid Concentration via Total Phosphorus Content.....	33
5.1.2	Determination of Liposome Size via Dynamic Light Scattering.....	34
5.2	Formation of Lipofectosomes	36
5.2.1	CE: Protein/Receptor-Decoration of the Liposomal Surface.....	36
5.2.2	CE / Chip: Specific Binding of Virus to Receptor-Decorated Liposomes	37
5.2.3	TEM: Visualization of Lipofectosomes.....	40
5.3	Genome Transfer.....	47
5.3.1	RT – Lipofectosomes: in-vitro detection of RNA transfer	47
5.3.2	HeLa system: Confirmation of RNase A dependent reduction of HRV2 infection.	56
6	Summary.....	59
7	References.....	61
8	Acknowledgements	65
9	Appendix.....	66
9.1	Publications	
9.2	Zusammenfassung der Dissertation (deutsch / englisch)	
9.3	Curriculum Vitae	

1 Abstract

The viral genome transfer through cellular membranes is a crucial process in the course of the early infection events of non-enveloped viruses; however, it is still poorly understood. To elucidate this mechanism, human Rhinoviruses are a valuable system. They contain an RNA genome of about 7kb in an icosahedral protein capsid, which needs to be transferred through the endosomal membrane to infect the host cell.

This work aimed at detecting *in-vitro* the minimal requirements necessary for proper genome transfer. The main criteria for the establishment of this model system were the membrane lipids, the receptors for virus binding and the triggers for viral conversion. Liposomes were prepared to mimic the cell surface. The suitability of this model was confirmed by capillary electrophoresis (CE) and transmission electron microscopy (TEM). The actual genome transfer however was demonstrated by a reverse transcription (RT) PCR assay.

The liposome-based model used a nickel chelating lipid implanted in the bilayer of the vesicle. Receptor constructs, derived from the very low-density lipoprotein-receptor (VLDLR), were attached onto the outer liposomal leaflet by a complex bond between its His6-tag and the nickel ions of the membrane. Human Rhinovirus serotype 2 (HRV2) was specifically bound to these receptor-decorated vesicles. Upon virus binding to the liposome, the assembly was primed for infection and thus called “lipofectosome”.

The stepwise assembly of this adduct was assessed by CE with laser-induced fluorescence (LIF) detection via tracing of fluorescence labeled liposomes. In addition, TEM imaging was applied to confirm the proper formation of the lipofectosome, and to identify the best proportion of its components and environmental conditions for its assembly. Subsequently, the trigger and the capacity of infection within this model system were examined by detecting different stages of virus conversion upon pH lowering and heating. Conditions for entire RNA release from the capsid were identified via screening of time series.

To confirm the ingress of the released RNA into the liposomal compartment, a RT protocol was adapted to allow for its application within the lipofectosomes. Technically, an entire RT kit was encapsulated in the liposomes prior to their assembly. Upon triggering the infection by either heating or acidification, lipofectosomes transferred the RNA genome from the virion into the interior of the vesicles. A specific cDNA template was produced by the encapsulated RT kit, and could be detected after amplification by PCR. Since these vesicles served as leak-tight compartment, to carry out reverse transcription, they can be considered a nano-reaction container.

Using RT-lipofectosomes, a system to monitor RNA transfer of non-enveloped viruses was invented. The minimal requirements for the genome transfer of HRV2 were identified by an *in-vitro* reconstitution of its putative key components. This work shows that even complex infection pathways can be resolved to discrete processes, such as the genome transfer, and can be described by defined technical terms.

2 Abbreviations

Abbrev.	Meaning
BGE	background electrolyte
CE	capillary electrophoresis
CE-LIF	CE equipped with laser induced fluorescence detector
Ch	cholesterol
cTEM / cryoTEM	cryo transmission electron microscopy
DLS	dynamic light scattering
dNTP	deoxyribonucleotide triphosphate
DOGS-NTA	1,2-dioleoyl-sn-glycero-3-{{N(5-amino-1-carboxypentyl)iminodiacetic acid}succinyl} (nickel salt)
DSPC	1,2-distearoyl-sn-glycero-3-phosphocholine
DTT	dithiothreitol
eIF4G1	eukaryotic translation initiation factor 4 G1
FITC	fluorescein isothiocyanate
FL	fluorescence
GPI	glycosyl-phosphatidylinositol
GUV	giant unilamellar vesicle
His6-tag	hexa histidine tag
HRV	human Rhinovirus
ICAM-1	inter-cellular adhesion molecule 1
inf MEM	infection medium
LDLR	low-density lipoprotein receptor
LIF	laser induced fluorescence
LRP	LDLR related protein
LUV	large unilamellar vesicle
MBP	maltose binding protein
MLV	multi-lamellar vesicle
mSEC	mini SEC
NBD-PC	1-oleoyl-2-[12-[(7-nitro-2-1,3-benzoxadiazol-4-yl)amino]dodecanoyl]-sn-glycero-3-phosphocholine
NTA	nitrilo-triacetate
PBS	phosphate buffered saline
PC	polycarbonate
PCR	polymerase chain reaction
PDI	polydiversity index
PE	phosphatidylethanolamine
PEG	polyethyleneglycol
PEG750PE	1,2-distearoyl-sn-glycero-3-phosphoethanolamine-N-[methoxy (polyethyleneglycol)-750] (ammonium salt)
POPC	1-palmitoyl-2-oleoyl-sn-glycero-3-phosphocholine
RT	reverse transcription
SDS	sodium dodecylsulphate
SEC	size exclusion chromatography
SF inf MEM	serum free infection medium
SM	sphingomyelin
SUV	small unilamellar vesicle
TEM	transmission electron microcopy
T _m	phase transition temperature (of lipid aggregates)
TX	Triton X100
VLDLR	very low-density lipoprotein receptor

3 Introduction

3.1 Virology of Rhinoviruses

Virus: human Rhinovirus serotype 2 (HRV2); Rhinoviruses are a valuable representative of the Picornavirus family. Besides Rhinoviruses, this family contains virus genera such as Enterovirus, Cardiovirus, Aphthovirus, Hepatovirus, Parechovirus, Erbovirus, Kobuvirus and Teschovirus. Common characteristics are their small size, a non-enveloped icosahedral capsid and their positive sensed RNA genome; therefore “pico-RNA virus”. Moreover, their capsid is basically built of four proteins, namely VP1 – VP4, which form protomers. A precursor, VP0, has to be cleaved to produce VP2 and VP4. The protomer, in turn, is the actual building block of the capsid. By self-assembly, 60 copies of this create an icosahedral shell, having a T=1, pseudo T=3 symmetry, as shown in Figure 1 and Figure 2 (Rossmann *et al.*, 1985).

Rhinoviruses are the major causative agent of the common cold. Based on the phylogenetic relationship of their >100 serotypes, they can be classified in the species HRV-A and HRV-B. A second classification focuses on the affinity of the respective serotype to specific receptors of the host cell. By this criterion, a major and a minor group can be differentiated. The major group uses a member of the immunoglobulin super-family as receptor, inter-cellular adhesion molecule 1 (ICAM-1) but also for some serotypes heparan sulfate. For most viruses of this group, ICAM-1 serves not only for binding but also catalyses uncoating upon internalization. The smaller, and thus called minor group, utilizes members of the LDLR family to bind their host cells. Here, the receptors mediate virus internalization; however they do not catalyze their uncoating. In contrast to major group viruses, viral uncoating and RNA release of minor group viruses are strictly dependent on pH lowering.

Both groups enter the host via endocytosis and accumulate in intracellular compartments - the endosomes – where they face pH lowering. To deliver their RNA genome from the endosome into the cytosol, it is believed that the major group disrupts these compartments, whereas the minor group forms a distinct pore through the membrane, which convoys the genome. It is not clear yet whether these two strategies are indeed due to different conversion mechanisms of the virion or only a matter of virus concentration at the endosomal membrane. Unpublished data suggest disintegration of vesicles also for minor group viruses, if applied in high concentration. This work aimed at elucidating the genome transfer via pore formation, thus human Rhinovirus serotype 2 (HRV2) was employed for the experimental setup. It is the best characterized member of the minor group (Brabec *et al.*, 2005; Prchla *et al.*, 1995; Semler & Wimmer, 2002; Vlasak *et al.*, 2003).

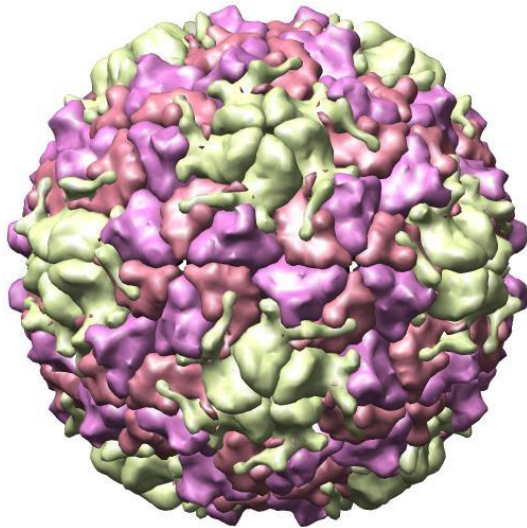


Figure 1: Structural reconstruction of an HRV2 virion via X-Ray crystallography (Verdaguer *et al.*, 2000). Yellowish vertex corresponds to 5-fold axis, built up by VP1; compare also with illustration in Figure 2.

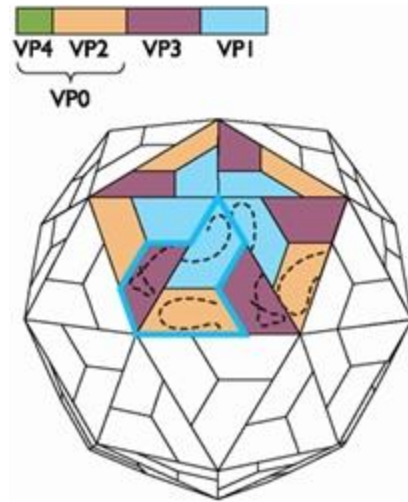


Figure 2: Illustration of arrangement of the viral proteins at the 5-fold axis of an icosahedral virus capsid (Flint *et al.*, 2004). VP4 is located inside the capsid and thus cannot be seen from top-view.

Receptors: from natural VLDLR to a recombinant receptor construct; VLDLR is part of the LDLR superfamily. Further prominent members of this family are the low-density lipoprotein receptor (LDLR) and the LDLR related protein (LRP). A common feature of these proteins is the various numbers of binding domains located at the N-terminus. Their primary sequence of 40 amino acids contains 6 cysteines each; all form disulfide bridges. LDLR possesses 7 (Yamamoto *et al.*, 1984), VLDLR 8 (Takahashi *et al.*, 1992) and LRP 2+8+18+11 of these repeats (Herz *et al.*, 1988), which enables for binding of multiple ligands. The structural integrity of the receptors is highly dependent on the calcium concentration. After those binding-repeats, a domain similar to the epidermal growth factor precursor and a heavily O-glycosylated domain follow. All receptors contain a transmembrane and a short C-terminal cytoplasmatic region. This C-terminus possesses an internalization signal, for receptor clustering and formation of coated pits, respectively (Semler & Wimmer, 2002). Each binding module binds with its inherent binding capacity to the star shaped dome of the virion. The dome is generated by VP1 at the 5-fold axis (see Figure 1). Three loop regions of VP1, namely the BC-, DE- and HI-loop are interacting with the receptor binding modules. Detailed information on amino acids involved in binding between VP1 loops of HRV2 and the binding module V3 of VLDLR are given in the article by Verdaguer published in 2004 (Hewat *et al.*, 2000; Verdaguer *et al.*, 2004). The receptor molecule folds around the fivefold vertex and attaches to virus with high avidity; Figure 3 shows binding of receptor fragments to a viral pentamer (Verdaguer *et al.*, 2004).

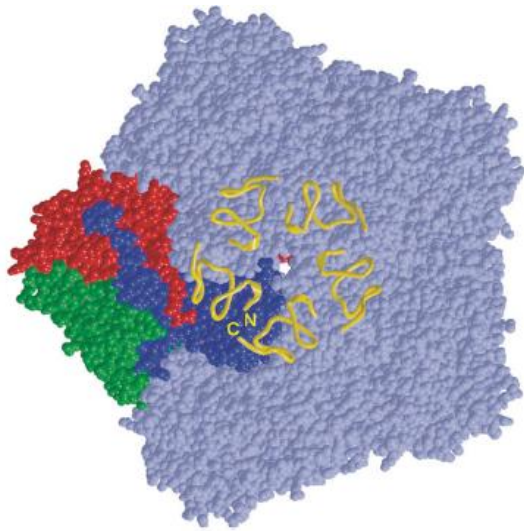


Figure 3: Electron density blot of a five-fold axis of HRV2 with bound receptor fragments (Verdaguer *et al.*, 2004). Color code of the reference protomer: VP1 (blue), VP2 (green), VP3 (red); Receptor constructs are shown as yellow stripes.

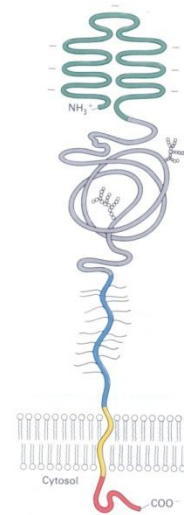


Figure 4: Illustration of a native very low-density lipoprotein receptor (Stryer, 1999). Domains from N- to C-terminus: ligand binding repeats (green), EGF precursor homology (gray), O-linked sugar domain (blue), transmembrane region (yellow) and short C-terminal cytoplasmatic region (red).

Recombinant receptor constructs are a valuable and versatile tool to study virus-receptor interactions. Due to their high solubility, they are expressed in high concentrations in *E. coli*. In this study, receptor molecules derived from the VLDLR were used. They can be designed in an adaptable way, concerning their number and composition of binding modules. Since module V3 possesses the highest binding affinity to virions, previous work intended to produce and study constructs with different numbers of this repeat. In the course of their expression and purification, a maltose-binding protein (MBP) and a His6-tag were needed and had thus been conjugated at each constructs N- and C-terminus, respectively. However, these constructs lack further domains, as mentioned for their natural counterpart; also the transmembrane domain has been left out (Marlovits *et al.*, 1998; Moser *et al.*, 2005; Neumann *et al.*, 2003; Ronacher *et al.*, 2000). Stoichiometric data for a receptor fragment, consisting of five times module V3 (His6-V33333-MBP, or short V33333) attaching HRV2 were derived by CE. The binding stoichiometry proposed the covering of the viral fivefold vertex by the receptor as a ring like structure (Konecni *et al.*, 2004). The receptor covering was proven by (Verdaguer *et al.*, 2004). Its good characterization and its high binding avidity to HRV2 was the crucial factor in the decision to use V33333 in this study.

Virus entry and genome transfer; In the course of the early steps in a viral infection pathway, viruses have to transport their genome into the host cell. Although this process is already well elucidated for enveloped viruses (Falanga *et al.*, 2009), for non-enveloped viruses the entire process is not yet clear in detail. An outline of the virus entry for minor group HRVs, is given in Figure 5. Briefly, the virion attaches the host cell via specific binding to receptors (Figure 5: 1-2). In the case of minor group viruses, this receptor belongs to the LDLR superfamily, which possesses clathrin-localization signals at their cytoplasmic region. This means that internalization happens via clathrin-coated pits (Figure 5: 3). Eventually, Rhinoviruses are transported to endosomes. The pH changes in early endosomes and the resulting mildly acidic pH (pH about 6.0) separates the virus from the receptor (Figure 5: 4-5). Subsequently, virus is transported to endosomal carrier vesicles and late endosomes, where further acidification of the compartments leads to a $\text{pH} \leq 5.6$ (Neubauer *et al.*, 1987). As a result of the acidic milieu, viral conversion is triggered and induces uncoating (Figure 5: 5) (Prchla *et al.*, 1994). In turn, these conformational changes are supposed to open a transport route for the RNA genome, in order to bridge the endosomal membrane and to reach the cytosol. (Fuchs & Blaas, 2008)

In the course of uncoating subviral particles are generated. They can be classified by their sedimentation behavior in a sucrose density gradient. Native virus particles sediment with 150 S (Swedberg) and are thus denoted 150S particles. First, they convert to intermediate hydrophobic particles, sedimenting at 135S. One can distinguish them from native virus by expelled VP4 (the inner-most viral protein) and externalized VP1 N-termini, but the capsid contains still its genome. The hydrophobic VP1 N-terminus and also VP4 are believed to insert into the endosomal membrane in order to generate a pore-like structure for genome transfer. VP4 contains a myristic acid as additional hydrophobic moiety. An illustration for this hypothesis is given in Figure 6. Such a pore could be a suitable gate for the hydrophilic RNA genome on its way through the lipid bilayer. Indications for an impact on the membrane integrity via the N-terminus of VP1, were shown by (Zauner *et al.*, 1995). For that work, leakage of a FL-dye from liposomes and erythrocytes was detected, depending on VP1-N concentration.

The second and final subviral particle is called 80S, according again to its behavior in sedimentation. In contrast to the 135S particle, it lacks the RNA genome and VP1-N-termini are retracted, hence it regained hydrophilic properties. Cryo TEM data showed an expansion of this particle in size by 4 % due to a relative movement of the viral proteins. A density corresponding to the N-terminus of VP1 was detected below the pseudo threefold axis. At the fivefold axis an iris-like movement opened a channel in the capsid with 10 Å in diameter. This channel was wide enough to allow the release the RNA genome (Hewat & Blaas, 2006). In conclusion, the hydrophilic virus (150S) passes during viral conversion through a hydrophobic stage (135S) and finishes up in a non-infectious

and hydrophilic empty capsid (80S). (Korant *et al.*, 1972; Lonberg-Holm *et al.*, 1976; Noble & Lonberg-Holm, 1973)

It is widely believed that the intermediate particle is involved in a pore-forming process at the endosomal membrane. Therefore, virologists suppose a contribution of the VP1 N-terminus and entire VP4 to either partly destabilize the membrane or to form discrete pore-complexes. Work on polio and Rhinoviruses gave already several indications that VP4 is needed for proper genome transfer. Similar to the N-terminus of VP1, also VP4 induced leakage in liposome-based assays (Danthi *et al.*, 2003; Davis *et al.*, 2008). Moreover, the hydrophobic feature of this viral protein, the N-terminal linked myristic acid, was under particular focus. This acid could very much be involved either in virus assembly and / or in cell entry (Chow *et al.*, 1987; Martin-Belmonte *et al.*, 2000).

A proof of the viral induced emergence of size specific pores was described by (Brabec *et al.*, 2005; Prchla *et al.*, 1995) for endosomal compartments. A brief outline of the principle of these works is shown in Figure 6, as well. Basically, two dye molecules of different sizes, namely 10 kDa and 70 kDa FITC dextran, were enriched within endosomes by fluid-phase uptake. In article by Brabec *et al.* the number of labeled vesicles and their pH values were determined by single-organelle flow analysis. Upon co-internalization with either adenovirus or HRV2, different impacts on the endosomal compartment could be detected. First, the presence of adenovirus in these compartments resulted in endosomal rupture and thus size-independent release of dye molecules. In contrast, cointernalized HRV2 only allowed release of the 10 kDa FITC dextran marker, whereas the larger one remained in the vesicle. These findings support the formation of pore-like structures. This was further confirmed by infection inhibitors, such as bafilomycin. It is described for its inhibition of the vacuolar ATPase, which in turn is responsible for pH-lowering in endosomes. Upon treatment of the cells with this drug, HRV2-infected cells showed no dye release at all. Since adenovirus infection is not dependent on pH-lowering, dye release was still detectable despite using bafilomycin.

These results raise the question about the minimal requirements necessary for pore formation and for subsequent genome transfer, which is addressed in this work. However, it is difficult to migrate experimentally from a native point of view towards a minimal system by stepwise excluding system elements. Therefore, an in-vitro system was used and successively equipped with the components necessary to acquire comparable infection skills as the natural system. The consequence was a liposome based model system, which was developed in the present doctoral thesis and will be described in more detail in the following sections.

As mentioned above biological membranes are an efficient barrier for cellular parasites, such as viruses. Non-enveloped viruses had to have found strategies to transport their genomes across this obstacle. The next section explains the basic building blocks of membranes and their compositions. Further, it should give a brief insight on the parameters influencing their consistency.

This will give an idea about the techniques viruses had to develop in order to interfere properly with this lipid bilayer to utilize the host cell.

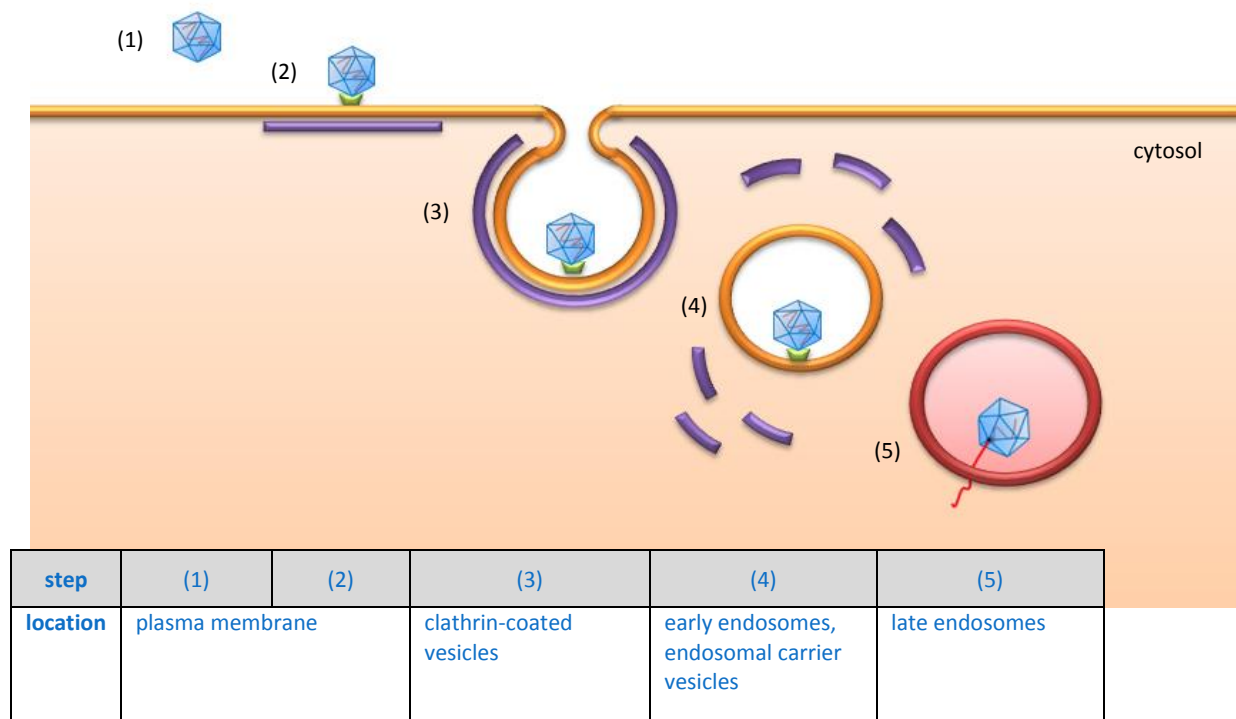


Figure 5: Viral entry of minor group HRVs via endocytosis in clathrin-coated vesicles. The following compartments / components are illustrated: plasma membrane (orange stripe), clathrin (purple stripes), receptor (green trapezoid), early endosome (orange circle), acidified late endosome (red circle), viral capsid (blue icosahedron) and viral RNA (red line). (Drawing by Gerhard Bilek)

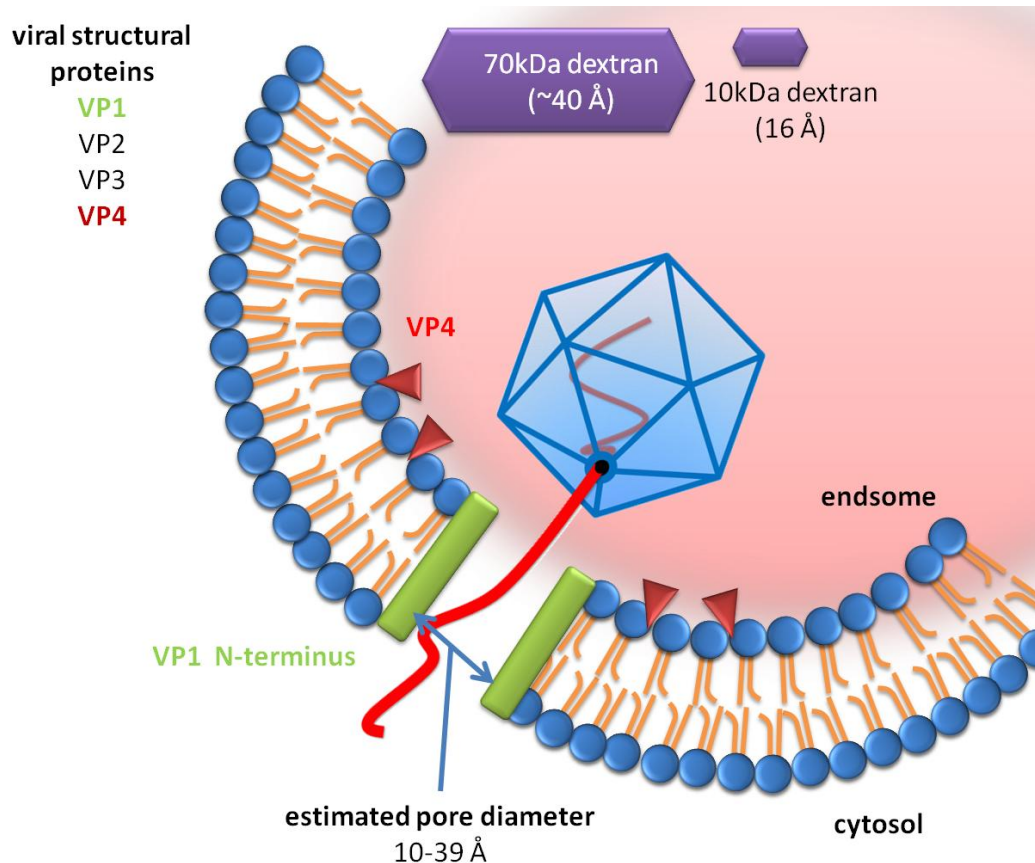


Figure 6: Model of virus induced pore formation in biological membranes and subsequent genome shuttling. The viral protein VP4 (red triangle) and the N-terminus of VP1 (green bars) are supposed to insert with their hydrophobic domains in the membrane of the respective cell compartment. Non-enveloped viruses could then transfer their genome through either an emerging pore or simple release it from a collapsing vesicle compartment. In any case, the genome must be transferred from the inner side of the compartment to the outer one, which in the case of picornaviruses would be the cytosol. (Drawing by Gerhard Bilek)

3.2 Biological Membranes

Lipids: central building block of membranes; Lipid molecules are amphipathic, which means that they possess a hydrophilic and a hydrophobic moiety within one molecule. The hydrophilic part is built by the so called polar head-group. Usually, a phosphoric acid or its derivatives form this end of lipids. In contrast, the hydrophobic unit consists of hydrocarbon chains, holding 14 to 24 carbon atoms. These chains are formed either from fatty acids esterified to glycerol or from sphingosine.

Figure 7 gives a scheme for the classification of membrane lipids, based on their structure. They are categorized in glycerophospholipids, sphingolipids and cholesterol. Moreover, this scheme points out a discrepancy concerning the former classification of phospholipids; they do not necessarily contain glycerol (branching in Figure 7). Anyway, glycerophospholipids (Figure 7a) do contain glycerol and build the main portion of membrane lipids. This group holds several members, which chiefly differ from each other by their head-groups. An ester bond links these alcohols, such as choline, ethanolamine, serine, glycerol and inositol, via a phosphate to the sn-3 carbon of glycerol. Position sn-1 and sn-2 links a saturated and an unsaturated fatty acid, respectively, to the glycerol. The saturated acid possesses 16 to 18 carbon atoms. Normally, the unsaturated one contains a longer chain with at least 18 carbons and one or more cis-double bonds. From a steric point of view, this attribute is of particular note, because it produces an obvious kink in the tail; this affects the membrane consistency. In fact, both, the length of the hydrocarbon chain as well as the cis-double bond are responsible for the packing capacity of the lipids and thus influence the membrane fluidity. Many membrane functions depend on a particular fluidity.

The next class contains the sphingolipids (Figure 7b). They are composed of a sphingosine, forming an amide linkage with a saturated fatty acid. The acylated sphingosine is also called a ceramide. Furthermore, a glycosphingolipid results from a β -glycosidic bond of a sugar or oligosaccharides to the 1-OH of the ceramide. The last class contains only cholesterol (Figure 7c). This lipid possesses an OH-molecule as polar head-group. Its hydrophobic moiety is composed of a sterane derivative, which holds an iso-octyl carbon chain. (Fantini *et al.*, 2002)

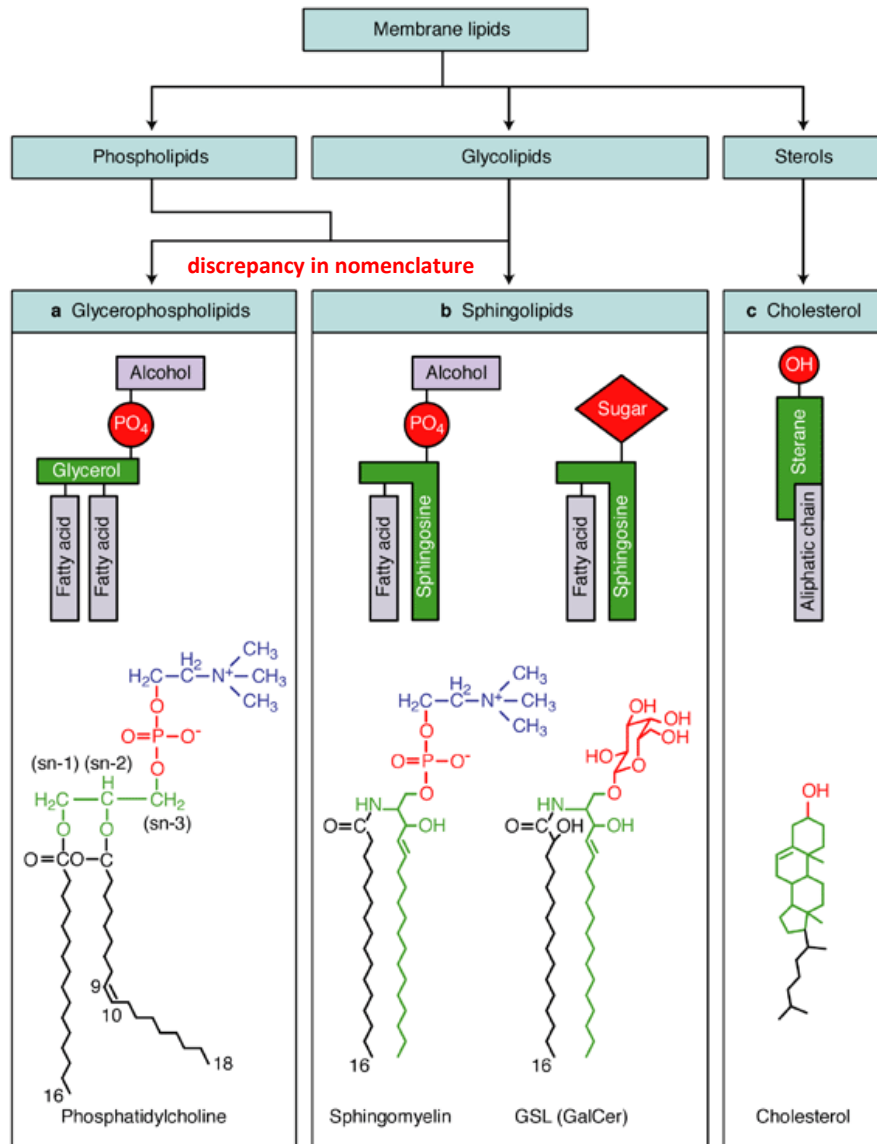
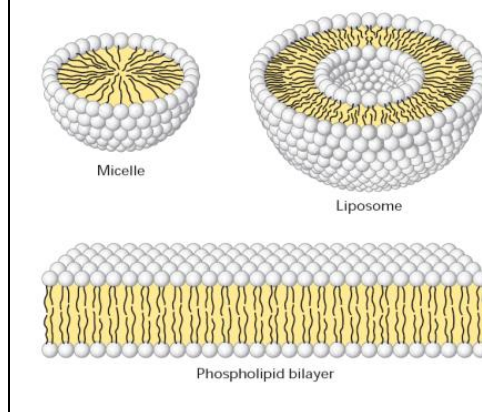


Figure 7: Classification of membrane lipids. (Fantini *et al.*, 2002)

Due to their amphipathic nature, lipids are able to form large assemblies in aqueous solutions only by self-aggregation. Depending on diverse lipid parameters, such as concentration, kind of head-group, length of fatty acids, etc., three major types of aggregates can be distinguished namely micelles, bilayers and liposomes; illustrated in Figure 8. All types have in common that the hydrophobic tails are turned towards the center of the aggregate or are sandwiched between bilayers. In any case, only the hydrophilic moieties face the aqueous solution. The cylindrical shape of phospholipids (Figure 10, a) favors formation of spherical aggregates. In this way, sealed compartments are produced (Alberts *et al.*, 2002).

Figure 8: Possible lipid aggregates in aqueous solutions. White spheres represent the polar head-group of lipids. (Lodish *et al.*, 2004)



Basal membrane model; The current theory on bio-membranes is mainly based on the work by Singer and Nicolson (Singer & Nicolson, 1972). They postulated in 1972 the “fluid mosaic model” which describes membranes as two-dimensional liquids, consisting of a lipid bilayer with embedded protein moiety; original illustration is given in the left-hand panel of Figure 9. A more developed model is given in the same figure on the right-hand panel. In addition to the earlier model, several membrane components have been discovered during the last decades, as mentioned in the figure legend. However, phospholipids remain still the main building block of all biological membranes. Indeed, the lipid content of an average animal cell represents up to 50% of the plasma membranes mass. The rest is constituted of proteins. One μm^2 of such membranes contains approximately 5×10^6 lipids. For a small animal cell, the plasma membrane would thus contain 10^9 lipid molecules (Alberts *et al.*, 2002).

Basically, two possible movements can change the position of a lipid within membranes. First, the lateral diffusion, with a diffusion coefficient of about $10^{-8} \text{ cm}^2/\text{sec}$, moves the lipid within a monolayer. This means that lipids migrate with a fast velocity on the surface of a sea of lipids. For instance, a large bacterial cell with a length of about $2 \mu\text{m}$ would be travelled across in one second by such a lipid. The second movement takes place within a bilayer of lipids. This phenomenon is called “flip-flop” and describes the migration of a lipid from one lipid mono-layer to the other. It occurs scarcely, about once a month (Alberts *et al.*, 2002).

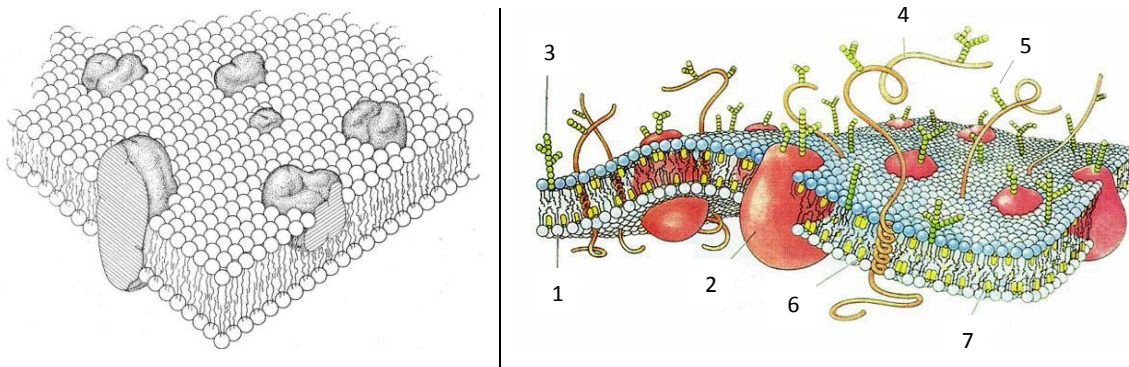


Figure 9: Obsolete and current scheme of the fluid mosaic model of biological membranes. The original drawing for the postulation of this model by Singer and Nicolson (Singer & Nicolson, 1972) is given on the left-hand panel, however over the last decades the model was subjected to further developments. Thus, the right-hand panel gives a more detailed view on additional building blocks of the membrane. Besides phospholipids (1) and globular proteins (2), further components, such as glycolipids (3), alpha-helix proteins (4), oligosaccharide side chains (5), transmembrane domains (6) and cholesterol (7), are mentioned. (Drawing by Dana Burns, (Bretscher, 1985))

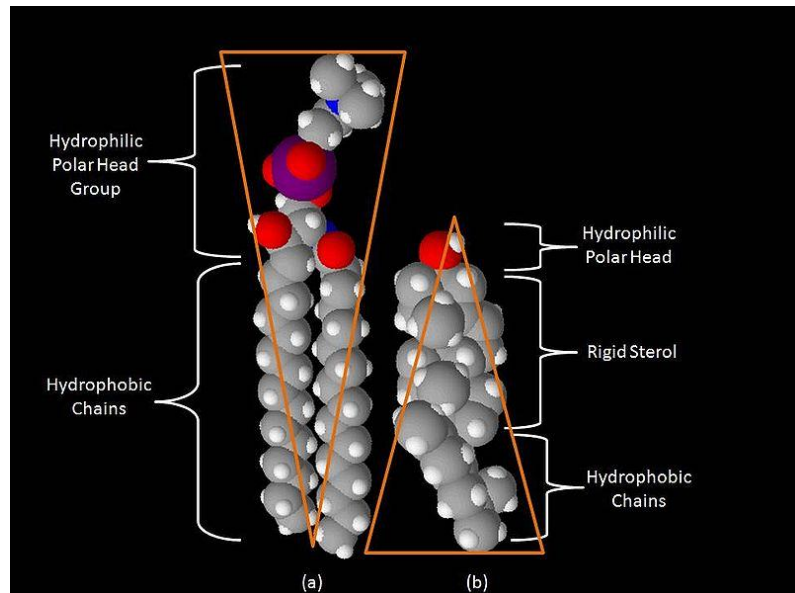
Membrane composition and fluidity; Overall, a defined membrane consistency is an important precondition for the proper function of a membrane as compartment forming entity. The lipid composition is responsible for membrane fluidity and thus enables or inhibits particular properties for an entire cell or rather for domains of the plasma membrane. A good criterion for defining the membrane fluidity is its “melting point”. At this point an obvious change in the membrane viscosity occurs due to a transition in its stage of aggregation; for review see also (Fantini *et al.*, 2002). Each aggregate, composed of one or several sorts of lipids possesses a rigid gel-like and a liquid crystalline stage. The point of transition is given by the so called phase transition temperature (T_m) and depends on the packing capacity of the respective lipid aggregate. Short hydrocarbon chains with double bonds hinder tight lipid packing and thus decrease the melting point of the membrane. Simple organisms are yet able to keep their membrane fluidity constant over a broad temperature range only by changing their lipid composition (Alberts *et al.*, 2002).

In contrast, many eucaryotic cells possess a buffer molecule to expand the range of phase transition. This buffer system uses cholesterol as additional membrane lipid, which hinders tight packing of hydrocarbon chains (Fantini *et al.*, 2002; Patty & Frisken, 2003); for its molecular orientation next to a phospholipid see Figure 10. Hence crystallization becomes more difficult for membranes. Its concentration can go up to one molecule per one phospholipid. Moreover, cholesterol decreases the permeability of lipid bilayers, with regard to small water soluble molecules. Cholesterol stabilizes the first few carbonyl-groups of a fatty acid chain. This part of the lipid is thus less deformable which results in less permeability for the whole compartment.

Mammalian cells contain four predominant types of phospholipids, namely phosphatidylcholine, sphingomyelin, phosphatidylserine and phosphatidylethanolamine. These lipids have very specific head-groups and thus differ very much in their properties. The variety of lipids is necessary to enable specific activity of proteins embedded in the membrane. In other words, lipids

serve as sort of solvent for these proteins and provide with that the proper environment to ensure their biological function. This effect is very much comparable to soluble proteins depending on a specific buffer composition, such as ionic strength or pH (Alberts *et al.*, 2002).

Figure 10: Molecular alignment of a phospholipid (a) and cholesterol (b) within lipid rafts. Figure from "Wikipedia" (free picture)



Lipids rafts; About one decade ago, an even more advanced membrane model was postulated. In fact, it was found that the different membrane lipids of a bilayer are not equally distributed around the complete entity. Yet, rather than forming a heterogeneous and chaotic mix of lipids, they seemed to form sort of definite islands, swimming on the lipid matrix (Simons & Ikonen, 1997). For this theory, the expression *lipid rafts* was born and added to the membrane model of Singer and Nicolson. Figure 11 shows a drawing of lipids rafts, flanked by a regular membrane area. Basically, they are micro domains within membranes, which are constituted of particular lipids, and thus can accommodate a unique collection of proteins. These regions build islands with specific functions, such as signaling events, intracellular trafficking of proteins and lipids, as well as putative entry site for pathogens.

The molecular structure of lipids and their phase transition stages gave a reasonable explanation for the emergence of lipid rafts; although, this theory is partly contradictive to the liquid mosaic model, which does not reflect on lipid clustering. In general, membrane lipids can exist in a gel-like phase, below their T_m , and in a liquid crystalline stage, above their T_m . A bilayer built up of one glycerophospholipid only, such as POPC, which possesses a T_m below 0°C , stays thus in a lipid crystalline stage at physiological temperature. As soon as more lipids are involved to build a membrane, its T_m will be a result of the respective T_m 's of the lipids. Cholesterol was proposed to equilibrate these differences and thus to keep the whole membrane in an intermediate stage of

aggregation. For sphingolipids, however, the situation looks different, from a molecular point of view. Due to their rigid acyl chains they can pack very tightly, and possess therefore a higher T_m than glycerophospholipids. This means that they are in a gel-like stage at 37°C.

Anyway, cholesterol favors such sphingolipids in its vicinity, because of steric reasons. Therefore, a mixture of glycerophospholipids and sphingolipids is supposed to unmix upon cholesterol addition. For a biological membrane, containing an enormous variety of lipids, this would mean the formation of at least two distinct regions. The entity composed of a glycerophospholipid would possess a low cholesterol concentration. It would still stay in a liquid crystalline stage, due to its low T_m . The second entity is supposed to contain most of the sphingolipids and cholesterol. The high cholesterol content, in turn, causes the intermediate stage of aggregation. This stage is characterized by tightly packed acyl chains but still a high mobility of its components. In conclusion, the latter entity forms small rafts, which are proposed to float on the glycerophospholipid part of the membrane. (Alberts *et al.*, 2002; Fantini *et al.*, 2002)

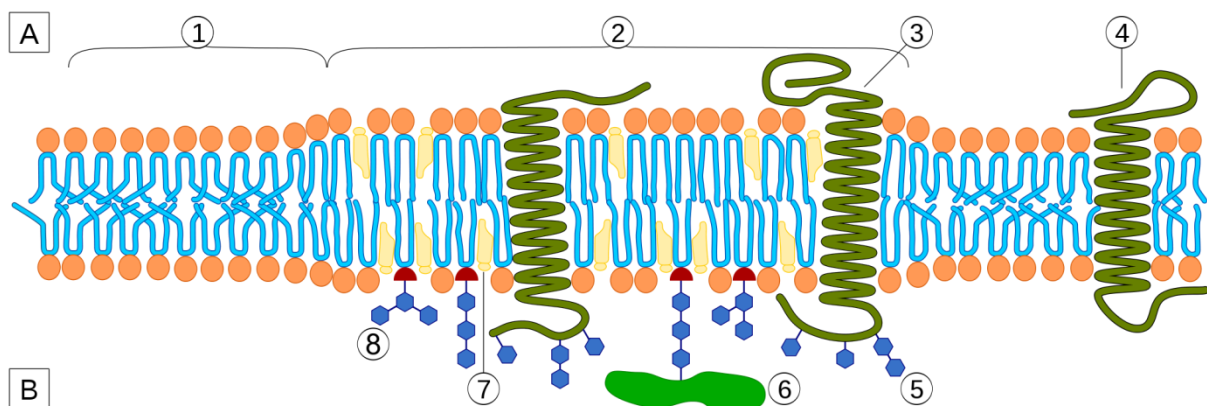


Figure 11: Schematic drawing of the arrangement of membrane lipids and proteins in a lipid raft region. In contrast to a non-raft membrane (1), lipid raft sections (2) contain a higher concentration of particular lipids, such as cholesterol (7), sphingomyelin or glycolipids (8), and form thus a dense packed and thicker micro domain. Due to a shorter transmembrane domain, non-raft proteins (4) are excluded from entering this area, whereas, proteins of specific functions can enrich in the raft section. The scheme shows examples such as transmembrane proteins (3) modified by glycosylation (5) and GPI-anchored proteins (6). Orientation of the bilayer: cytosol (A), Golgi apparatus lumen (B). Figure modified from "Wikipedia" (originated by Artur Jan Fijalkowski)

Membrane Permeability and Transport; Important physiologic substances, such as sugars or amino-acids, are transported through the membrane by transport mechanisms. Porins, which form protein aggregates in membranes, are a good example for those systems. They have been found in the outer membrane of many bacteria and allow for diffusion of dissolved molecules of up to 600 Da. Further examples are ion-transporters, which carry charged molecules through the amphipathic membrane.

Instead of using such transporters, lipid soluble substances can overcome the lipid bilayer on their own by diffusion. However, for this purpose the substances have to possess a high distribution

coefficient between the membrane and water phase. Then, they can shed their solvation shell and dissolve in the lipophilic core of the bilayer. Inside the core the dissolved substances migrate only by diffusion across the lipophilic phase. Upon reaching the hydrophilic end, they become resolvated in water again. Since ions carry charges, they are poorly soluble in lipid phases. This can be easily explained by the electrostatic energy necessary to transfer a charged particle from a medium with a high dielectric constant, such as water, to one of a very low constant. For that reason, Na^+ and K^+ diffuse by a factor 10^9 slower across the membrane than water and thus need transport systems. For its part, water covers an intermediate position. Its high degree of permeability results from the small size of the molecule, the high concentration and the lack of complete charges. The lipid solubility of some substances might also depend on the respective pH and the resulting charge of the molecule. Therefore, the degree of permeability cannot be assigned for any particle *per-se*. Nevertheless, to gain an overview in this regard about several physiologic substances a convenient assignment is shown in Table 1. (Adam *et al.*, 2003; Alberts *et al.*, 2002; Stryer, 1999)

membrane permeability to substances	
high permeability	low permeability
CHCl_3	Ions, e.g. Na^+ , K^+ , Cl^-
$\text{CH}_3\text{CH}_2\text{OH}$	amino acids (amphoteric ionic), nucleic acids (RNA, DNA)
$\text{CH}_3\text{CH}_2\text{OCH}_2\text{CH}_3$	sugar (several OH-groups)
(H_2O)	(H_2O)
CH_3COOH^*	CH_3COO^-*
NH_3^*	NH_4^{+*}

* Depending on molecule charge and pH, respectively.

Table 1: Examples of substances with high and low membrane permeability. Table modified from (Adam *et al.*, 2003)

As hydrophilic and charged molecule, nucleic acids need transport mechanisms to pass a lipid bilayer. With their about 7 kb long RNA genome, Rhinoviruses had to develop such mechanisms to conquer cellular membranes. Indeed, minor group HRVs are believed to form a pore in the endosomal membrane to shuttle their RNA. The minimal requirements for pore formation are defined in this work and will be addressed by an *invitro* model system

3.3 Model System: Lipofectosome

Construction of artificial membranes / liposomes; Biological membranes of living cells are very heterogeneous aggregates. As described above, they consist of a number of different lipids and a substantial content of embedded or associated proteins. In principle, one can prepare *in-vitro* vesicles from isolated cell membranes. They are certainly handy tools to study membrane phenomenon, such as fusion between membranes and the activity of embedded ion channels. However, they are very heterogeneous and thus badly defined with regard to their lipid and protein content. For that reason, this approach is not well suited for an experimental setup, requiring a defined vesicle material.

In contrast, a well defined lipid composition in vesicles can be guaranteed, if they have been *de-novo* synthesized. Technically, this means adding the required lipids sort by sort into a reaction container and to hydrate them. The resulting sort of aggregate, such as micelles or liposomes, can be selected via concentration and type of applied lipids. The chosen preparation technique and buffer composition for vesicle hydration are also parameters for the formation of lipid aggregates. In any case, the prepared lipid membrane will contain only the chosen lipids and thus possess a defined lipid ratio (Bilek *et al.*, 2006a; b; Torchilin & Weissig, 2003).

By using standard procedures for liposome preparation, they can be generated within a size range of 25 nm to 2.5 μ m. Concerning this diameter, unilamellar vesicles are referred to small (SUV), large (LUV) or giant unilamellar vesicles (GUV). Moreover, the incorporation of functional lipids can clearly expand and improve the experimental possibilities without great effort or costs. This includes for instance tracing vesicles upon insertion of homeopathic amounts of FL-lipids or prolonging the vesicle serum half-life via grafting their surface with polyethyleneglycol (PEG) derivatized lipids. The latter technique is well established for liposomes applied in drug delivery (Woodle, 1998). To conclude, self-made vesicles are very adaptable and clean tools suitable for an enormous spectrum of applications. Figure 12 shows the typical appearance of *de-novo* prepared LUVs (diameter about 100 – 200 nm) as used in this work, in TEM and cryo-TEM, respectively. Uniform size distribution of unilamellar vesicles was conveyed by extrusion of multi-lamellar vesicles. Cryo-TEM image even resolves the bilayer of vesicles and shows a low portion of multi-vesicular bodies, which remained after extrusion (lower panel).

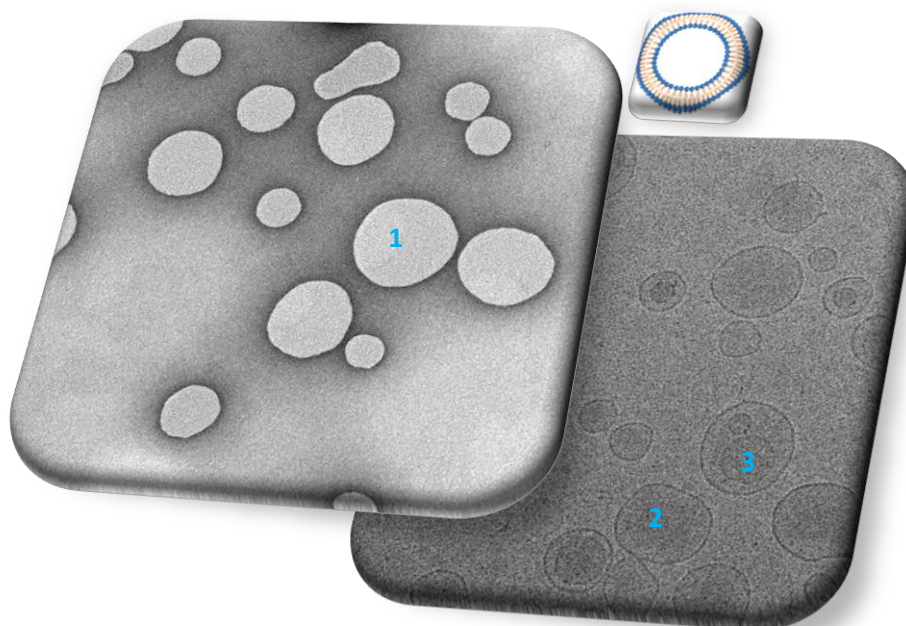


Figure 12: TEM (upper panel) and cryo-TEM images (lower panel) of liposomes. Unilamellar vesicle (1 + 2) and multi-vesicular body (3) are shown. Negative stain TEM image by Angela Pickl-Herk taken at of 5.6×10^4 fold magnification, cryo-TEM image by Günter Resch taken at of 3.1×10^4 fold magnification. (Drawing by Gerhard Bilek)

Liposome based model system for virus infection; based on the phospholipid composition of biological membranes the major building block of the prepared liposomes consisted of the lipids 1-palmitoyl-2-oleoyl-sn-glycero-3-phosphocholine (POPC), L- α -phosphatidylethanolamine (PE), cholesterol (Ch), sphingomyelin (SM); structural formula given in Table 2. In spherical compartments, POPC lipids accumulate on the outer leaflet while PE tends to enrich in the inner one. This separation is explained by the steric arrangement of their head groups (choline and ethanolamine) and promotes even the generation of vesicles. Ch and SM were added to mimic a raft like surface.

1,2-dioleoyl-sn-glycero-3-[(N-(5-amino-1-carboxypentyl)iminodiacetic acid)succinyl] (DOGS-NTA) and 1-oleoyl-2-[12-[(7-nitro-2-1,3-benzoxadiazol-4-yl)amino]dodecanoyl]-sn-glycero-3-phosphocholine (NBD-PC) were employed as functional lipids. Table 2 shows the structural formula of these lipids and their functional moiety. The DOGS-NTA lipid was implanted to complex nickel ions by its NTA group. Nickel-loaded lipids, in turn, attached His6-tagged proteins (Bubeck *et al.*, 2005; Tuthill *et al.*, 2006). Receptor constructs, possessing these tags, were used to decorate the lipid surface and then bind specifically the virions. In this work a recombinant receptor construct, derived from the VLDLR, was used to decorate the liposomes. Its binding module number V3, which possess

high binding affinity, was arranged in a pentameric concatemer (V33333) to obtain an even stronger binding to HRV2 (Bubeck *et al.*, 2005; Moser *et al.*, 2005).

For fluorescence detection, a FL-lipid, NBD-PC, was incorporated into the bilayer. An acyl chain is here modified with a FL-dye in order to trace the prepared liposomes by FL-detection. Figure 13 shows an outline of the model and TEM images, confirming the proper formation of the model cell; see background image and lower right-hand panel. Moreover, these images confirm the consistency of liposomes and the stage of viral conversion. In other words, one can examine whether infectious 150S particles or only sub-viral particles, such as 135S and 80S, are attached to the model surface.

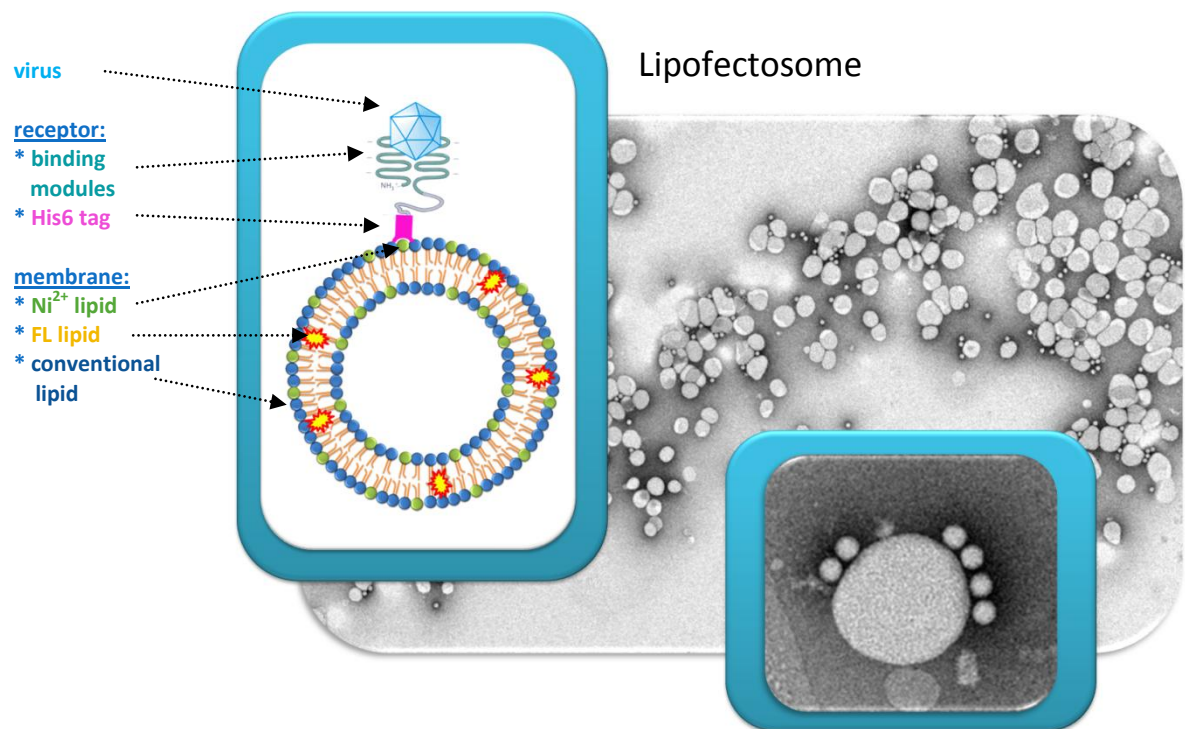


Figure 13: Scheme and TEM images of the liposome based model to mimic cell surfaces. The basic outline of the model system (left-hand panel) indicates nickel-chelating lipid head-groups as green circles inside the lipid bilayer. These lipids are supposed to complex His6-tags (pink rectangle) of receptor constructs. Virus, in-turn, can bind specifically to these receptor constructs and thus completes the system. Background of this figure and lower right-hand panel show TEM visualizations of these assemblies. (TEM images by Angela Pickl-Herk; drawing by Gerhard Bilek)

Basically, this model cell is now constituted by the minimal components necessary to allow viral genome transfer. It possesses an infectious virion, a receptor to keep it in proximity to the lipid membrane and a sealed lipid compartment which serves as recipient for RNA. Since this system is primed for “infecting” the liposomal compartment, it was called a “lipofectosome”.

3.4 Liposomes in Capillary Electrophoresis

A central topic of this work is the use of liposomes to mimic the cellular membrane of a human plasma membrane. As pointed out above, liposomes have been preferred to entire cells, because of their versatility and adaptability. In contrast to cell organelles, they can be easily prepared for their analysis in CE. By choosing a particular lipid composition, the resulting liposomal membrane can certainly mimic that of human cells. These properties made liposomes a suitable deputy cell and also a brilliant analyte for CE. However, in the genre of high-performance separation science, the use of liposomes as analytes is only one range of application. Several separation principles in analytical chemistry take also advantage by the use of liposomes as separation medium. Popular representatives are methods such as electrokinetic chromatography (EKC) or capillary electrochromatography (CEC). Both, the analysis of liposomes, as well as their application in separation methods was described in the following review (Bilek *et al.*, 2006a). It was published in the course of the doctoral thesis and thus inserted in this manuscript:

Working title:

**“Analysis of liposomes by capillary electrophoresis
and their use as carrier in electrokinetic chromatography”**

State of publication: published in “Journal of Chromatography B” 2006, 841: 38-51.

Contributing authors: **Bilek, G.**
Kremser, L.
Blaas, D.
Kenndler, E.

See review (Bilek *et al.*, 2006a) from publication section of appendix_____

4 Materials and Methods

4.1 Liposome Preparation

Preparation of multi-lamellar vesicles (MLV); Dissolved lipid stocks were prepared from lyophilized lipids as provided by *Avanti Polar Lipids*. An appropriate amount of each lipid was dissolved in chloroform to obtain a final lipid concentration of 10 mM. In order to generate a membrane with biological relevance, a composition similar to that from literature was prepared (Alberts *et al.*, 2002; Evans & Hardison, 1985; Kobayashi *et al.*, 2002; White & Helenius, 1980; Wubbolts *et al.*, 2003). Therefore, the dissolved lipid stocks from POPC : PE : SM : Ch : DOGS-NTA : NBD-PC (formula shown in Table 2) were mixed in the molar ratio 1 : 1 : 1 : 1.5 : 0.5 : 0.05 in a round-bottom flask. The solvent was removed under a constant flow of nitrogen gas while rotating the flask for at least 3 hours. The resulting dry lipid film was hydrated by the respective buffer for further 2 to 3 hours. To facilitate detachment of the lipid film from the flask wall, the suspension was frequently shaken on a vortex. The buffer volume was chosen to obtain a final lipid concentration between 5 and 20 mM. The resulting multi-lamellar suspension of vesicles was either immediately used for extrusion or stored at -20°C (Torchilin & Weissig, 2003).

Formation of large uni-lamellar vesicles (LUV) by extrusion; A mini-extruder (*Avanti Polar Lipids*) was used to prepare a liposome population of uniform size distribution. The extruder apparatus was equipped with two polycarbonate (PC) filters with a particular pore diameter. Normally, the extrusion was started with a filter diameter of 400 nm and was then reduced to the desired diameter in a second and third procedure of extrusion, respectively. The extruder was prewarmed to a temperature of about 30 to 50°C (depending on lipid concentration and vesicle cargo) and the MLV suspension was applied via a flat-needle Hamilton syringe. For each procedure 35 passages of the suspension through the filters were performed, collecting the extruded suspension finally in the syringe not used for its introduction. In the end, large uni-lamellar vesicles (LUV) were ready for immediate use in experiments or were stored at +4°C (*AvantiPolarLipids_Inc.*, 2009; Hope *et al.*, 1993; Patty & Frisken, 2003; Torchilin & Weissig, 2003).

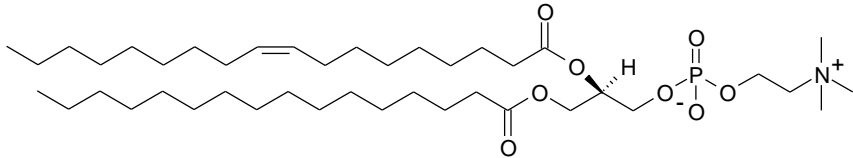
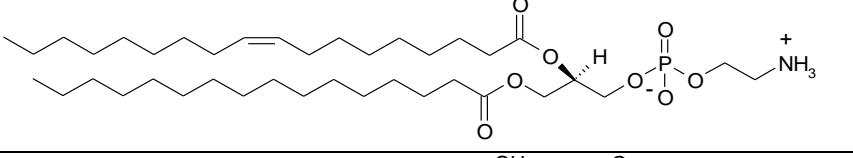
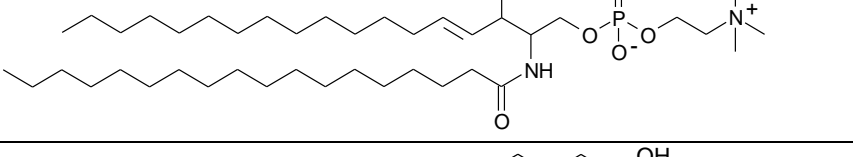
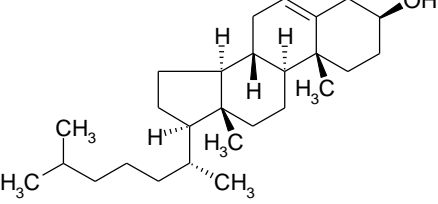
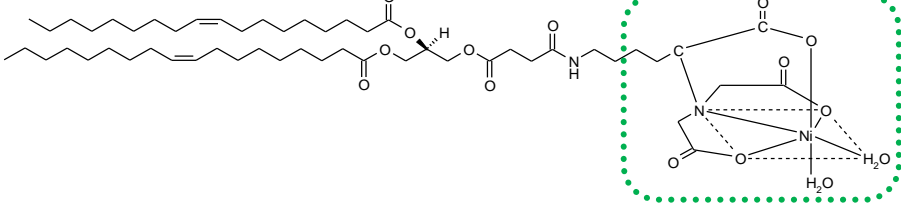
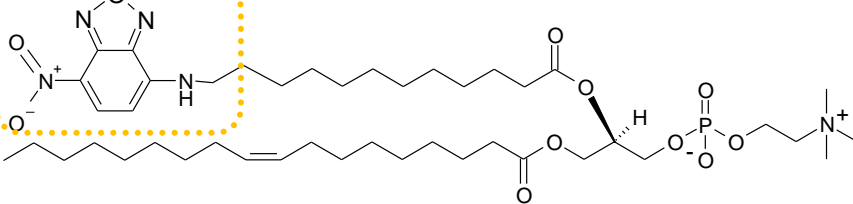
abbrev.	structural formula		formal charge
	hydrophobic moiety	hydrophilic moiety	
POPC			0
PE			0
SM			0
Ch			0
DOGS-NTA			-1
NBD-PC			0

Table 2: Overview of the lipids and their corresponding structural formula, as used for liposome preparation. Functional domains are indicated by colored boxes. Table modified from (Bilek *et al.*, 2009)

4.2 Liposome Purification

Flotation; For their application in TEM, receptor-decorated LUVs were floated to separate them from unbound receptor prior to incubation with HRV2. 20 μ L DOGS-NTA LUVs of 200 nm [\sim 150 nmol lipid] were mixed with 2 μ L of soluble receptor fragments [0.15 nmol V33333] and incubated for one hour at ambient temperature. The receptor-decorated LUVs were mixed with a 67% sucrose solution to obtain a final sucrose concentration of 50%. 200 μ L of the 50% LUV'sucrose mix were overlaid by 900 μ L of a 25% sucrose solution and finally by 900 μ L of pure buffer, 50 mM Tris-HCl pH 8.0. The gradient was subjected to 45.000 rpm at 4°C for 4 hours, in a TLS55 swing-out rotor. Subsequently, fractions of 164 μ L were taken from the top of the gradient and transferred to a

96-well plate. The NBD-PC fluorescence lipid, incorporated in the liposomal membrane, was used to trace the liposomes. All fractions were measured on a Wallac 1420 Victor V plate reader (Perkin Elmer; Software: Wallac 1420 Manager Version 2.0) at an excitation wavelength of 485 nm and an emission wavelength of 535 nm to isolate the main fraction of liposomes. In fact, the liposomes accumulated at the interface of 25% and 0% sucrose (Airaksinen *et al.*, 2001; Fricks & Hogle, 1990; Lonberg-Holm *et al.*, 1976).

Size exclusion chromatography; High molecular weight particles, such as HRV and liposomes, can be separated from significantly smaller molecules by gel filtration, also known as size exclusion chromatography (SEC). A very fast and effective SEC method is described in (Torchilin & Weissig, 2003). In contrast to regular SEC, this technique utilizes a semidry medium and subjects the filtration columns to centrifugation while filtering the particles. A further benefit of this SEC is their potential for downscaling to a micro range, with regard to applied gel medium and sample volume. Upon downscaling, this manuscript refers to this technique as mini-SEC (mSEC). In our laboratory, we adapted this technique to enable buffer exchange and purification of used biological particles; such as viruses, liposomes and receptors. Moreover, via mSEC sample dilution was significantly reduced, compared to regular SEC.

The sieving material, Sephadex G50 (DNA grade / fine, from Amersham Biosciences), was freshly swelled in the respective buffer over-night at +4°C. From the settled material an aliquot of 450 µL was transferred into a *Corning Spin-X* centrifuge tube, which was equipped with a cellulose acetate membrane, pore size 0.45 µm (Sigma Aldrich). Excess of buffer was removed via centrifugation in a tabletop centrifuge; 30 sec. at 800 rpm. Another 450 µL of sieving material were added. In order to obtain an appropriate dried column, it was centrifuged at 2000 rpm and 3000 rpm for one minute each.

Ten µL of a liposome suspension [~17 mM] were slowly added on the prepared mSEC column, filled with semidry G50 sieving material. The liposomes were filtrated through the column via centrifugation at 3000 rpm for one minute. For rinsing, 5 µL of buffer were added and the tube was again centrifuged with the same setup. The resulting filtrate, containing liposomes, was subjected to a second round of purification, using a freshly prepared mSEC column. Finally, the filtrate contained a slightly diluted (factor 2-4), but well purified suspension of liposomes.

4.3 Liposome Characterization

Determination of total phosphorus content; A standard protocol for the assessment of inorganic ortho-phosphate via ammonium molybdate (VI) tetra hydrate and its subsequent photometric detection was provided by (AvantiPolarLipids_Inc., 2009) and modified with regard to the needed working scale. Upon downscaling to the micro range, the protocol was used to confirm the lipid concentration of prepared liposome batches.

KH₂PO₄ (Sigma) was used to prepare a dilution series and thus to create a calibration function for phosphorus consisting of the following amounts: 0, 0.010, 0.020, 0.050 and 0.100 µmol. Both, the standard solutions, as well as 5 µL of each liposome batch, with a calculated phosphorus concentration of between 0.020 and 0.030 µmol, were transferred in glass vials. To digest the organic sample, 129 µL of H₂SO₄ [8.9 N] (MERCK) were added to each vial and the samples were heated without sealing in an oven at 210°C for 25 minutes. The sample vials were chilled for five minutes before 43 µL H₂O₂ [30 wt %] (MERCK) were added. Heat-treatment was continued for additional 30 minutes. All samples were supposed to be colorless; if not additional 14 µL of H₂O₂ were added and heating was continued for further 15 minutes. Glass vials were chilled at ambient temperature and diluted with 1.11 mL deionized water. For the color reaction, 145 µL of a 2.5% solution of ammonium molybdate (VI) tetra hydrate (Sigma) were added followed by a short vortex step for sample and standard. Finally, 145 µL of a 10% solution of ascorbic acid (MERCK) were added to each vial before sealing and subjecting them to heat-treatment, at 100°C for seven minutes.

For the spectral-photometric analysis, an Eppendorf instrument (BIOphotometer) was used. The zero value for the instrument was set with the 0 µmol standard. The absorbance of all five standard solutions and all samples was determined at 820 nm. The calibration curve was generated by using the standard values and the resulting linear regression was used to derive the unknown phosphorus concentration of the samples. For additional information, see also protocol 1 (p170-171) of (Torchilin & Weissig, 2003).

Dynamic light scattering (DLS); Non-functionalized liposomes were prepared for subjection to DLS. These testing liposomes were composed of POPC, PE and Ch. Before measuring the respective liposome suspensions, they were diluted in 50 mM Tris HCl pH 8.0 accordingly, to reach the linear range of the instrument. Liposome diameter and poly-diversity index (PDI) were assessed on a Malvern Nano ZS (Malvern Instruments; United Kingdom) at the department of pharmaceutical technology and biopharmaceutics (university of Vienna; Vienna 1090). The instrument was kindly put to our disposal by the group of Univ.Prof.Mag.Dr. Michael Wirth and was operated by Mag. Gerda Ratzinger.

Electrophoresis of labeled liposomes and lipofectosomes; Capillary and chip electrophoresis were employed to detect liposomes and their assemblies. Detailed information on the instrumentation and methodology is given in the respective publication, which are mentioned in the results and have been inserted in the appendix of this manuscript. Therefore, see the publications (Bilek *et al.*, 2006b; Bilek *et al.*, 2007) for information on conventional capillary electrophoresis, and (Bilek *et al.*, 2009; Weiss *et al.*, 2009) for detailed descriptions on chip electrophoresis.

TEM imaging; Liposomes or liposome assemblies were prepared and diluted as described in the respective section. Four μL of the sample were applied on a glow discharged (20 mA / 30 sec.) carbon-coated copper grid and incubated for one minute. Then excess of solution was blotted and samples were negatively stained with 2% phosphotungstic acid (pH 7.3) for one minute. The preparation of samples, as well as the operation of the TEM instrument was performed by DI(FH) Angela Pickl-Herk at the IMBA – institute of molecular biotechnology of the Austrian academy of science GmbH (1030, Vienna). The images were taken with a Morada CCD camera at magnifications of 8.9×10^4 , 5.6×10^4 , 3.6×10^4 or 1.8×10^4 (Bilek *et al.*, 2009).

4.4 Genome Transfer / Monitoring of Pore Formation

Reverse transcription (RT) – PCR; A dry lipid film was prepared as described above. For its hydration, however, the RT-kit, SuperScript III – Reverse Transcriptase, from *Invitrogen* was applied. This kit was used with a reverse primer, which was designed to anneal at the 3' end of the HRV2 genome; primer sequence is given in Table 5 (P/R: HRV2_3end). The RT-kit consisted of 150 μL nuclease-free water, 30 μL primer [2 pmol], 15 μL dNTP [10 mM], 60 μL 5x first-strand buffer, 15 μL DTT [0.1 M], 15 μL RNasin [40 units/ μL] and 15 μL SuperScript III RT [200 units/ μL]. As a consequence of the first-strand buffer, the buffer milieu was lastly composed of 50 mM Tris HCl pH 8.3, 75 mM KCl and 3 mM MgCl_2 . Prepared MLVs had a lipid concentration of about 17 mM and were allowed to mature over night at $+4^\circ\text{C}$. Before subjecting them to RT experiments, they were extruded through a set of 400 nm PC-filters at ambient temperature.

Upon mSEC-purification, 15 μL of purified RT-liposomes were reloaded with NiSO_4 , the nickel concentration reached 1 mM. Subsequently, 2 μL of the soluble receptor construct, V33333, with a concentration of about 5 mg/mL were added and incubated for 30 minutes at ambient temperature. To finally prime the receptor-decorated liposomes, 1 μL of HRV2 was added and again incubated for 30 minutes at ambient temperature; respective virus concentration is given in the results section.

Infection was triggered by either heating or pH-lowering. For the heat-treatment, samples were directly subjected to the PCR-instrument, running the RT-program (see Table 3). The first step of this program, 56°C for 10 minutes, is known to uncoat the virus. To trigger uncoating and thus RNA

release by pH-lowering, 1 μ L of a 1 M sodium acetate buffer pH 5.0 was added. After incubation for 15 minutes at ambient temperature, the acidic solution was re-neutralized with 0.5 μ L of a 1 M sodium hydroxide solution. Subsequently, the sample was subjected to PCR, while running the second step of the RT-program (4°C / 3 minutes). In any case, upon triggering infection, the RNA genome was expected to enter the liposomal lumen. Inside this nano-container, the RT kit was allowed to reverse transcribe an about 1kb region from the HRV2 genome.

step	parameters	commentary
1	56°C / 10 min	virus conversion / RNA release, RNA unfolding
2	4°C / 3 min	reduce RNA refolding
3	37°C / 1h	reverse transcription of RNA genome
4	70°C / 15 min	inactivation of RT
5	4°C / hold	final hold

Table 3: Program for reverse transcription of the HRV2 genome.

PCR: Amplification of the 3 prime end of HRV2; after finishing RT, the liposomal compartment had to be disintegrated in order to reach the synthesized cDNA template. Triton X100 (TX) was added, adjusting a final concentration of 1 % TX, in the liposome suspension. Two μ L of this mixture were subjected to a common pfu-polymerase PCR kit (Promega). The PCR mix contained 40 μ L nuclease-free water, 5 μ L pfu buffer (10xbuffer with 20 mM $MgSO_4$), 1 μ L dNTPs [10 mM], 0.5 μ L forward primer [10 μ M]; 0.5 μ L reverse primer [10 μ M], 2 μ L template (TX – treated) and finally 1 μ L of pfu DNA polymerase [3 units/ μ L]; sequence of oligo-DNA used as primer is given in Table 5. Further, Figure 14 shows the entire primary sequence of the HRV2 genome and indicates a 923 bp long amplicon at its 3 prime end. This region is flanked by the primers (also indicated), and hence being amplified. Subsequently, the PCR sample was again transferred in the PCR instrument, and the temperature program, shown in Table 4, was applied.

The samples together with a 1kb DNA ladder (Gene Ruler, Fermentas) were applied on a 1 % agarose gel. Electrophoresis was performed at 80 V for 30 minutes. The gel was incubated in an ethidium bromide bath for 10 minutes. Stained DNA bands were visualized and imaged under UV light.

step	parameters	commentary
1	95°C / 2 min	initialization
2	95°C / 45 sec	denaturation
3	50°C / 45 sec	annealing
4	72°C / 2 min	elongation
5	GoTo 2 / 60 repeats	cycle adjustment
6	72°C / 10 min	final elongation
7	4°C / hold	final hold

Table 4: Temperature program of PCR

primer name {position}	orientation	sequence	T _a [°C]
P/F: HRV2-7A {6126-6148}	forward (5'--> 3')	gagttgacttacctatggtcacc	62°C
P/R: HRV2 3end {7028-7048}	reverse (5'--> 3')	ccactcatgcaaaagcaaattc	60°C

Table 5: Primer sequences for RT and PCR. For RT-reaction “P/R” was applied in a concentration of 1µM, whereas a concentration of 10µM of each primer was used for PCR. T_a: annealing temperature of oligo nucleotides.

RNA genome of HRV2

```

1  uuaaaacugg auccagguug uucccaccug gauuucccac agggaguggu acucuguuau uacgguaacu uuguacgcca guuuuauuc
91  ccuuccccca uguaacuuaag aaguuuuuca caaagaccaa uagccgguaa ucagccagau uacugaaggu caagcacuuc uguuuccccg
181 gucaauguug auaugcucca acaggggcaa aacaacugcg aucguuaacc gcaaagcgcc uacgcaaagc uuaguagcau cuuugaaauc
271 guuuggcugg ucgaucggcc auuuccccug guagaccugg cagaugagcg uagaaauacc ccacuggcga caguguuuaa gccugcgugg
361 cugccugcac acccuauagg ugugaagcca aacaauaggc aaggugugaa gagccccgug ugcucgcuu gaguccucg gccccugaau
451 guggcuuaac uuaaccucgc agcuagagca cguaacccaa uguguaua gucguuauga gcaauugcgg gaugggacca acuacuuugg
541 guguccgugu uucacuuuuu ccuuuauuuu ugcuuauugg gacaauauau acaauauaia uauuggcacc augggugcac agguuucaag
631 acaaauguu ggaacucacu ccacgcaaaa cucuguauca aaugggucua guuuuuuuua uuuuaacauc aaauuuuaa aagaugcugc
721 uucaaauggu gcaucaaaaac uggaauucac acaagaucuu aguaaaauua cugacccagu uaaggauuuu uuggaaaagg gaauaccaac
811 acuacagucc cccacagugg aggcuuuggg auacucugau aggauuuuac agauuaccag agggagauua accauaacuu cacaagaugu
901 ggcuaaugcu aucguugcgu augguguuug gccacauuau cuauccucca aggaugccuc ugcaauugau aaaccucuc aaccagauac
991 aucuucuaa agauuuuuaa cucuaaggag ugugaccugg agcaguuccu caaagggguug gugguggaaa cuaccugaug cacucaagga
1081 caugggguuu uuuggugaaa acauguuuua ucauuaccug gguaggagug gauacacaau acaugugcag uguaaugcua guaaaauua
1171 ccagggguua cuauuugug cucugauacc ugagcaucag auugcaagug ccuucacaug caaugugaau guugguuua acuacacaca
1261 cccaggguua acaggcgagg aaguuuaagc ugagacgaga uugaauccug aucuacaacc uacugaagag uauuggcuaa acuuugaugg
1351 gacacuccuu ggaauuuuaa ccuuuuuccc ucaucauuuu aucaacuuga ggaguuuuua uucugccaca auuuuugccc cuuugucuaa
1441 ugcauuccu auggaaucaa ugcggagcca caauauuugg aguugguuaa uauuaccaau auguccccuu gagacaucaa gugcauuuaa
1531 cacaauaccu auuacaauau cuauaagccc caugugugca gaguuuuccg gcgcgcgugc caagcgucua ggauuaccag uuuuacacac
1621 accagguuaa ggacaguuuu ugacaacaga ugaauuucca ucccacugug cacuucccug guaucacca acuaaggaaa uuucuuuucc
1711 agguagaggu aaaaauuugg uugaauuug ucaaguagac agccuaguc cauuuuuuua cacugacacc uacaucaaua gugaaaaau
1801 guauucuguu guauugcaau caucauuuaa ugcaccagau aagaucuuu cuauucgaac agauguugcu ucccacuuu uagcuacuac
1891 uuugauuggu gagauaucua gcuauuuac ccacuggaca gggagucucc guuucagcuu cauguuuugu gguacugcca acacuacugu
1981 uaagcuuuug uuggcauaca caccaccugg uaucgcagaa cccaccaca gaaaggaguc aaugcuaggc acucauguua uauuggaugu
2071 gggguugcag ucuacaauau caaugguagu gccauggauu agcgcuguc auuuuagaaa cacaucacca gguagauua caucugggua
2161 cauaacaugc ugguauacga cuagauuagu cauuccaccu cagacccac caacagcuag auuguuuuugu uuuguauucg ggugcaaaaga
2251 cuuugcugug cgauggcac gagauacuaa ccuacaccug caaaguggug caauagcaca gaaccuuguu gagaauuaa uagaugaagu
2341 ucuuaaugga guuuuaguug ucccaauuau uauuaguagu aacccacaa cauaaaauuc ugccccagca uuagauugcg cagaacagg
2431 gcacacuagu aguguuacac cagaggauu cauugaauu agguaugugc agacauaca aacaagagau gaaugaguug uagagaguuu
2521 ucuuggcaga ucaggauca uacugaauu uaaauuagag guuacacug caauuuuaa caaggagaau uuacagugu gggucauuua
2611 ucuacaagaa auggcuaaaa uuagaaggaa auuuuauug uucacuaa cuagguuuga uucugaaa uaccuaguuc caugcauuuc
2701 cgcccuuagu caggacauug gacacauac aaugcaauac auguauugc caccaggugc accggugccc auuagauagg acgauuugc
2791 auggcagucu ggcacuaaag ccucuguuuu cuggcaacau ggacaggcuu auccaagauu uuccuuaccu uuccuaagug uggcaucugc
2881 uuauuacaug uuuuauaug gguuugauga acaagaucua aacuaugua cagcaaacac aaauaacau gggucacua gcucuaggau
2971 aguaacagag aaacacauuc auuauuaga uauuauagac agaauuauac acaaggcuua acauguaag gcaugugugc cagccccacc
3061 cagagcgcuu gaguauacuc gugcuacug cacuaauuuu aaaaauaggg auaggaguau ucagacagca auugugacca gaccauuuau
3151 cacuacagcu ggccccagug acauguauu ucauguaggu aaccuuuuu auagaaauu ucaucuuuuc aacucugaga ugcaugaauc
3241 uauuuuugua ucuuuuauu cagaauuuau cauuuaccga acaaacacug uaggugauga uuacauucc ucuugugauu guaccaagc
3331 uacuuaauu ugcaaacuaa aaaaauagaa cuucccauu acaguuuaca gccaugacug guaugaaau caggaaagug aguacauucc
3421 caaacacua caguacaauu uguugauugg ugagggcccu ugugaaccag gugacugug uggaaaguug cuaugcaaac auggugucua
3511 agguauagua acagcugug gugauaaua uguggcuuu auugaccua gacacuuca uugugcugaa gaacaagggg uuacagauua
3601 uauacauaug cuaggagaag cauuuggaaa uggauuugug gauaguguaa aagaacauu acaugccaua aaccagugag gaaauuacag
3691 caagaaaaau auuauuagga uguugagaau aauuacagca auggucaua uauuagaaa cucuucugac ccccaacua uauuagcaac

```

```

3781 acucacacug auugggguguu cuggaucacc cuggagauuu uaaaaggaaa aaucucguua auggacacag cuuaauuaua uacacaaaaga
3871 aucagauuca ugguuaaaga aauiuacuga agcaugcaau gcagcuagag ggcuugaau gauagggaau aagauaucua aauiuuuuga
3961 auggaugaag ucgaugcucc cgcaagcuca auugaagguu aaguacuuua acgagcuuaa aaaacucaac cuuacgaaa agcaaguuga
4051 gagcuugcgg guggcugaca ugaaaacaca agaaaaauu aaaauggaaa uagacacuuu acaugauuug ucacguaaa uucuaacuuu
4141 guaugcaagu gaggcaaaaa ggauaaaaac ccuauacauu aaugugaua auaucauca gcagaagaaa agaugugaac caguagcuau
4231 aguuuuuau ggaccaccug gugcuggcaa aucuauaaca acaauuuucc uggccaaaau gauaacuaau gauagugaca uauacucucu
4321 accuccugau ccaaaaauuu uugaugguua ugaccaacag aguguaguua uaauggauga cauuaugcag aauccagccg gggaugacau
4411 gacacuguuc ugccaaaugg uuucugugu uacauuuaua ccaccaauug cugaucuaac agauaaaggc aaggcuuuug auucagguu
4501 uguuuuauug agcacaauu auuccuuuc aaccccccg acauaacuu cacuaccugc aaugaauga agauuuuuu uagauuuuga
4591 uauaaugua cauguaacu ucaaagaucc acagggcaaa cuuaaugug cagcagcguu ucgaccaugu gaugugaua auagaauagg
4681 aaugcacguu uguuguccau uugugugug aaaagcagu ucuuucaaa aucguaacuc uugcaacaaa uacagccuug cgagggugua
4771 caacauaau auugaagaag acagacggag aagacaagug guugaugua ugacagcuau auuccaaggc ccaauugua ugaaaaacc
4861 accaccaccu gcuauuacug acugcucca gucuguuaga accocugaag uuauuaugua uugugagggg aaugaugga uauuccagc
4951 agaaucaag auagaaaagg aguugaacu ggcuacaca aucuaaaca ucauugcaa uguuuuuggu auggcgagaa uauuuuauu
5041 uuuuuacaaa cuuuuuugca cauucaggg accauuuua ggagaaccaa agcccaagac uaaaaucca gaaaggcgug uaguaacaca
5131 gggaccagag gaggaauuug ggaugucuu aauiuaacau aacucaugug uuauuacaac agaaauggg aaauccagc gucuuggagu
5221 auacgacaga uuugugugc uaccaacaca ugcagauccu ggaagggaau uucagguuga ugguuuaacu acaaaugua uugacucaua
5311 ugaccuauac aacaagaau ggauaaagcu agaaauaaca guacuuaau uagauagaaa ugaaaauuu agagauauca ggagauuuu
5401 accuaacaa gaagaugau accccaaug caacuagca cugcuagcaa accagccuga accaacuaa aucaauugug gagauuguu
5491 auccuauugc aaauacugc ucagugcaa ccaaacggcu agaauugcu aaucaguuu ccaacuuaa ucugguuacu guggaggugu
5581 cuuauacaaa auugggcaag ugcuuugaa acauguggg ggcaauugua gggaugguu cucagcuau uuacucagau ccuauuucac
5671 ugaugucag ggccaaaaua cguuuacaaa gaagaccagu gaauuaacc uaccaguuu acacaccca ugcaaaacca aaugcagcc
5761 uaguguuuuc uagaugauu ucccugguuc aaaagaacca gcugugugu cugaaaaaga ugcccguua caaguugau ucauugaagc
5851 acuuuuuuc aauuacaaag ggaauacaga uuguccauu aaugaccaca uaagaauugc aucaucacu uaugcagc aacucuuuac
5941 cuuagauuu gacccaaaac cuuuuacacu ugaggacagu gucuuugca cugaugguu agaggcucu gauuuaga cuagcgagg
6031 auuuccauu auugcaauug gaguuaaaa gagagauuuu auaaacaaca agaccaagga uauaagcaaa cuuaaagaag caauugacaa
6121 auacggaguu gacuuaccua uggucacuu cuugaaagau gaacucagaa agcaugaaaa gguaauuaa gguaaaacua gaguuuuga
    P/F: Primer HRV2-7A {6126-6148}
    >>.....Amplicon 3end (923 bp).....>
6211 agcuaguau gugaugaua ccuauuuu uagaacaau uuuggcaacc ucuuuucuaa guuccacuug aauccggaa uuguuacug
    >.....Amplicon 3end (923 bp).....>
6301 aucagcagu ggaugugau cagaggguu uuggucaaaa auaccagaa uguuggauga uaauguuu auggcuuu auuauacaaa
    >.....Amplicon 3end (923 bp).....>
6391 uuaugaugu aguauacacc cuuuuuguu ugaagcucu aaacaggua uguuagauu aucauuuuu ccaacuua uagauagau
    >.....Amplicon 3end (923 bp).....>
6481 augcaaguc aaacacauu ucaaaaau acuaugaa guggaggag guguaccau ugguguuu gguacuaga uuuuuacac
    >.....Amplicon 3end (923 bp).....>
6571 uaugaucau aaauuuaua uaaggacuu aguuuagau gcauacaaga auauagauu agauaagcu aagauauug ccuauugga
    >.....Amplicon 3end (923 bp).....>
6661 ugaugucau uucucaua uacauaacu ggcauggag gcuauagca uagaggguu uaaauauggu uugacuuaa cuccugcuga
    >.....Amplicon 3end (923 bp).....>
6751 uaaaucaac acauuugua aauiagacu uagcauugu acuuuuuu aaagaggguu uaagcaagu gagauguau acuuucuaa
    >.....Amplicon 3end (923 bp).....>
6841 acauccaau uuccugaag augaaauuu ugaaucau agauaggaa agaaaccau acaauugcu gaacauugu ugucucug
    >.....Amplicon 3end (923 bp).....>
6931 ucacuuauug uggcacaug gacugacgc auacaaaaa uuugggaga agauacgcag ugaagcgcu ggucugcac uguacuucc
    >.....Amplicon 3end (923 bp).....>
7021 uccguaugau ugcuuuugc augagugua ugaaaaauu uaaagauua gaaauagua acugauugu uuuuaguuu au
    P/R: Primer HRV2_3end {7028-7048}
    >...Amplicon 3end (923 bp)....>

```

Figure 14: Entire RNA sequence of the HRV2 genome with indications for forward primer, reverse primer and the resulting 923bp amplicon at the 3' end. Modified from embi|X02316|X02316 Human rhinovirus 2

Infection from plasma membrane and determination of eIF4G1 marker protein for early infection (eIF4G1 cleavage assay); HeLa cells were seeded in parallel in two 48-well plates and allowed to grow to 90 % confluence. They were washed with 500 μ L PBS each well and subsequently incubated in 150 μ L infection medium (infMEM), containing 40 nM bafilomycin, for 30 minutes at 37°C. Before adding virus, the 48-well plates were chilled for 15 minutes at +4°C. The medium on chilled cells was exchanged by 150 μ L of virus with a MOI of 30, suspended in infMEM containing 20 nM bafilomycin. To prevent fluid phase uptake and thus bind the virus only to the plasma membrane, the samples were incubated for one hour at +4°C. Upon virus attachment, the samples were washed twice with 500 μ L serum-free infMEM (SF-infMEM) and then incubated with 100 μ L of SF-infMEM containing 20 nM bafilomycin, 100 mM MES buffer pH 5.2 containing 20 nM bafilomycin and the latter mixture plus holding RNase [2 mg/mL], respectively. To perform the actual infection from the plasma membrane, the samples were again subjected for one hour at +4°C. Acidified samples were re-neutralized by exchanging MES buffer with regular SF-infMEM with 20 nM bafilomycin. Further, the infected cells were incubated for five hours at 34°C in order to initialize virus replication. Since eIF4G1 cleavage happens at an early time point in HRV infection, five hours of incubation are sufficient to assess this marker protein. Finally, all samples were washed with 500 μ L PBS each and collected in a vial upon addition of 25 μ L cell lysis buffer. In addition to these samples, controls were prepared in parallel. Positive controls have not been incubated with bafilomycin, whereas negative controls have not been infected with virus. Further controls tested the effect of applied RNase and the effect of the whole treatment (mock) on the cells (Brabec *et al.*, 2003).

Ten μ L of each sample and each control were separated on a 6% SDS polyacryl-amide gel (I=20 mA / 1h) and subsequently blotted on a transfer membrane (I=400 mA / 1.5h; Millipore Immobilon). The membrane was incubated with a primary antibody from rabbit against eIF4G1, which recognizes both, the cleaved, as well as the native eIF4G1, for one hour at ambient temperature. Upon washing with PBS the membrane was incubated again for one hour at ambient temperature with a secondary antibody against rabbit, conjugated with a horse radish peroxidase. Afterwards, a peroxidase substrate (SuperSignal West Pico - stable peroxide solution and luminol/enhancer solution from Pierce) was added, and a chemoluminescence film (Kodax BioMax MR Film) was exposed for 30 minutes to the membrane (Gradi *et al.*, 1998). Employing the program *ImageJ*, the signal intensity was assessed. In this way the extent of darkening was quantified and plotted in a chart.

5 Results and Discussion

5.1 Liposome Characterization

5.1.1 Determination of Lipid Concentration via Total Phosphorus Content

An important characterization of batches of lipid aggregates is their lipid concentration. Especially for the formation of assemblies, such as lipofectosomes, which are composed of three building blocks, accurate information about the concentration of the components is needed. Otherwise, their reproducible preparation is impeded. From the input concentration of lipids, used for MLV preparation, a theoretical lipid concentration can be derived. Since liposome preparation can bear unexpected losses of applied lipids, this calculated value needs experimental confirmation. Therefore, the total phosphorus content of different liposome batches was assessed by photometric means. The resulting lipid content was related to the theoretical value.

Three liposomes species (MLV, LUV, LUV-DSPC) were oxidatively decomposed. The resulting phosphate reacted in acidic solution with ammonium molybdate-(VI) tetra hydrate and formed molybdenum blue, which in turn, was detected at 820 nm. Potassium dihydrogenphosphate (Sigma) was used to calibrate the system; its calibration function and linear fit are given in Figure 15 (left-hand panel).

The applied liposome samples were measured in duplicates. Their measured phosphorus content was in good agreement with the theoretical value. Both values, experimental as well as theoretical lipid concentration, are given in the bar diagram of Figure 15 (right-hand panel). The precision of the assay was dependent on the respective liposome species, as indicated by their error bars. Due to their heterogeneity, MLVs were more difficult to examine in comparison to processed and thus more homogeneous liposome species. As can be seen from the diagram, measurement of the first LUVs sample (middle bars), extruded through a 200 nm filter, had a significantly higher precision. Both species (MLV and LUV) were composed of the standard lipid composition, as used to mimic biological membranes. The last batch, however, was composed of 1,2-distearoyl-sn-glycero-3-phosphocholine (DSPC) as a substitute for POPC and PE of the regular mixture. Since DSPC consists of saturated fatty acids, the resulting lipid aggregates are more rigid and thus more difficult to process. In fact, although extruded in the same way, as the previous LUV batch, concentrations of DSPC-LUVs were still difficult to determine with high precision.

In any case, the experimental estimation of the lipid content of three different liposome samples confirmed good correlation with their theoretical value, in terms of phospholipid concentration. Therefore, the lipid concentration, derived from lipid input, was considered suitable

to refer for the calculation of particle ratios. This is of particular interest for the reproducible composition of lipofectosomes, consisting of virions, receptor-molecules and liposomes.

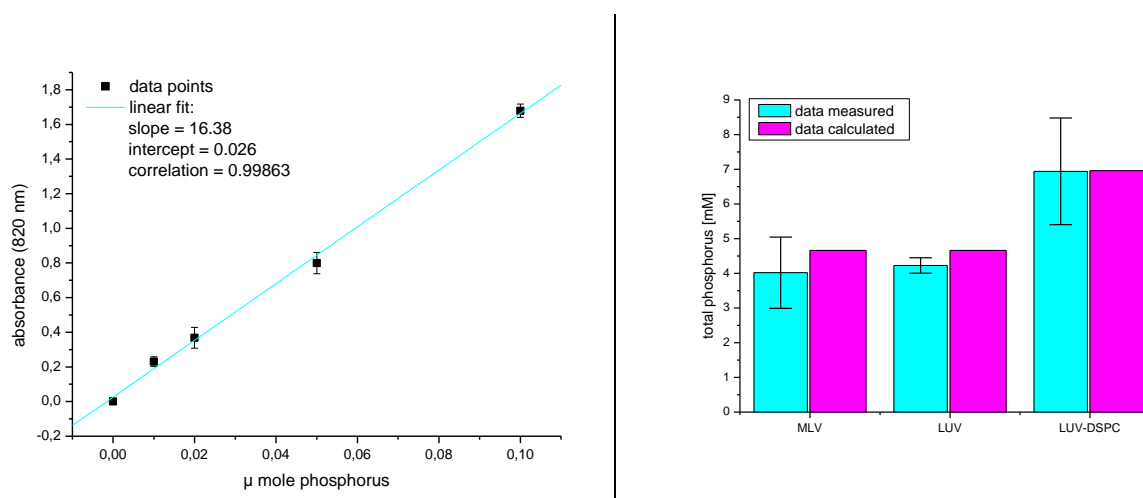


Figure 15: Determination of total phosphorus in liposomes. The calibration function and its linear regression are shown on the left-hand panel. The right-hand panel compares, the resulting concentrations [mM phospholipid] of three liposome samples (data measured) with data, derived from their lipid-input concentration (data calculated), as used for liposome preparation. Data were measured in duplicates.

5.1.2 Determination of Liposome Size via Dynamic Light Scattering

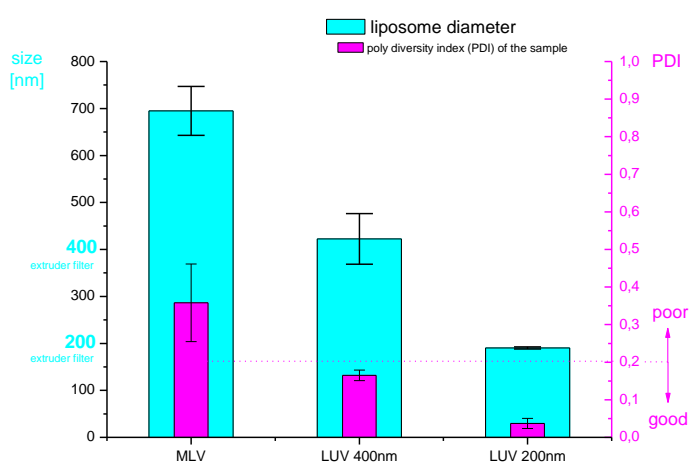
An important quality criterion of lipofectosomes is their uniformity, with regard to size distribution, of applied liposomes. Moreover, concerning assays for RNA transfer, prepared LUVs should not contain multi-vesicular bodies; see Figure 12. Both properties can be conveyed on liposomes by extrusion of the MLV suspension through PC filters. The resulting LUVs are expected to possess a uniform size population and only one lamella. However, the efficiency of this technique needed to be confirmed. For that purpose, DLS was chosen to assess the diameter of MLVs and of the corresponding LUVs, upon extrusion through 400 nm and 200 nm filters, respectively.

The derived liposome diameters, as well as the respective poly diversity index (PDI) are shown in Figure 16. MLVs appear in DLS as huge particles with a size up to 700 nm. As expected, due to the heterogeneity of this raw liposomal material, their PDI was too high and the data thus not reliable; the Figure gives an indication for the PDI-threshold at 0.2 (magenta-dotted line). However, for the extruded suspension, the PDI fit the acceptance specifications. LUVs, extruded through a 400 nm filter, showed a mean diameter of indeed about 400 nm although their size distribution was still rather broad. Particle diameters varied by about ± 50 nm. Significant tighter distributions (± 2.5 nm) were obtained in the liposome suspension, which was serially extruded through a 400 nm and a 200 nm filter set. For each extrusion procedure, 35 passages were performed to

produce a very uniform vesicle population. Therefore, the determined diameter was, as expected, around 200 nm.

From these results, it can be seen that extrusion is an essential step towards a defined working material. Moreover, DLS demonstrated a significant increase in LUV homogeneity upon serial extrusion through two sets of filters. As far as allowed by the experimental setup, liposomes were therefore extruded to a final diameter of 200 nm. However, for RT-assays only one extrusion step, using a 400 nm filter set, was applied to prevent mechanic forces on the enzymes and impairing knock-on effects, such as foam formation.

Figure 16: Dynamic light scatter confirms liposomal diameters of MLV and obtaining LUV. Bars in cyan give the measured liposome diameter, whereas bars in magenta give the corresponding poly diversity index (PDI). Samples were measured in triplicates.



5.2 Formation of Lipofectosomes

5.2.1 CE: Protein/Receptor-Decoration of the Liposomal Surface

In Figure 13 the outline shows the basal building blocks of the lipofectosome, namely liposome, receptor and virion. A crucial step for accurate formation of this assembly was the decoration of the liposomal surface with receptor molecules prior to its incubation with virus. In fact, virus forms only receptor-mediated aggregates with the liposomes. In our model, a chelator enabled receptor decoration of the membrane. Briefly, a nickel chelating lipid was incorporated in the liposomal membrane in the course of the MLV preparation. The nickel ions, in turn, formed a complex bond with the histidines of His6-tagged receptor molecules.

Protein decoration of liposomal surfaces was established via nickel DOGS-NTA containing liposomes, which were incubated with two different His6 containing receptor molecules. The liposomes contained a FL-dye in their aqueous core to allow their tracing via CE-LIF. Protein decoration was confirmed by detection of a shift in the electrophoretic mobility of liposomes upon protein binding. The results of this project are described in detail in the following publication (Bilek *et al.*, 2006b), which is inserted in this manuscript:

Working title:

“Capillary electrophoresis of liposomes functionalized for protein binding”

State of publication:

Published in “Electrophoresis” 2006, 27: 3999-4007.

Experimental contributing authors:

Bilek, G. – 80%
Kremser, L. – 20%

Contributing items by Bilek, G.:

- * MLV preparation
- * LUV preparation and purification
- * Production of liposomes stable for CE
- * Characterization of particle size - DLS
- * CE of liposomes – CE-LIF

See article (Bilek *et al.*, 2006b) from publication section of appendix_____

5.2.2 CE / Chip: Specific Binding of Virus to Receptor-Decorated Liposomes

As demonstrated above, liposomal surfaces can be decorated with soluble proteins via a His6/Ni-NTA bond. The following two papers, (Bilek *et al.*, 2007) and (Weiss *et al.*, 2009) accomplished the formation of lipofectosomes via specific binding of virus to these receptor-decorated liposomes. These articles were also published in the course of the doctoral thesis and describe in detail the stepwise formation of lipofectosomes and their examination by electrophoretic means.

The first article inserted below, (Bilek *et al.*, 2007), utilizes liposomes, which were FL-labeled via encapsulation of FITC dextran. These vesicles were detected on a home-made capillary electrophoresis instrument, employing LIF detection. Using this method, gradual mobility shifts of liposomes were found, which corresponded to the extent of their receptor decoration. After decorating the liposome with receptor, HRV2 specifically bound to them. This resulted in an additional shift in the mobility of the liposome signal. However, upon virus attachment the consequential FL-trace of liposomes rendered a spike-covered signal rather than a neat peak. This phenomenon was explained by aggregating virus in capillary instruments. In fact, detergents, such as SDS, are normally applied in the BGE to run virus particles and thus prevent aggregation (Kremser *et al.*, 2006b). However, detergents affect the consistency of liposomes and were thus avoided in this setup. Moreover, due to multiple receptor binding sites on the virus, most probably more than one liposome was bound via receptor-mediation and this effect also increased aggregation. The specific complex formation was confirmed by replacing HRV2 with a major group virus, HRV14, as a negative control. Viruses of this group bind ICAM-1 or heparan sulfate. The utilized receptor fragments derived from VLDLR, and targets only minor group viruses. As expected, HRV14 did not bind and the liposome signal was not shifted.

The second publication in this context, aimed at solving the aggregation problem upon virus binding (Weiss *et al.*, 2009). As found in previous work of our group, virions can be examined by chip electrophoresis with a detergent free BGE (Kolivoska *et al.*, 2007; Weiss *et al.*, 2007). Therefore, the experimental method for measuring lipofectosomes was transferred from the capillary to the chip format. In contrast to CE, chip electrophoresis uses shorter distances for separation and thus requires significant less time for sample analysis. Whereas the former assay traced only one component of the lipofectosome, in this work the setup was improved yet by FL-labeling of two components: the liposome again via dye encapsulation and this time the virus via protein labeling of its capsid. In conclusion, chip electrophoresis indeed overcame the aggregation problem and rendered reproducible and neat peaks for lipofectosomes.

Working title:

**“Mimicking early events of virus infection:
Capillary electrophoretic analysis of virus
attachment to receptor-decorated liposomes”**

State of publication:

Published in “Analytical Chemistry” 2007, 79: 1620-1625.

Experimental contributing authors:

Bilek, G. – 80%
Kremser, L. – 10%
Wruss, J. – 10%

Contributing items by Bilek, G.:

- * MLV preparation
- * LUV preparation and purification
- * Binding studies on CE-LIF instrument

See article (Bilek et al., 2007) from publication section of appendix_____

Working title:

**“Mimicking virus attachment to host cells employing liposomes:
Analysis by chip electrophoresis”**

State of publication:

Published in “Electrophoresis” 2009, 30: 2123-2128

Experimental contributing authors:

Weiss, V.U. – 55%

Bilek, G. – 30%

Pickl-Herk, A. – 15%

Contributing items by Bilek, G.:

* MLV preparation

* LUV extrusion

See article (Weiss et al., 2009) from publication section of appendix_____

5.2.3 TEM: Visualization of Lipofectosomes

TEM experiments were designed, to confirm and visualize the previous data on complex formation between liposomes, receptors and viruses. This method enables utilization and detection of unlabeled material. Therefore, putative interfering effects due to dye molecules can be excluded. In a first attempt bare liposomes and virus were visualized. Subsequently, receptor-decorated liposomes were incubated with HRV2 to follow complex formation. Receptor molecules, however, were too small to allow visualization. Consequently, images of the ternary complex render only liposome and virus particles visible.

A section of a recent article of our group described the approach of visualization of these assemblies in detail and hence was added to this chapter. The demonstrated data show the specific attachment of HRV2 to receptor-decorated liposomes and thus confirms formation of lipofectosomes. For inclusion in this manuscript, the TEM section from (Bilek *et al.*, 2009) was inserted and slightly modified to preserve the integrity of the document.

Working title:

***“Chip electrophoretic characterization of liposomes with biological lipid composition:
Coming closer to a model for viral infection”***

State of publication:

Accepted for publication in “Electrophoresis” 2009; XX

Experimental contributing authors:

Bilek, G. – 55%
Weiss, U.V. – 30%
Pickl-Herk, A. – 15%

Contributing items by Bilek, G.:

- * MLV Preparation
- * LUV Preparation
- * Incubation series of vesicles for TEM imaging

Begin of insertion from (Bilek *et al.*, 2009)

Receptor-mediated formation of liposome/virus assemblies; Virus binding to receptor-decorated liposomes was also assessed via electron microscopy. Figure 17 shows pictures of liposomes, virus, assemblies resulting from mixing receptor-decorated liposomes with virus, and a mixture of bare liposomes (lacking receptor) with virus, respectively. Samples were applied to glow discharged carbon coated copper grids and negatively stained with 2% phosphotungstic acid, pH 7.3. Liposomes appeared as circular density with diameters ranging from about 50 to 200 nm (Figure 17A). Due to adsorption and dehydration as part of sample preparation, they are not perfectly round. The image

confirmed that extrusion leads to a size distribution with a maximum diameter of 200 nm, limited by the pore size of the polycarbonate filter. HRV2 is shown in Figure 17B. The particles are well dispersed and not aggregated. Figure 17C shows receptor-decorated liposomes after incubation with virus. The virions are no longer distributed randomly but are preferentially seen attached to liposomes and only few free virus particles are detected. To again confirm the specificity of the interaction, virus was incubated with bare liposomes (Figure 17D). Liposomes and virus particles are randomly distributed and no virions are attached to the lipid vesicles. This confirms that the virus does not interact with the membrane *per se* but depends on the receptor for attachment.

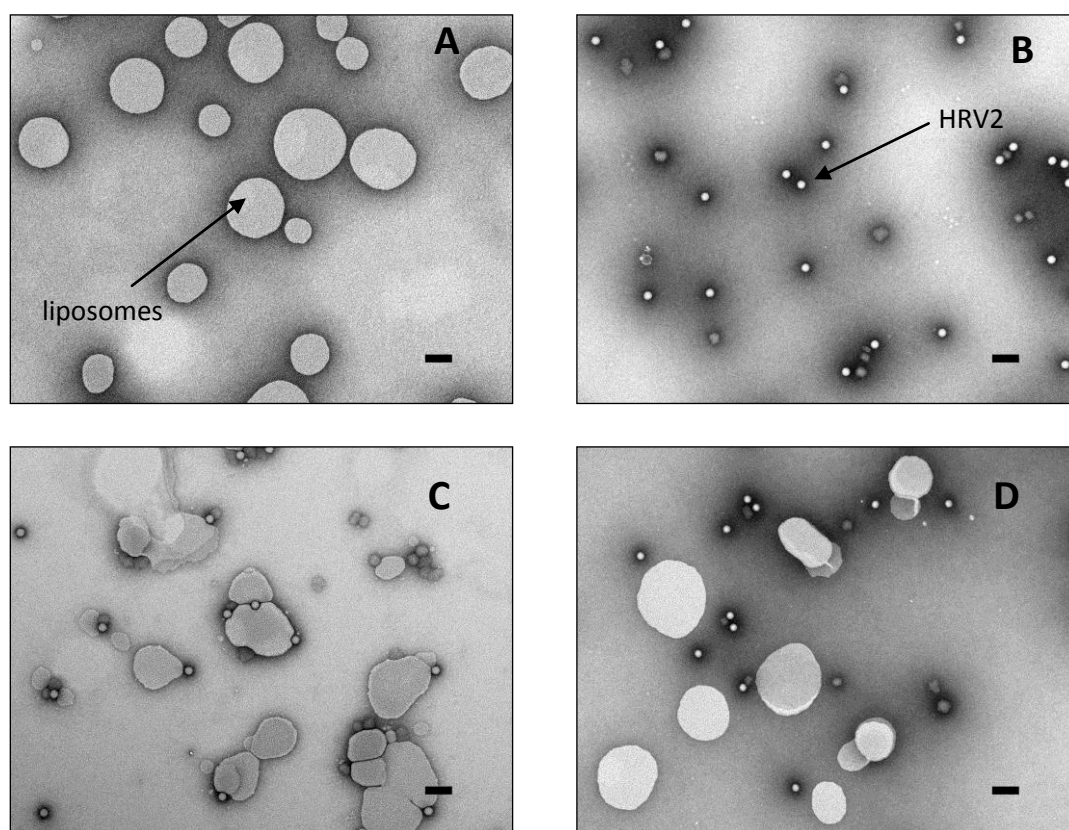


Figure 17: Virus binding to liposomes depends on the receptor. TEM images of liposomes (A); HRV2 (B); a mixture of virus and receptor-decorated liposomes (C); a mixture of virus and bare liposomes (D). Sample staining: samples were adsorbed to glow-discharged carbon coated copper grids and negatively stained with 2% phosphotungstic acid, pH 7.3. Images were taken at a 5.6×10^4 fold magnification. Size bar = 100 nm

The inserted TEM data confirmed findings from capillary electrophoresis that is receptor-mediated formation of assemblies. In addition, these TEM images clearly show that attached virus particles are still infectious 150S particles, with their RNA genome inside. This means that the produced lipofectosomes are indeed primed for genome transfer. The following TEM images will explain the optical differentiation of infectious and non-infectious virions. Two experimental techniques are known to trigger HRV2 conversion *in-vitro* and so release viral RNA from the capsid. An effective but artificial approach is the heat-treatment. Incubation at 56°C for 10 minutes was shown to release RNA from the viral capsid (Kremser *et al.*, 2006a). The second and more subtle approach is pH-lowering. For this technique, viral conversion is induced via acidification in order to generate a similar milieu as present in endosomal compartments during virus infection (Prchla *et al.*, 1994). So far, both techniques have only been tested for the conversion of bare virus particles. Therefore, their efficiency for triggering RNA release needed to be confirmed for virions engaged in lipofectosomes. Consequently, lipofectosomes were prepared and different stages of viral conversion were examined upon triggering uncoating. Negative stain TEM distinguishes these viral stages easily by a variable and stage-depending ingress of staining material into the viral capsid. As a result, contrast and appearance of the capsid are unique for each stage and can thus serve as indicator for differentiation.




Heat induced conversion of virus in lipofectosomes; First, heat treatment was tested for its efficiency in triggering RNA release. Receptor-decorated LUVs with a diameter of about 200 nm were separated from free receptor (V33333) by flotation. 19 µL of the flotation fraction were incubated with 1 µL of 14.5 nM or 7.25 nM HRV2, resulting lipofectosomes containing either 0.73 nM or 0.36 nM virus. They were incubated at 56°C for 10 minutes to trigger infection. Subsequently, lipofectosomes were imaged by negative stain TEM, in order to examine viral and liposomal stages and the degree of RNA release (Figure 18). Independent of applied viral concentration, the liposomal appearance was still homogeneous; liposomes were of integrity and did not produce aggregates. Despite heat-treatment, the majority of viral particles were still attached to the membrane. Since the difference in applied virus concentration was only by a factor of two, it did not lead to any differences in the saturation of lipofectosomes with virions.

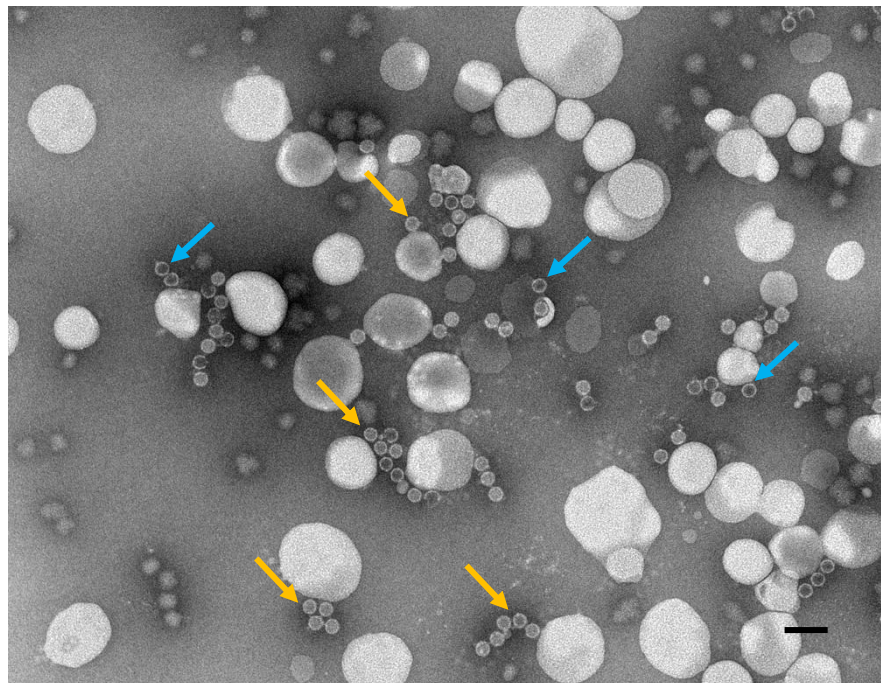
After heating, the majority of HRV2 appeared either as intermediate particle (Figure 18; yellow arrow) or empty capsid (Figure 18; blue arrow). The intermediate corresponded most likely to the 135S particle. Due to the ingress of stain media into the empty capsids, in negative stain TEM 80S particles are visible with a dark stained center and a bright protein corona. Intermediates retain more internal density. Almost no native virus was detected after heat-treatment. This means that RNA release had clearly been initialized but complete release was not found for all particles. Several intermediates keep at least to some extent their genome. Further or stronger heat-treatment

however, broke viral capsids apart and affected liposome integrity; data not shown. Since the heating procedure could not be changed for this reason, it was endeavored to obtain a more efficient degree of RNA release by pH-lowering. This technique meets closer the native situation.

(A) Heat-treatment of lipofectosomes containing **0.73 nM HRV2**




Arrow key:

-  native (150S)
-  intermediate (135S ?)
-  empty (80S)



(B) Heat-treatment of lipofectosomes containing **0.36 nM HRV2**

Arrow key:

-  native (150S)
-  intermediate (135S ?)
-  empty (80S)

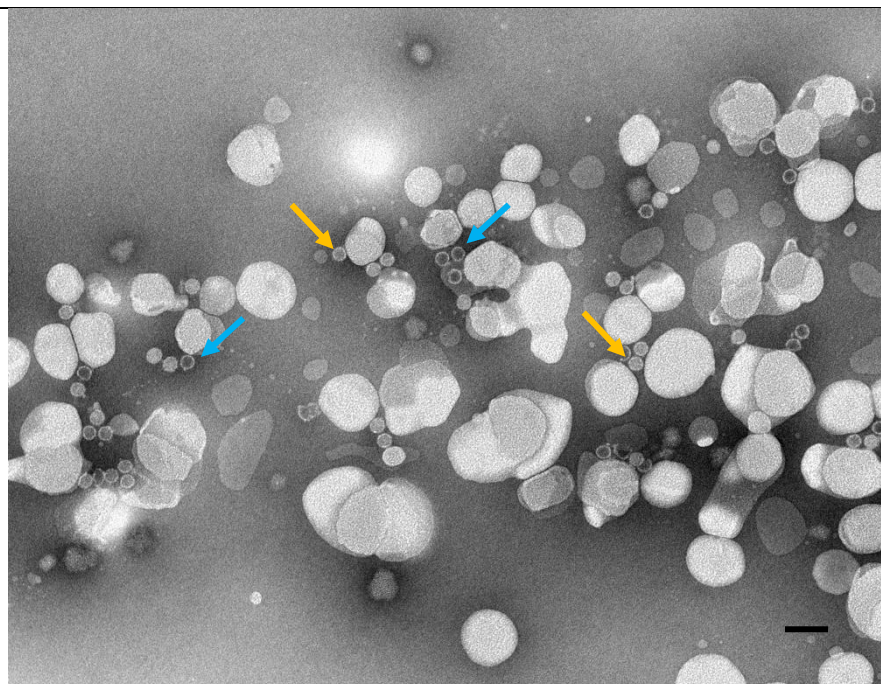






Figure 18: Negative stain TEM images of lipofectosomes upon heat-treatment. Receptor-decorated liposomes were incubated with HRV2 of two concentrations (indicated in the figure). Heat-treatment: 56°C for 10 minutes. Arrows indicate the converting stage of virions (color code is given by the arrow-key at the left-hand side of each picture); sample staining as in Figure 17; images were taken at a 5.6×10^4 fold magnification; size bar = 100 nm.

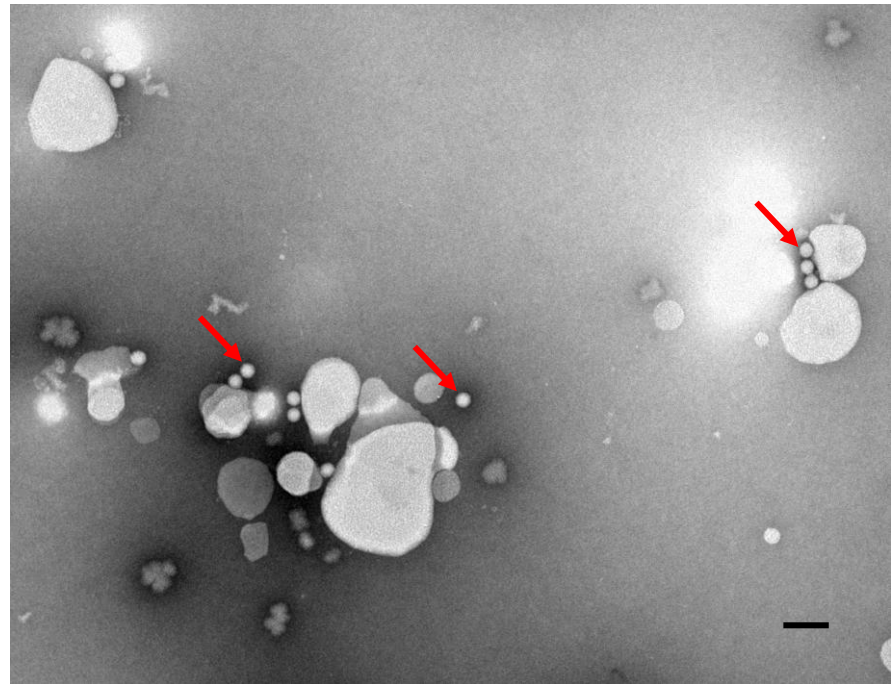
HRV2 uncoating in lipofectosomes upon pH lowering; Nothing was known about HRV2 uncoating on model cells. Only vague protocols existed on *in-vitro* generation of 135S particles upon pH lowering (Prchla *et al.*, 1994). These protocols were modified and used to monitor uncoating in lipofectosomes. Therefore, receptor decorated liposomes were floated as described before and subsequently incubated with HRV2 to produce lipofectosomes. Again 19 μ L of the flotation fraction were incubated with 1 μ L of HRV2 [12.6 nM]. The resulting lipofectosomes hold thus a virus concentration of about 0.63 nM. Next, this sample was acidified with 1 M sodium acetate pH 5.4 to achieve a pH of about 5.4. Aliquots of the acidified sample were taken at particular time points after pH drop and applied on TEM grids for negative staining. Grid adsorption and staining procedure captures and holds lipofectosomes at different stages of uncoating. Figure 19 shows the images for the sample prior to acidification (Figure 19 A), immediately after acidification (< 30sec, Figure 19 B), after 2 minutes (Figure 19 C) and 15 minutes (Figure 19 D), respectively. Before pH lowering (Figure 19 A), infectious 150S particles are attached to the liposome membrane via receptor mediation. Immediately after acidification of this sample, the virus started converting (Figure 19 B). Occasionally, 150S particles were still detected and few 80S particles were already found. However, most of the virions were not classifiable to either of those. Apparently, the intermediate stage of sub-viral particle was again detected (intermediate I, yellow arrow). In contrast to 80S particles, it retained some internal density. Thus it appeared dark in its center but held still bright pattern inside. This indicated that RNA was not completely released from the capsid. Furthermore, upon 2 minutes of acidification (Figure 19 C), all virions have been converted, hence no 150S particles were detectable anymore. In addition to the 80S particles, and the just mentioned intermediate I, a further intermediate stage appeared at this time point (intermediate II, green arrow). Characteristic for this intermediate was a dense rod-like structure inside the capsid. Apparently, both intermediate particles were seen at specific time points upon acidification and could be distinguished by an unambiguous pattern of the capsid. After incubation for 15 minutes at low pH (Figure 19 D), almost all viral and sub-viral particles reached the final point of conversion, the 80S particle.

This experiment determined different time depending stages of viral conversion during pH lowering. At least 2 intermediate particles were resolved. Concerning the genome transfer, it was shown that entire RNA content was released from the viral capsids after incubation of the lipofectosome for 15 minutes at pH ~5.4. Here, almost exclusively 80S particles were detected. Therefore, pH lowering can be considered a very effective way to trigger uncoating of HRV2 in the context of lipofectosomes. Moreover, this technique certainly resolves more intermediate viral stages than heat-treatment, which apparently works too rapidly to do so. Proper uncoating is the prerequisite for genome transfer. This is why the pH treatment will be employed for the following experiments using RT-lipofectosomes to detect the ingress of RNA in the nano-container.

(A) No pH lowering





Arrow key:

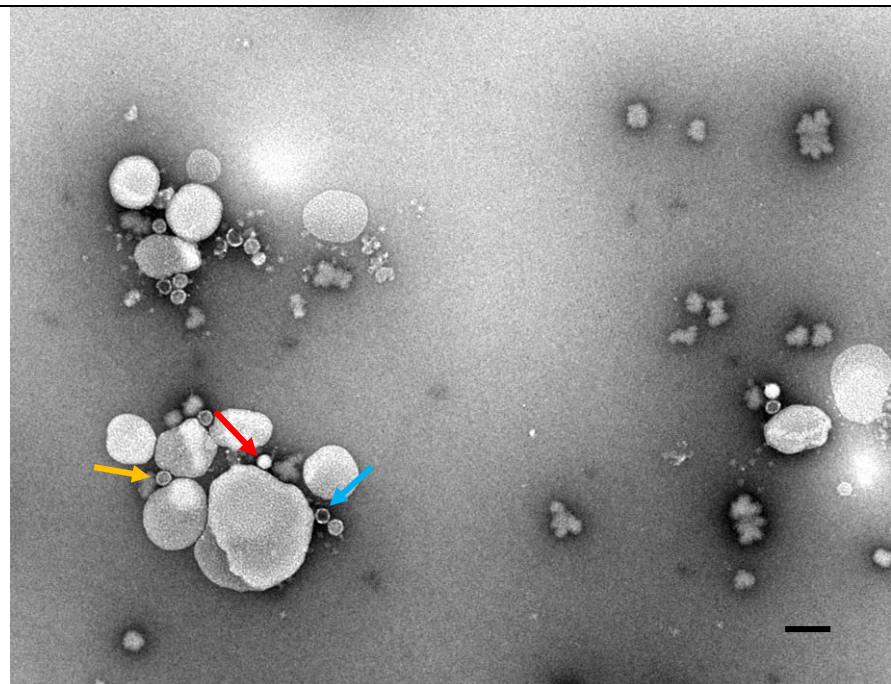
-  native (150S)
-  intermediate I (135S ?)
-  intermediate II -rod structure- (135S ?)
-  empty (80S)



(B) <30 sec / pH 5.4





Arrow key:

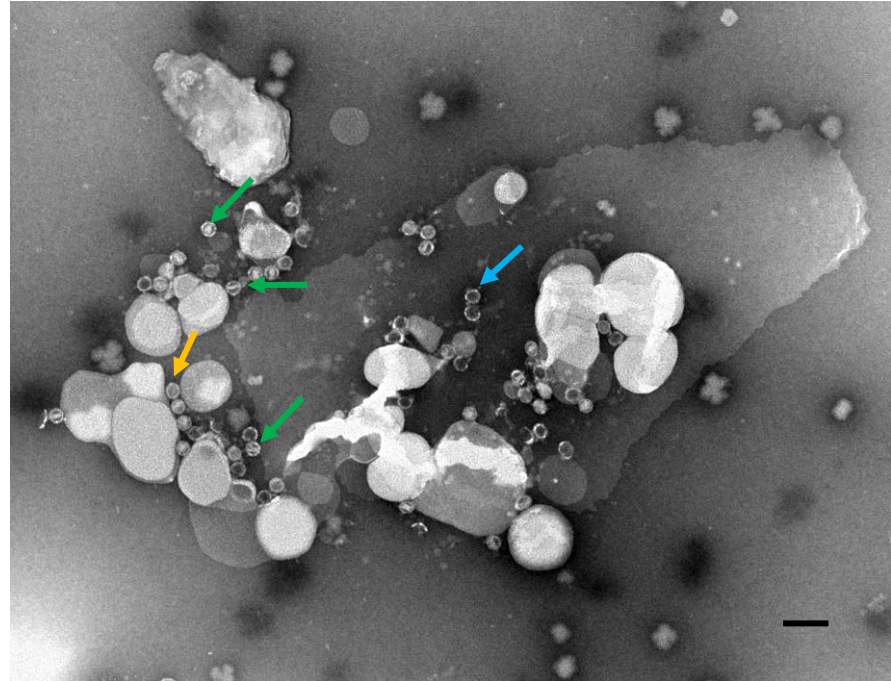
-  native (150S)
-  intermediate I (135S ?)
-  intermediate II -rod structure- (135S ?)
-  empty (80S)



(C) 2 min / pH 5.4





Arrow key:

-  native (150S)
-  intermediate I (135S ?)
-  intermediate II -rod structure- (135S ?)
-  empty (80S)



(D) 15 min / pH 5.4

Arrow key:

-  native (150S)
-  intermediate I (135S ?)
-  intermediate II -rod structure- (135S ?)
-  empty (80S)

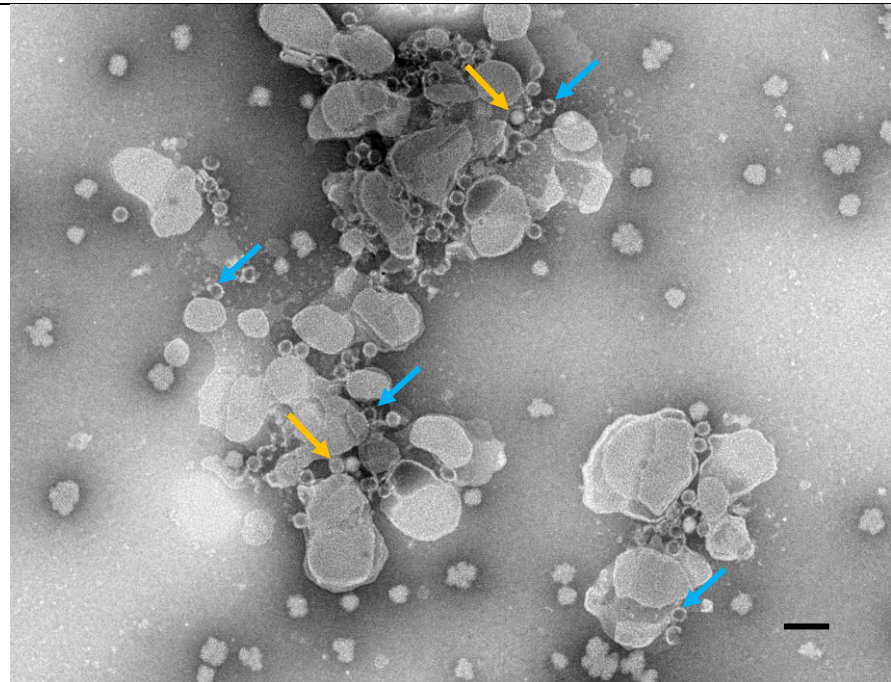


Figure 19: Time series of lipofectosomes incubated at low pH and visualized via negative stain TEM. Lipofectosomes (A) were formed and subsequently incubated at pH 5.4 for <30 sec (B), 2 min (C), and 15 min (D), respectively. pH was adjusted with 1 M sodium acetate pH 5.4 . Lipofectosomes were prepared in the presence of 0.63 nM HRV2. Arrows indicate the converting stage of virions (color code is given by the arrow key at the left-hand side of each picture); sample staining as in Figure 17; images were taken at a 5.6×10^4 fold magnification; size bar = 100 nm.

5.3 Genome Transfer

5.3.1 RT – Lipofectosomes: in-vitro detection of RNA transfer

To detect the genome of HRV upon being transferred into liposomes, the hydration buffer for MLV preparation was completed with a reverse transcription (RT) kit. Upon purification of the resulting liposomes, the RT-kit worked only in their interior. This means that the outer buffer was exchanged by a buffer not suited for RT. As target for RT and PCR, a 923bp long region at the 3' end of the genome of HRV2 was chosen. In this area, a loop was found within the secondary structure of the RNA where primer molecules easily bind. The detection of this amplicon inside the liposomal nano-container by an RT-PCR assay is the proof for genome transfer through membranes using minimal requirements.

The current section contains several figures, demonstrating images from agarose gels. For the sake of clarity and simplicity, several images have been rearranged by leaving out redundant or irrelevant lanes. However, one figure represents always one gel only and its original numbering is written on the very top of each gel image. Further, a blue stripe has been added to the marker lane at the beginning of each gel to highlight its 1kb band.

Testing robustness of the RT enzyme for liposome encapsulation; To ensure that the RT kit still works efficiently after being encapsulated in liposomes, conditions as for MLV preparation were simulated. 1 μ L HRV2 [~ 620 nM $\equiv \sim 5$ mg HRV2 /mL] was mixed with 19 μ L of the RT kit, resulting in viral concentration of ~ 31 nM, and incubated at ambient temperature for at least two hours. Frequently, the incubation was interrupted for vigorous vortexing. Even under these harsh conditions, it turned out that the expected amplicon was detectable. The gel from Figure 20 confirms that the RT-kit was indeed able to endure the conditions for liposome preparation. Clear bands can be detected upon incubation of the RT-reaction mixture with HRV2. Lane 2 shows the signal after incubation of RT for two hours and vigorous vortex treatment. The sample on lane 3 contained additionally 0.5 % Triton X100 to simulate conditions for cDNA template recovery by vesicle disruption. Both samples were incubated in the presence of liposomes, to mimic the lipid matrix.

Validation of the RT-PCR system; The limit of detection for the HRV2 concentration was estimated. 1 μ L HRV2 of concentrated virus stock [~ 620 nM], a dilution 1:200 and 1:2500, respectively, were mixed with 19 μ L of the RT-Mix. Moreover, it was tested whether RT can be inhibited by buffer exchange using mSEC. This would show if non-encapsulated RT-kit can be separated from RT-liposomes by gel filtration.

Lane 1 to 3 in Figure 21 show three dilution steps of HRV2. Upon mixing with the RT-kit the virus concentration in the system corresponded to 31 nM (conc.), 0.15 nM (1:200) and 0.012 nM (1:2500). The dilution 1:200 rendered still an obvious band, whereas the dilution of 1:2500 was under the detection limit. Further, lane 4 shows the effect of mSEC purification prior to RT. For that purpose, the RT mixture, consisting of RT, primer and dNTPs, was applied on a G50-mSEC, and its filtrate was incubated with undiluted HRV2. Since no signal is visible in this lane, it can be concluded that mSEC inhibits the reaction completely. Most probably, it was stopped due to buffer exchange and retardation of components of the RT-kit. On the one hand, these findings confirmed the sensitivity of the method; on the other hand they demonstrated an effective way to purify RT-liposomes from non-encapsulated RT material. A proper purification is essential to avoid any background noise, and to stress that positive signals need leak-tight nano-containers.

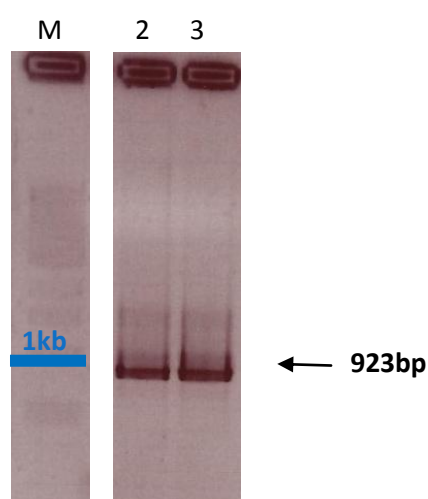


Figure 20: RT-PCR of a 923bp region of HRV2 under conditions similar to MLV-preparations. HRV2 conc. in RT system: ~31 nM

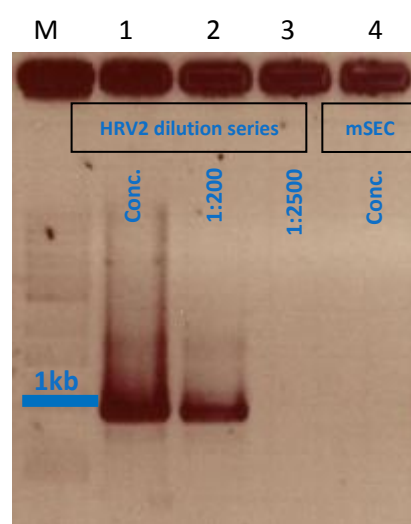


Figure 21: Dilution series of HRV2 to estimate the limit of detection for virus in the RT-PCR assay. HRV2 conc. in RT system: 1: concentrated [31 nM], 2: 1:200 [0.15 nM], 3: 1:2500 [0.012 nM].

Encapsulation of the RT-kit inside of liposomes; since the RT-kit appeared to be very robust in terms of temperature and mechanic stress, it was encapsulated. For this purpose, a lipid film, consisting of POPC:PE:SM:Ch:DOGS-NTA:NBD-PC = 1:1:1:1.5:0.5:0.05 (molar ratio as used for lipofectosomes), was produced and hydrated with buffer containing the RT-kit. Beside the commercial kit components, the kit contained a reverse primer, which annealed at the 3' end of the HRV2 genome. It produces a cDNA template, which, in turn, had to serve as template for a PCR amplicon of about 923 bp; with a resulting DNA band as shown in the gels above.

TEM: Visualization of RT-liposomes upon mSEC purification; As mentioned above, mSEC was perfectly suited to separate non-encapsulated RT-kit from the RT-liposomes. However, nothing definite was known about the appearance, concentration and stage of aggregation of the vesicles upon mSEC purification. To check these issues, TEM images were taken of RT-liposomes before (Figure 22, A+B) and after mSEC (Figure 22, a+b). As shown in Figure 22 the liposomal appearance did not change upon purification. They still appear as homogeneous vesicles and did not tend to aggregate. A closer look on the RT-liposomes at 5.6×10^4 fold magnification confirms that their appearance had not changed; compare images before (Figure 22B) and after mSEC (Figure 22b). Only the vesicle concentration was significantly reduced upon purification. The overview images taken at 1.8×10^4 fold magnification show this reduction (compare Figure 22A + a) which is expected due to dilution after mSEC subjection. The extent of dilution is usual for this procedure and vesicle rupture can be excluded. Therefore, one can assume that the nano-container was not damaged in the course of its purification. This is an important prerequisite for correct function of the RT-assay using lipofectosomes.

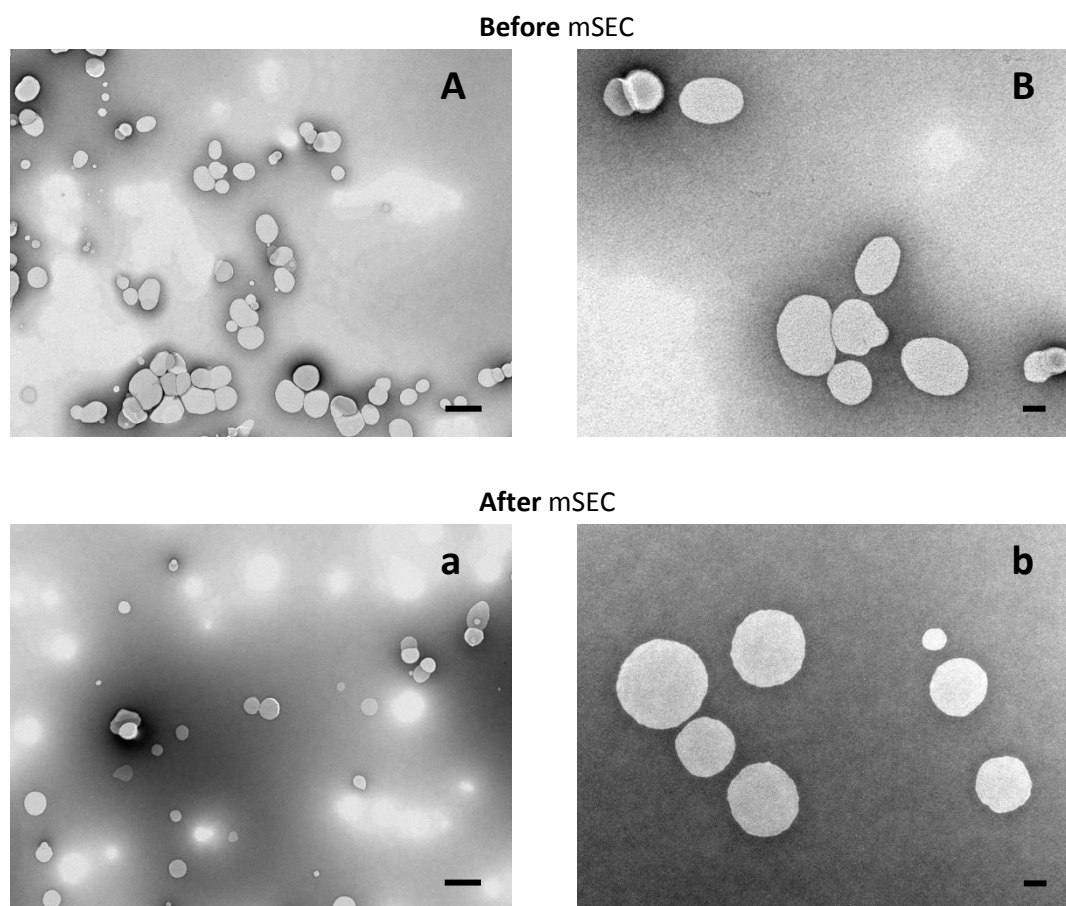


Figure 22: Negative stain images of freshly prepared RT-liposomes before (A+B) and after mSEC purification (a+b). Images were taken at a 1.8×10^4 (A+a) and 5.6×10^4 (B+b) fold magnification. Size bars = 500 nm (left-hand panels) and 100 nm (right-hand panels), respectively. LUVs were diluted 1:20 before applying them on the grid; sample staining as in Figure 17.

Heat-trigger on lipofectosomes; Liposomes were purified from non encapsulated RT by mSEC. Subsequently, the membrane was decorated with V33333 prior to incubation with HRV2. Infection of the so formed lipofectosomes was triggered via incubation at 56°C for 10 minutes. The resulting band at about 923 bp on lane 1 of Figure 23 demonstrated the RNA transfer into the lumen of the vesicle and thus confirmed the suitability of the method. If V33333 was not added to the mixture (lane 3), the band is still visible but certainly weaker. By comparing lane 1 and 3 it is obvious that the receptor plays an important role for correct transport of RNA. The remaining signal in lane 3 can be explained by the presence of 135S particles. These hydrophobic particles can attach to membranes in the absence of receptor and thus do not need receptor mediation (Lonberg-Holm *et al.*, 1976). To confirm the need of a leak-tight nano-container and infectious virus particles, respectively, two controls were added. First, the lipofectosome was disintegrated before triggering RNA transfer. In lane 5 of the same figure, no band was detected, because membrane integrity has been affected by adding 1% of Triton X100; thus no RT was carried out. 1% TX had no affect on the RT reaction *per-se* (data not shown). Second, the gel gives a good control for the need of infectious particles in this assay. The sample in lane 6 used 80S particles instead of 150S. Again, no signal can be detected. However, in this case the virion, lacking its genome inside the capsid, was responsible for the failed signal, rather than the consistency of the nano-container. It is of note that viral RNA was still present from 80S preparation but was not capable of entering the nano-container. These findings suggest that only infectious material, where RNA is still primed for its transfer in the capsid, can finally overcome the membrane.

Triggering genome transfer by heating and pH-lowering showed differences in efficiency of infection; An efficient and useful way to release RNA from virus in solution can be initialized by heating a diluted virus sample up to 56°C for 10 minutes; concentrated virus samples do not release their genome under these conditions (unpublished data). However, this technique is very artificial and does not represent the natural way, where virus faces pH lowering within endosomal compartments. Therefore, it was of interest how these two strategies of virus conversion, differ in their efficiency to deliver the genome properly through the membrane. TEM experiments (see previous section) suggested already more efficient transport upon pH lowering. The signals, shown in Figure 24, stressed again this difference in transport efficiency. Here the lanes 1 – 3 corresponded to a genome transfer in lipofectosomes triggered by no-trigger, heat- and low pH-treatment, respectively. Apparently, also without trigger several RNA genomes were transferred (lane 1). This effect can be explained by stimulated “viral breathing” at 37°C during RT. “Viral breathing” describes a dynamic change in the viral capsid. For Rhinovirus this phenomenon allowed digest of the inner

VP4 protein by exposing it transiently on the virus surface (Lewis *et al.*, 1998). In the absence of pH lowering the membrane decorated receptor keeps holding virus in proximity to the membrane of the nano-container. Dynamic changes in the capsid could thus insert transiently exposed hydrophobic domains of the virus into the membrane. This hydrophobic attachment is suggested to catalyze the RNA transfer even without proper trigger and results in a background signal. However, by using heat triggering the signal appeared significantly stronger (lane 2). The strongest signal was obtained after triggering the transfer by pH lowering (lane 3). The actual conditions for pH lowering, pH 5.4 for 15 minutes at ambient temperature, were shown by TEM to be very efficient to uncoat the virion; see TEM section. In TEM, it was not possible to trace the route of the RNA after its release. Now, RT-PCR confirmed that the genome was indeed transferred through the membrane upon release from the capsid.

Besides a very efficient way to uncoat HRV2 in lipofectosomes, pH lowering served as further indication for pore formation. As mentioned above, the RT needs a particular buffer milieu for its proper function. By changing the outer buffer composition, the RT buffer inside the nano-container should not be affected. In the presence of HRV2, however, after pH lowering RT reaction was inhibited; data not shown. Complete disintegration of the liposomes can be excluded, because upon re-neutralization with a sodium hydroxide solution [500 mM] of the whole mixture, as performed for the presented data, the activity of the enzyme was recovered. These findings suggest again the formation of a pore, which allows passage for polar molecules or protons.

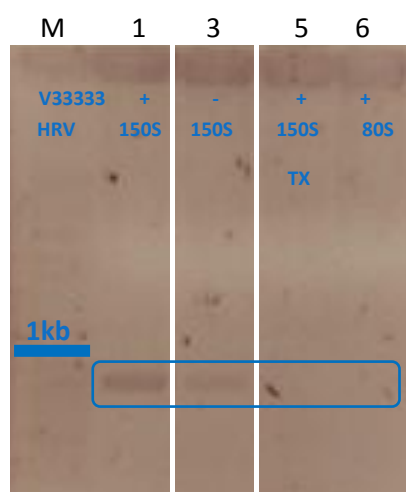


Figure 23: Heat-triggered RNA transfer of lipofectosomes and liposome/virus mixtures.

Incubation of lipofectosomes at 56°C for 10 minutes transferred viral genomes from the capsid into the liposomal compartment (lane 1). Significantly less RNA was transported if no receptor kept the virus on the membrane (lane 3). Disintegrated nano-containers were not able to carry out RT at all (lane 5). Non-infectious particles, such as 80S, could not transport their released RNA in the liposomal compartment (lane 6). Lipofectosomes were prepared in the presence of 33 nM HRV2, TX: Triton X100 [1%], V33333: Receptor construct, 150S: native virus, 80S: empty capsid;

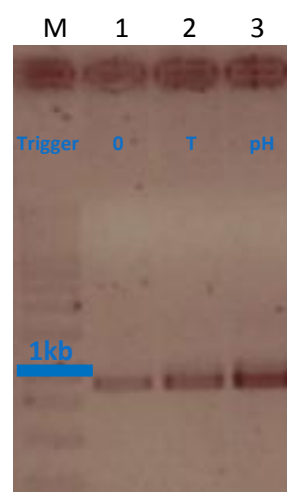


Figure 24: RT-PCR of lipofectosomes upon triggering infection by either heat-treatment or pH-lowering.

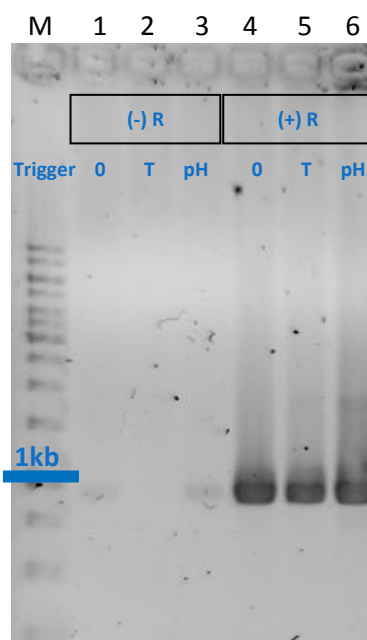
No trigger for uncoating gave a weak signal (lane 1), whereas heating at 56°C for 10 minutes (lane 2) resulted in a significant higher signal. The strongest signal, was obtained by pH lowering (lane 3); Lipofectosomes were prepared in the presence of 33 nM HRV2, 0: no trigger, T: heat treatment (56°C/10min), pH: pH-treatment (pH ~5.4 / 15 minutes / re-neutralization)

Importance of receptor-mediation for RNA transfer; As already indicated in Figure 23, the decoration of the liposomal membrane with receptors significantly increased the genome transfer presumably by binding more viral particles in proximity of liposomes. To estimate the effect of the receptor in more detail, two assays were performed: one with bare RT-liposomes without receptor decoration, and the other with V33333-decorated liposomes. Both were incubated with HRV2. The following bands in Figure 25 confirmed the need of receptors for an efficient genome transfer into the liposomal nano-container. The respective trigger (temperature, pH) showed here a negligible contribution to the resulting signal. For the first three lanes, the mixture lacked receptors molecules. Sample in lane 1 was not triggered, whereas samples from lane 2 and 3 were triggered by heat and pH-lowering, respectively. Despite applying the appropriate triggers, this series did not give clear bands due to the lack of receptor decoration. With the same sequence of triggering, lane 4, 5 and 6, showed the expected bands by using receptor-decorated RT-liposomes. Apparently, receptor-decoration is necessary for proper genome transfer *in-vitro*. This would mean that immediately before virus conversion starts, virions need the proximity to the membrane, to release the genome correctly. For unknown reasons, the intensity of the signal in this experiment could not be correlated with the respective trigger; all signals reached the saturation. One has to be aware of the fact that

regular PCR systems are not suited for proper quantification in a subtle concentration range. Although keeping all parameters constant (e.g.: cycles of amplification, concentrations of components, etc.) the final signals varied always slightly in intensity; data not shown.

Figure 25: Comparison of bare and receptor decorated RT-liposomes upon RT-PCR with focus on their efficiency of genome transfer.

Liposomes lacking receptor molecules on their surface, where not capable of transferring the RNA properly (lane 1-3). Only assemblies, containing receptor molecules showed a significant signal after RT-PCR (lane 4-6). Lipofectosomes were prepared in the presence of 33 nM HRV2, R: receptor (V33333), 0: no trigger, T: heat treatment (56°C / 10 minutes), pH: pH treatment (pH ~5.4 / 15 minutes / re-neutralization)



Formation of lipofectosomes with a dilution-series of HRV2; A rough estimation of the limit of detection to reaffirm the presence of HRV2 RNA was shown above. However, that assay used only HRV, and the virion was not engaged by receptor-decorated liposomes. As described in the last paragraphs, released RNA can be detected upon its ingress in the liposomal compartment. This meant a change in the methodology and thus it was of interest whether the limit of detection had changed. If not using nano-containers, even viral RNA, not being transferred through the membrane gives a signal. It is thus expected that higher virus concentrations are required for signal detection.

The gel from Figure 26 used lipofectosomes prepared in the presence of different virus concentrations. It shows a stepwise reduction of the DNA signal, depending on virus concentration in the system. Virus dilutions of 1:100 [~ 0.33 nM] and 1:1000 [~ 0.033 nM] were still detectable, whereas those of 1:10.000 [~ 0.0035 nM] and 1:50.000 [~ 0.0005 nM] were not; nM values correspond to virus concentration present while forming the lipofectosome. For the latter dilutions, a slight signal was detected for the expected 923 bp band. However, also negative controls, for instance upon TX treatment for testing the need of a leak tight nano-container, showed occasionally such weak signals (compare lane 13 in Figure 26). Therefore, signals of this extent have always been considered background noise and have never been considered RNA transfer. Since regular PCR does not work for subtle quantification of DNA templates, it is difficult to judge whether the use of lipofectosomes resulted also in a profit for the limit of detection. However, it was confirmed that it

did not result in a significant loss of sensitivity. Moreover, the main goal of this method, using nano-container, was not the achievement of better sensitivity but better selectivity for RNA transferred by infectious virus.

Based on the idea that a pore must be formed through the leak-tight nano-container, in order to form a gate for a hydrophilic RNA molecule, two negative controls have been designed, and are also shown in Figure 26. The putative pore must possess a particular diameter to carry out genome transfer. The extent of this diameter can roughly be estimated, with regard to data presented by (Brabec *et al.*, 2005). The group compared leakage of two dyes, which only differed in their size (10 and 70kDa FITC dextran), from an endosomal compartment to the cytosol. Only the small dye (10kDa) was able to migrate to the cytosol upon co-internalization with HRV2. Considering the hydrodynamic diameter of this dye molecule, the putative pore must possess a diameter in the range of 10 to 39 Å; see Figure 6. Therefore, a small enzyme, such as the 14 kDa RNase A, could readily pass this gate, as well. Lane 12 of Figure 26 shows a control, where lipofectosomes, which were already tested to give a clear positive signal (HRV2 dilution of 1:100; compare lane 2), were exposed to 50 µg/mL RNase A during heat-triggering and RT. As a result of this incubation, no signal was detectable anymore. The RNA genome has been degraded, either inside the capsid, on its route through the pore or within the liposome. This finding is in agreement with the theory of pore formation upon viral conversion to transfer the RNA (Hewat & Blaas, 2006; Prchla *et al.*, 1995).

To confirm the proper function of RNase A in the given RT environment, two HRV2 samples were diluted in RT-mix to obtain a concentration of 0.33 nM as used for lipofectosomes. During heat-triggering and subjection to RT-PCR, one of these samples was treated with RNase A [50 µg/mL]. Lane 11 in Figure 27 shows the 923 bp band, which corresponds well to the applied HRV2 concentration. The same sample, but incubated with RNase A (lane 12), did not give any signal. In this attempt, RNA was clearly degraded, where RNase A was added. Even the presence of the RNase-inhibitor could not avoid the degradation.

The second control in this context emphasized again the need of a leak-tight nano-container. For that reason, a tested lipofectosome (prepared in presence of 0.33 nM HRV2) was treated with 1% Triton X100, prior to heat triggering. The detergent had certainly a negative effect on membrane integrity. Lane 13 (Figure 26) gives the remaining and very weak signal of this control. If compared to lane 2 the major part of the signal is lost due to destabilization of the nano-container. This demonstrates once more that reverse transcription only works inside the liposomal compartment, in its favorable buffer conditions.

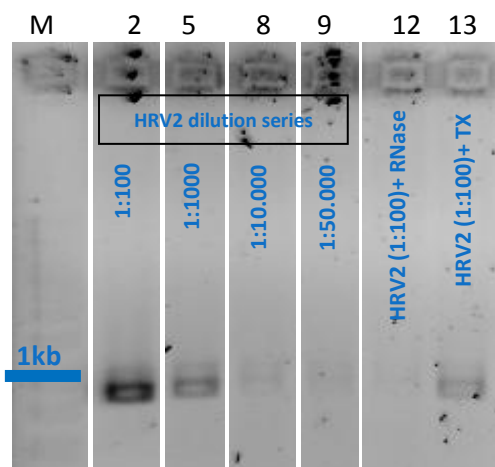


Figure 26: Concentration of applied HRV2 correlates with the intensity of a lipofectosome-derived RT-PCR signal.

Lipofectosomes were prepared in the presence of 0.33 nM (1:100), 0.033 nM (1:1000), 0.0035 nM (1:10.000) and 0.0005 nM (1:50.000) HRV2; Trigger: 56°C for 10 minutes; RNase A in the mixture: 50 µg/mL (applied upon formation of the lipofectosome); Triton X100 (TX): 1% ;

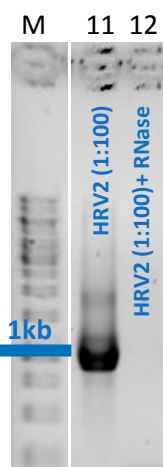


Figure 27: Inhibition of RT-PCR by degradation of the viral genome with RNase A.

HRV2 concentration: 0.33 nM; RNase A: 50µg/mL;

Whether or not a pore has formed in the course of minor group HRV infection is still a crucial question. A certain answer to this question could give new insights into the mechanism of infection of non-enveloped viruses. As demonstrated above, RNase A interferes with the RT system by degrading the RNA genome. To do so, the enzyme has entered either the nano-containers or the viral capsid via pores. Therefore, the experiments around RT-PCR of lipofectosomes in the presence of RNase A must be examined in more detail. To test these *in-vitro* findings and to confirm their biological relevance, it was endeavored to transfer and repeat the experiments in a cell culture system. Hence, the next section describes HRV2 infection of HeLa cells from the plasma membrane, using native receptor and membrane composition, and its inhibition upon RNase A treatment.

5.3.2 HeLa system: Confirmation of RNase A dependent reduction of HRV2 infection. (eIF4G1 cleavage assay)

To confirm whether the findings from the *in-vitro* experiments can keep validity in a tissue culture approach, the experimental setup was transferred into a living cell system. By using a protocol to infect HeLa cells from plasma membranes, one can easily manipulate parameters of infection. In this approach infection occurs artificially on the cell surface and virions are not internalized into endosomes (Berka *et al.*, 2009; Brabec *et al.*, 2003). By changing buffer conditions to lower pH values, infection can be triggered similar to the *in-vitro* manipulation on lipofectosomes. This protocol was used to correlate the presence of RNase A with the infection capacity of HRV2 on HeLa cells.

HeLa cells were incubated with HRV2 [MOI 30] in the presence of 40 nM bafilomycin to inhibit infection via endosomal routes. The pH of the medium was changed to pH 5.2 to trigger infection from the plasma membrane. Additionally, a further sample also changed to pH 5.2, contained RNase A [2mg/mL] in order to reduce infection on cells.

Western blot applying antibodies against eIF4G1, a marker for early infection (Pain, 1996), was used to detect the extent of infection in these cells. Since cleaved eIF4G1 protein is a clear proof for early infection, cells were harvested after incubation for only 5 hours at 34°C. As can be seen from the Figure 28, the controls (+ / -) worked as expected. The absence of bafilomycin led to regular infection of the cells (lane 1 and 2; cleaved product). However, infection was completely stopped in the presence of bafilomycin, as demonstrated in lane 3 only uncleaved product is detectable. Upon changing the pH to 5.2, still in the presence of bafilomycin, cleaved eIF4G1 can again be detected (lane 4). In other words, infection from the plasma membrane has occurred. This signal, in turn, is reduced after incubation with RNase A (lane 5).

For sake of quantitation the films were scanned and the intensity of the signals of cleaved product was quantified, using *ImageJ*. The diagram in Figure 29 shows the resulting values of film darkening for the three samples of interest. A detailed overview of the respective treatment of each sample is given in the corresponding table at the lower end of the figure. Figure 29 demonstrates in more detail that the presence of bafilomycin inhibited infection from plasma membranes almost completely (1. Column = 3. Lane). As soon as exposed to low pH, infection was restored (2. Column = 4. Lane). However, infection, directly from the plasma membrane, can be effectively inhibited by addition of RNase A (3. Column = 5. Lane), reducing eIF4G1 cleavage to values of the bafilomycin value (1. Column = 3. Lane).

The presented data from HeLa experiments support clearly the *in-vitro* findings using lipofectosomes. Both systems detected a significant decrease in HRV2 infection upon treatment with RNase A. This data is in agreement with the postulation of pore-formation during minor group HRV infection. Indeed, it is very likely that a pore, generated for genome transfer, allows also small proteins, such as RNases, to pass the membrane. Thus the RNase A could readily pursue the RNA genome on its way from the capsid into the cytosol and into the interior of an artificial nano-container, respectively. Upon ingress in the new compartment, it is very likely that the RNase degrades the genome and thus inhibits infection. However, additional data is required to exclude RNA digest prior to its release from the capsid. Moreover, future experiments should also aim at assessing the persistence of the putative pore.

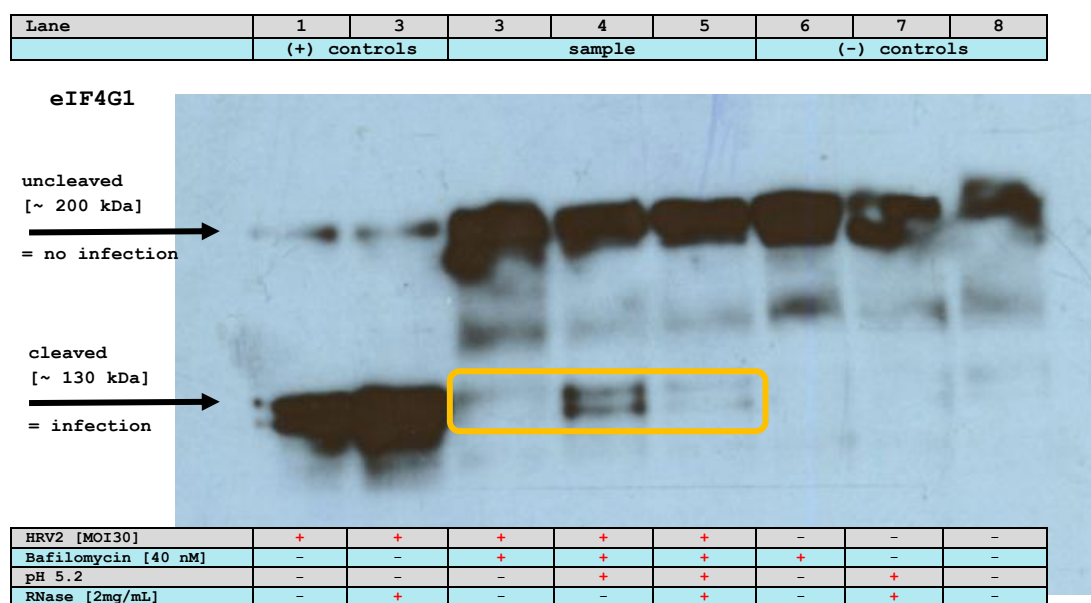


Figure 28: Western Blot of eIF4G1 - Assessment of HRV2 infection from the plasma-membrane upon treatment with RNase A.

Uncleaved eIF4G1 possesses a size of ~200 kDa. In the course of infection it is cleaved by the viral protease 2A^{pro} (Liebig *et al.*, 2002) to a fragment of ~130 kDa. Upon infection with HRV2, normally the cleaved protein is the predominant species and indicates infection (lane 1 + 2). Non-infected HeLa cells possess only uncleaved protein (lane 6-8). In the presence of bafilomycin, HRV2 cannot infect the cells via endosomal routes and thus no cleavage product can be seen (lane 3). However, infection can be induced from the plasma membrane by pH lowering (lane 4). Upon incubation with RNase A, infection from the plasma membrane was reduced (lane 5). HRV2: MOI 30, representative result from two independent experiments is shown.

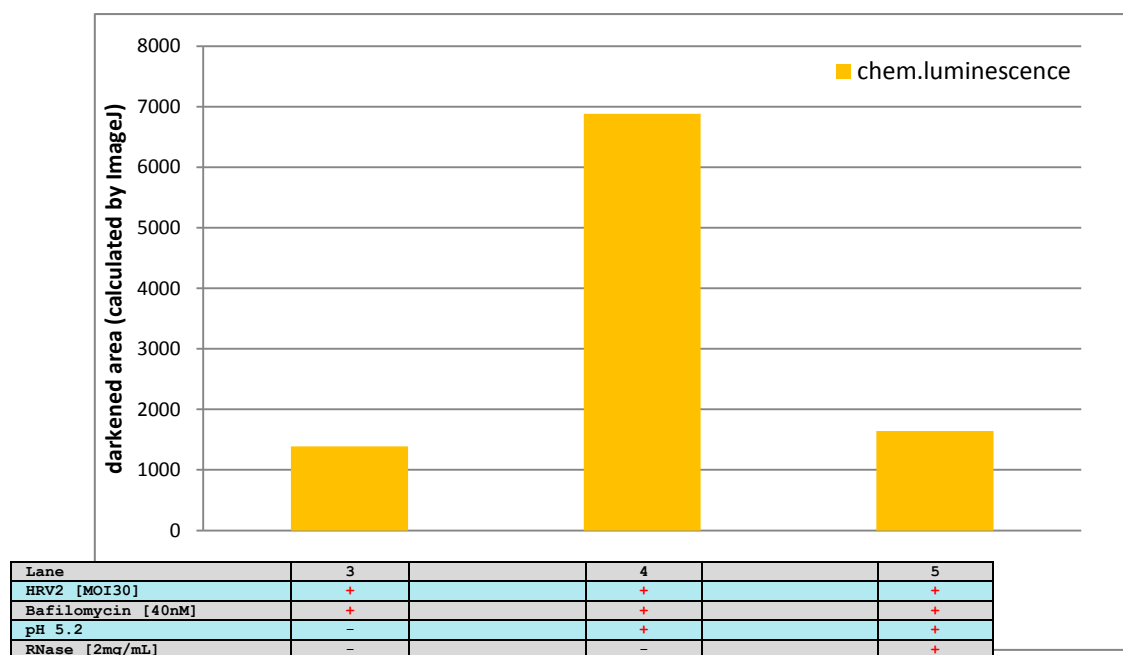


Figure 29: Quantitative assessment of infection from the plasma membrane by eIF4G1 cleavage assay. The bars correspond to the intensity of darkening of the Western blot film, shown in Figure 28. Representative result from two independent experiments is shown.

6 Summary

The actual infection process of minor group human Rhinoviruses takes place on the endosomal membrane. Driven by acidic pH, uncoating of the virion is initialized and the viral genome reaches the cytosol of the host cell. How this actual transfer of the genome - a RNA molecule of about 7 kb - operates is not yet clear. It is widely believed that a pore, consisting of viral proteins, must be formed to transport the hydrophilic RNA through the amphipathic bilayer. However, the building blocks of this putative pore are not known. Also, whether its components were only of viral origin or additional host factors were needed to carry out proper genome transfer, was left unanswered since long.

This work endeavored thus to generate an appropriate model system in order to elucidate the minimal requirements for the correct transport of the genome. For this purpose, an *in-vitro* system was successively equipped with components, which seemed likely to be involved in this transport mechanism. To mimic the surface of a human cell, liposomes were prepared and decorated with receptors onto their outer leaflets using a complex bond. As a representative of the minor group of human Rhinoviruses, HRV2 was bound via its receptors to this liposomal compartment. The resulting construct was called a lipofectosome and was used to render a minimal system for genome transfer.

Different liposome batches were characterized to choose for preparation techniques suitable for further experimental approaches. Their characterization focused on the lipid concentration and the vesicle diameter, which were assessed via determination of total phosphorus content and dynamic light scattering, respectively. The correct formation of lipofectosomes was monitored by electrophoretic means, such as capillary- and chip-electrophoresis, and confirmed by transmission electron microscopy. Moreover, the latter technique was used to examine conditions for complete and reproducible viral uncoating. Finally, a reverse transcription kit was encapsulated inside the liposomal compartment. These vesicles served as nano-container to generate a DNA template of the viral genome. Using this method the ingress of the viral genome from the liposome surface was detected upon triggering uncoating from the outside of the liposomal vesicle.

The resulting data confirmed the successful transfer of viral RNA from the virion to the liposomal compartment within a lipofectosome. Moreover, the data allows to derive several conclusions from the minimal system requirements and to apply them to the natural situation in living cells. First, the system needs to keep the virus in vicinity to the membrane while triggering infection, to transport the genome. This model used a recombinant receptor to do so. This receptor construct consisted only of binding repeats for targeting the viral capsid and lacked most of its natural building parts. Also its transmembrane domain and cytoplasmatic region were not present in

the construct and thus do not seem to be required for the genome transport. Besides membrane and receptor, host factors, such as additional membrane or cytoplasmatic proteins, can be considered not being involved in this process, as genome transfer occurs in their absence. Moreover, the results demonstrated that not only the native trigger of uncoating can cause the genome to migrate through the membrane. Indeed, a very synthetic stimulus, the heating of virions at 56°C for 10 minutes, which was only known to release RNA, was also capable of transferring it properly. Apparently, the proper trigger, such as the mimicry of endosomal pH conditions, is of minor importance to carry out genome transfer. Upon providing the viral capsid with enough energy to leave its meta-stable stage, the resulting uncoating process and pore-formation proceeds independently of the environment.

For future perspectives, a so far untouched criterion for the minimal system of RNA transport is the membrane composition. In this regard, the contribution of lipid rafts needs to be examined. One could easily test this criterion by the RT-assay invented here but employing different lipid compositions for the liposomal nano-container. Further, the proposed pore needs to be confirmed and described in more detail. For instance, leakage data could offer information about the persistence of a formed pore. Moreover, detailed data on the structure of a putative pore complex could be obtained via visualization of lipofectosomes by high resolution means. Such data can provide a base for image-reconstruction. First attempts with cryo electron microscopy looked very promising. In turn, the knowledge about the persistence and the structural assembly of such a pore complex will provide supplementary information about the early steps in the infection process of non-enveloped viruses.

7 References

- Adam, G., Luger, P. & Stark, G. (2003). Physikalische Chemie und Biophysik - 4. Auflage. Springer.
- Airaksinen, A., Somerharju, P. & Hovi, T. (2001). Variation in Liposome Binding among Enteroviruses. *Virology* **279**, 539-545.
- Alberts, B., Johnson, A., Lewis, J., Raff, M., Roberts, K. & Walter, P. (2002). Molecular Biology of The Cell, 4th edition. *GS Garland Science*, 589-622.
- AvantiPolarLipids_Inc. (2009). <http://www.avantilipids.com>.
- Berka, U., Khan, A., Blaas, D. & Fuchs, R. (2009). Human rhinovirus type 2 uncoating at the plasma membrane is not affected by a pH gradient but is affected by the membrane potential. *J Virol* **83**, 3778-3787.
- Bilek, G., Kremser, L., Blaas, D. & Kenndler, E. (2006a). Analysis of liposomes by capillary electrophoresis and their use as carrier in electrokinetic chromatography. *J Chromatogr B Analyt Technol Biomed Life Sci* **841**, 38-51.
- Bilek, G., Kremser, L., Blaas, D. & Kenndler, E. (2006b). Capillary electrophoresis of liposomes functionalized for protein binding. *Electrophoresis* **27**, 3999-4007.
- Bilek, G., Kremser, L., Wruss, J., Blaas, D. & Kenndler, E. (2007). Mimicking early events of virus infection: capillary electrophoretic analysis of virus attachment to receptor-decorated liposomes. *Anal Chem* **79**, 1620-1625.
- Bilek, G., Weiss, V. U., Pickl-Herk, A., Blaas, D. & Kenndler, E. (2009). Chip electrophoretic characterization of liposomes with biological lipid composition: Coming closer to a model for viral infection *Electrophoresis*, submitted.
- Brabec, M., Baravalle, G., Blaas, D. & Fuchs, R. (2003). Conformational changes, plasma membrane penetration, and infection by human rhinovirus type 2: role of receptors and low pH. *J Virol* **77**, 5370-5377.
- Brabec, M., Schober, D., Wagner, E., Bayer, N., Murphy, R. F., Blaas, D. & Fuchs, R. (2005). Opening of size-selective pores in endosomes during human rhinovirus serotype 2 in vivo uncoating monitored by single-organelle flow analysis. *J Virol* **79**, 1008-1016.
- Bretscher, M. S. (1985). The molecules of the cell membrane. *Scientific American* **253**, 86-90.
- Bubeck, D., Filman, D. J. & Hogle, J. M. (2005). Cryo-electron microscopy reconstruction of poliovirus-receptor-membrane complex. *nature structure & molecular biology*.
- Chow, M., Newman, J. F., Filman, D., Hogle, J. M., Rowlands, D. J. & Brown, F. (1987). Myristylation of picornavirus capsid protein VP4 and its structural significance. *Nature* **327**, 482-486.
- Danthi, P., Tosteson, M., Li, Q. H. & Chow, M. (2003). Genome delivery and ion channel properties are altered in VP4 mutants of poliovirus. *J Virol* **77**, 5266-5274.
- Davis, M. P., Bottley, G., Beales, L. P., Killington, R. A., Rowlands, D. J. & Tuthill, T. J. (2008). Recombinant VP4 of human rhinovirus induces permeability in model membranes. *J Virol*.
- Evans, W. H. & Hardison, W. G. (1985). Phospholipid, cholesterol, polypeptide and glycoprotein composition of hepatic endosome subfractions. *Biochem J* **232**, 33-36.
- Falanga, A., Cantisani, M., Pedone, C. & Galdiero, S. (2009). Membrane fusion and fission: enveloped viruses. *Protein Pept Lett* **16**, 751-759.
- Fantini, J., Garmy, N., Mahfoud, R. & Yahi, N. (2002). Lipid rafts: structure, function and role in HIV, Alzheimer's and prion diseases. *Expert Rev Mol Med* **4**, 1-22.
- Flint, S. J., Enquist, L. W., Racaniello, V. R. & Skalka, A. M. (2004). Principles of Virology - Molecular Biology, Pathogenesis, and Control of Animal Viruses. *ASM Press ISBN 1-55581-259-7*, 101.
- Fricks, C. E. & Hogle, J. M. (1990). Cell-induced conformational change in poliovirus - externalization of the amino terminus of Vp1 is responsible for liposome binding. *Journal of Virology* **64**, 1934-1945.
- Fuchs, R. & Blaas, D., (eds) (2008). *Human rhinovirus cell entry and uncoating*: World Scientific and Imperial College Press.
- Gradi, A., Imataka, H., Svitkin, Y. V., Rom, E., Raught, B., Morino, S. & Sonenberg, N. (1998). A novel functional human eukaryotic translation initiation factor 4G. *Mol Cell Biol* **18**, 334-342.

- Herz, J., Hamann, U., Rogne, S., Myklebost, O., Gausepohl, H. & Stanley, K. K. (1988). Surface location and high affinity for calcium of a 500-kd liver membrane protein closely related to the LDL-receptor suggest a physiological role as lipoprotein receptor. *EMBO J* **7**, 4119-4127.
- Hewat, E. A. & Blaas, D. (2006). Nonneutralizing human rhinovirus serotype 2-specific monoclonal antibody 2G2 attaches to the region that undergoes the most dramatic changes upon release of the viral RNA. *J Virol* **80**, 12398-12401.
- Hewat, E. A., Neumann, E., Conway, J. F., Moser, R., Ronacher, B., Marlovits, T. C. & Blaas, D. (2000). The cellular receptor to human rhinovirus 2 binds around the 5-fold axis and not in the canyon: a structural view. *Embo J* **19**, 6317-6325.
- Hope, M. J., R. Nayar, L. D. Mayer & Cullis, P. R. (1993). Reduction of liposome size and preparation of unilamellar vesicles by extrusion techniques. *Liposome Technology*, 2nd ed, 124-139.
- Kobayashi, T., Beuchat, M. H., Chevallier, J., Makino, A., Mayran, N., Escola, J. M., Lebrand, C., Cosson, P. & Gruenberg, J. (2002). Separation and characterization of late endosomal membrane domains. *J Biol Chem* **277**, 32157-32164.
- Kolivoska, V., Weiss, V. U., Kremser, L., Gas, B., Blaas, D. & Kenndler, E. (2007). Electrophoresis on a microfluidic chip for analysis of fluorescence-labeled human rhinovirus. *Electrophoresis* **28**, 4734-4740.
- Konecsni, T., Kremser, L., Snyers, L., Rankl, C., Kilar, F., Kenndler, E. & Blaas, D. (2004). Twelve receptor molecules attach per viral particle of human rhinovirus serotype 2 via multiple modules. *FEBS Lett* **568**, 99-104.
- Korant, B. D., Lonberg-Holm, K., Noble, J. & Stasny, J. T. (1972). Naturally occurring and artificially produced components of three rhinoviruses. *Virology* **48**, 71-86.
- Kremser, L., Petsch, M., Blaas, D. & Kenndler, E. (2006a). Capillary electrophoresis of affinity complexes between subviral 80S particles of human rhinovirus and monoclonal antibody 2G2. *Electrophoresis* **27**, 2630-2637.
- Kremser, L., Petsch, M., Blaas, D. & Kenndler, E. (2006b). Influence of detergent additives on mobility of native and subviral rhinovirus particles in capillary electrophoresis. *Electrophoresis* **27**, 1112-1121.
- Lewis, J. K., Bothner, B., Smith, T. J. & Siuzdak, G. (1998). Antiviral agent blocks breathing of the common cold virus. *Proc Natl Acad Sci U S A* **95**, 6774-6778.
- Liebig, H. D., Seipelt, J., Vassilieva, E., Gradi, A. & Kuechler, E. (2002). A thermosensitive mutant of HRV2 2A proteinase: evidence for direct cleavage of eIF4GI and eIF4GII. *FEBS Lett* **523**, 53-57.
- Lodish, H., Berk, A., Matsudaira, P., Kaiser, C. A., Krieger, M., Scott, M. P., Zipursky, L. & Darnell, J. (2004). Molecular Cell Biology - 5th edition. *WH Freeman & Co* ISBN-10: 0716764040, 45.
- Lonberg-Holm, K., Gosser, L. B. & Shimshick, E. J. (1976). Interaction of Liposomes with Subviral Particles of Poliovirus Type 2 and Rhinovirus Type 2. *Journal of Virology* **19**, 746-749.
- Marlovits, T. C., Abrahamsberg, C. & Blaas, D. (1998). Very-low-density lipoprotein receptor fragment shed from HeLa cells inhibits human rhinovirus infection. *Journal of Virology* **72**, 10246-10250.
- Martin-Belmonte, F., Lopez-Guerrero, J. A., Carrasco, L. & Alonso, M. A. (2000). The amino-terminal nine amino acid sequence of poliovirus capsid VP4 protein is sufficient to confer N-myristoylation and targeting to detergent-insoluble membranes. *Biochemistry* **39**, 1083-1090.
- Moser, R., Snyers, L., Wruss, J., Angulo, J., Peters, H., Peters, T. & Blaas, D. (2005). Neutralization of a common cold virus by concatemers of the third ligand binding module of the VLDL-receptor strongly depends on the number of modules. *Virology* **338**, 259-269.
- Neubauer, C., Frasel, L., Kuechler, E. & Blaas, D. (1987). Mechanism of entry of human rhinovirus 2 into HeLa cells. *Virology* **158**, 255-258.
- Neumann, E., Moser, R., Snyers, L., Blaas, D. & Hewat, E. A. (2003). A cellular receptor of human rhinovirus type 2, the very-low-density lipoprotein receptor, binds to two neighbouring proteins of the viral capsid. *J Virol* **77**, 8504-8511.

- Noble, J. & Lonberg-Holm, K. (1973).** Interactions of components of human rhinovirus type 2 with Hela cells. *Virology* **51**, 270-278.
- Pain, V. M. (1996).** Initiation of protein synthesis in eukaryotic cells. *Eur J Biochem* **236**, 747-771.
- Patty, P. J. & Frisken, B. J. (2003).** The pressure-dependence of the size of extruded vesicles. *Biophys J* **85**, 996-1004.
- Prchla, E., Kuechler, E., Blaas, D. & Fuchs, R. (1994).** Uncoating of human rhinovirus serotype 2 from late endosomes. *Journal of Virology* **68**, 3713-3723.
- Prchla, E., Plank, C., Wagner, E., Blaas, D. & Fuchs, R. (1995).** Virus-mediated release of endosomal content in vitro: different behavior of adenovirus and rhinovirus serotype 2. *J Cell Biol* **131**, 111-123.
- Ronacher, B., Marlovits, T. C., Moser, R. & Blaas, D. (2000).** Expression and folding of human very-low-density lipoprotein receptor fragments: neutralization capacity toward human rhinovirus HRV2. *Virology* **278**, 541-550.
- Rossmann, M. G., Arnold, E., Erickson, J. W., Frankenberger, E. A., Griffith, J. P., Hecht, H. J., Johnson, J. E., Kamer, G., Luo, M., Mosser, A. G., Rueckert, R. R., Sherry, B. & Vriend, G. (1985).** Structure of a human common cold virus and functional relationship to other picornaviruses. *Nature* **317**, 145-153.
- Semler, B. L. & Wimmer, E. (2002).** Molecular Biology of Picornaviruses. *ASM Press* ISBN 1-55581-210-4.
- Simons, K. & Ikonen, E. (1997).** Functional rafts in cell membranes. *Nature* **387**, 569-572.
- Singer, S. J. & Nicolson, G. L. (1972).** The fluid mosaic model of the structure of cell membranes. *Science* **175**, 720-731.
- Stryer, L. (1999).** Biochemie. *Spektrum Akademischer Verlag*, 487-422, 737.
- Takahashi, S., Kawarabayasi, Y., Nakai, T., Sakai, J. & Yamamoto, T. (1992).** Rabbit very low density lipoprotein receptor: a low density lipoprotein receptor-like protein with distinct ligand specificity. *Proc Natl Acad Sci U S A* **89**, 9252-9256.
- Torchilin, V. & Weissig, V. (2003).** Liposomes Second Edition. *Oxford University Press*, 1-8.
- Tuthill, T. J., Bubeck, D., Rowlands, D. J. & Hogle, J. M. (2006).** Characterization of Early Steps in the Poliovirus Infection Process: Receptor-Decorated Liposomes Induce Conversion of the Virus to Membrane-Anchored Entry-Intermediate Particles. *Journal of Virology* **80**, 172-180.
- Verdaguer, N., Blaas, D. & Fita, I. (2000).** Structure of human rhinovirus serotype 2 (HRV2). *Journal of Molecular Biology* **300**, 1179-1194.
- Verdaguer, N., Fita, I., Reithmayer, M., Moser, R. & Blaas, D. (2004).** X-ray structure of a minor group human rhinovirus bound to a fragment of its cellular receptor protein. *Nature Struct Mol Biol* **11**, 429-434.
- Vlasak, M., Blomqvist, S., Hovi, T., Hewat, E. & Blaas, D. (2003).** Sequence and structure of human rhinoviruses reveal the basis of receptor discrimination. *Journal of Virology* **77**, 6923-6930.
- Weiss, V. U., Bilek, G., Pickl-Herk, A., Blaas, D. & Kenndler, E. (2009).** Mimicking virus attachment to host cells employing liposomes: Analysis by chip electrophoresis. *Electrophoresis* **30**, 2123-2128.
- Weiss, V. U., Kolivoska, V., Kremser, L., Gas, B., Blaas, D. & Kenndler, E. (2007).** Virus analysis by electrophoresis on a microfluidic chip. *J Chromatogr B Analyt Technol Biomed Life Sci* **860**, 173-179.
- White, J. & Helenius, A. (1980).** pH-dependent fusion between the Semliki Forest virus membrane and liposomes. *Proc Natl Acad Sci U S A* **77**, 3273-3277.
- Woodle, M. C. (1998).** Controlling liposome blood clearance by surface-grafted polymers. *Adv Drug Deliv Rev* **32**, 139-152.
- Wubbolts, R., Leckie, R. S., Veenhuizen, P. T., Schwarzmann, G., Mobius, W., Hoernschemeyer, J., Slot, J. W., Geuze, H. J. & Stoorvogel, W. (2003).** Proteomic and biochemical analyses of human B cell-derived exosomes. Potential implications for their function and multivesicular body formation. *J Biol Chem* **278**, 10963-10972.

- Yamamoto, T., Davis, C. G., Brown, M. S., Schneider, W. J., Casey, M. L., Goldstein, J. L. & Russell, D. W. (1984).** The human LDL receptor: a cysteine-rich protein with multiple Alu sequences in its mRNA. *Cell* **39**, 27-38.
- Zauner, W., Blaas, D., Kuechler, E. & Wagner, E. (1995).** Rhinovirus-mediated endosomal release of transfection complexes. *J Virol* **69**, 1085-1092.

8 Acknowledgements

In the beginning of my acknowledgements, I would like to thank my team-mates, **Angela** and **Victor**, for great teamwork, for their professional support in the fields of molecular biology and analytical chemistry, and in general for their awesomeness.

(“Awesomeness”, either you have it – or you want it; definition by Thomas Kern)

Next, I want to thank **Leopold Kremser** for introducing me into the mystery of capillary electrophoresis and for teaching me how to fix CE instruments (with a minimum of rage).

Of course, thanks go to my coordinators, Prof. **Ernst Kenndler** and Prof. **Dieter Blaas**, for rock solid guidance in my doctoral thesis. Further, I like to express my thanks to **Irene Gösler**, who managed to prepare virus batches for this work in an almost as reproducible and flawless way as Chuck Norris performs a round house kick.

Certainly, I want to acknowledge my girlfriend, **Irene**, for always being awesome company and support. And finally, I would like to mention my brother, **Miguel**, because he just wanted be mentioned in my acknowledgements and moreover helped me with the spelling of the word of “acknowledgement”.

(It is by far not the easiest word in the English language; remark by the author)

Further thank go to ...	
L-Dorf...	for providing brilliant writing atmosphere.
Mark...	for as independent as flawless inspection of this manuscript and for checking my punctuation.
Abdul...	for explaining western blots properly in the dark room.
Sony and again to my girlfriend...	for the notebook I am writing on.
rest of the lab members	for sharing digital <i>information</i> .
the English people...	for using their language in this work.
my mother...	for having drinks together.
the producers of “The IT crowd” and Kevin Sorbo...	for providing a lot of entertainment during my writing pauses.
me...	for doing the whole work.

9 Appendix

9.1 Publications

The following articles, published in the course of the doctoral thesis, have been inserted in this manuscript:

(Bilek et al., 2006a)

“Analysis of liposomes by capillary electrophoresis and their use as carrier in electrokinetic chromatography”

(Bilek et al., 2006b)

“Capillary electrophoresis of liposomes functionalized for protein binding”

(Bilek et al., 2007)

“Mimicking early events of virus infection: Capillary electrophoretic analysis of virus attachment to receptor-decorated liposomes”

(Weiss et al., 2009)

“Mimicking virus attachment to host cells employing liposomes: Analysis by chip electrophoresis”

Review

Analysis of liposomes by capillary electrophoresis and their use as carrier in electrokinetic chromatography[☆]

Gerhard Bilek^a, Leopold Kremser^a, Dieter Blaas^b, Ernst Kenndler^{a,*}

^a Institute for Analytical Chemistry, University of Vienna, Währingerstrasse 38, A-1090 Vienna, Austria

^b Max F. Perutz Laboratories, University Departments at the Vienna Biocenter, Department of Medical Biochemistry, Medical University of Vienna, Austria

Received 9 January 2006; accepted 15 March 2006

Available online 6 May 2006

Abstract

This contribution reviews work about liposomes in the context of electrically driven separation methods in the capillary format. The discussion covers four topics. The one broaches the application of liposomes as pseudo-stationary phases or carriers in vesicle or liposome electrokinetic chromatography (EKC) in the way as microemulsions and micelles are used; it includes the chromatographic use of liposomal bilayers as stationary phases attached to the wall for capillary electrochromatography (CEC). The second topic is the characterization and separation of liposomes as analytes by capillary electrophoresis (CE). Then the determination of distribution coefficients and binding constants between liposomes and ligands is discussed, and finally work dealing with peptides and proteins are reviewed with lipid bilayers as constituents of the electrically driven separation system.

© 2006 Elsevier B.V. All rights reserved.

Keywords: Liposome; Phospholipids; Capillary electrochromatography; Capillary electrophoresis; Vesicles; Pseudostationary phase; Proteins; Peptides

Contents

1. Introduction	38
2. Liposomes for electrically driven capillary chromatography	41
2.1. Liposomes as pseudo-stationary phases	41
2.2. Immobilized phospholipids as stationary phases	42
3. Analysis and characterization of liposomes by capillary electrophoresis	44
4. Distribution coefficients and binding constants	46
5. Work related to proteins and peptides	48
6. Conclusion	49
Acknowledgement	50
References	50

1. Introduction

Liposomes are self-assembled vesicles commonly consisting of phospholipid bilayers enclosing an aqueous solution, with

other lipid aggregates found as well. These model organelles have been widely used to mimic processes occurring at cell membranes. The main phospholipids of *Eukarya* are phosphatidylcholine (PC, the most common phospholipid in natural membranes), phosphatidylserine (PS), phosphatidylethanolamine (PE), sphingomyelin (SM); for the abbreviations and symbols of the compounds and for their structures see Table 1. These substances are amphiphilic (they possess a hydrophilic and a lipophilic entity) and many are zwitterionic. Liposomes can be multi- or unilamellar. The diameter of unilamellar vesicles

[☆] This paper is part of a special volume entitled "Analysis of proteins, peptides and glycans by capillary (electromigration) techniques", dedicated to Zdenek Deyl, guest edited by I. Miksik.

* Corresponding author. Tel.: +43 1 4277 52305; fax: +43 1 4277 9523.
E-mail address: ernst.kenndler@univie.ac.at (E. Kenndler).

Table 1

List of compounds for liposome formation including structural formulae and symbols used in the text

Compound	Symbol	Structure	R
Phosphatidylcholine	PC		
Dilauroylphosphatidylcholine	DLPC		R_1, R_2
Dimyristoylphosphatidylcholine	DMPC		R_1, R_2
Dipalmitoylphosphatidylcholine	DPPC		R_1, R_2
Distearoylphosphatidylcholine	DSPC		R_1, R_2
Dioleoylphosphatidylcholine	DOPC		R_1, R_2
Palmitoylphosphatidylcholine	Mono-PPC		R_1 R_2
Palmitoyloleoylphosphatidylcholine	POPC		R_1 R_2
Palmitoylinoeoylphosphatidylcholine	PLPC		R_1 R_2
Phosphatidylethanolamine	PE		a
Sphingomyelin	SM		a
Phosphatidylglycerol	PG		
Distearoylphosphatidylglycerol	DSPG		R_1, R_2
Dipalmitoylphosphatidylglycerol	DPPG		R_1, R_2
Phosphatidylserine	PS		

Table 1 (Continued)

Compound	Symbol	Structure	R
Dipalmitoylphosphatidylserine 1,2-Dipalmitoyl-sn-glycero-3-phosphoserine	DPSP		R_1, R_2
Phosphatidic Acid	PA		^a
Phosphatidylinositol	PI		^a
Cardiolipin	CL		^a
Cholesterol	Ch		
Dicetylphosphate	DCP		

^a R_1, R_2 depend on source.

ranges between several tens and thousands of nanometers. With diameters from ~25 to ~100 nm they are usually termed “small unilamellar vesicles” (SUVs) and from ~100 nm to ~1 μm “large unilamellar vesicles” (LUVs). “Giant unilamellar vesicles” (GUVs; 20–150 μm) are formed rather from bipolar tetraether lipids like those occurring in *Archaea* than from esters like the phospholipids [1]. *Archaea* are microorganisms which are adapted to extreme environmental conditions like high temperatures, low pH or absence of oxygen.

Phospholipid liposomes have been utilized since about two decades in liquid chromatography (LC) and became popular for the investigation of interactions between ligands and biomembranes (for recent reviews, see refs. [2,3]). In electrically driven separation methods in the capillary format liposomes were less frequently used and investigated. However, since their introduction into these methods [4,5] they have raised two-fold interest; on the one hand, they were considered attractive separation media especially as models for the partition of analytes into cell membranes. On the other hand, capillary electrophoresis (CE) turned out to be an effective tool to investigate the properties of liposomes as analytes, like their charge and size distribution, or their interaction with ligands. It is interesting that most types of liposomes carry a charge (normally they are anions) even

when they are composed of neutral compounds or of zwitterionic lipids in their isoelectric range, at pH values where the opposite charges should compensate each other. In this respect the liposomes behave similarly to other colloidal particles composed of apparently electrically neutral compounds like polyethylene, polyvinylchloride or elementary gold [6].

The use of liposomes as stationary or pseudo-stationary phase in electrically driven techniques has some advantages as compared to column chromatography. The setup of the separation systems is much less complicated; in liquid chromatography, the liposomes have to be attached to the stationary phase. This is not the case in electrokinetic chromatography (EKC). Here, the vesicles are freely dispersed in solution without steric restrictions thus better mimicking conditions such as they prevail for lipid vesicles within cells. Similar to micellar electrokinetic chromatography (MEKC) and microemulsion electrokinetic chromatography (MEEKC) consumption of sample and chemicals is very low as compared to classical column LC. For reviews on the use of liposomes in separation techniques and on their characterization and analysis by CE see refs. [2,3,7,8].

First the application of phospholipids as pseudo-stationary phase added to the background electrolyte (BGE), and as real stationary phase, when they form a coating layer at the capillary

wall is discussed. In both cases, separation of the analytes is based on their partition between the aqueous buffers and the lipid membranes; in principle the system is a chromatographic one. Migration is due to electrokinetic movement, by electrophoresis for charged analytes and dispersed charged vesicles, and by the superimposed electroosmotic flow (EOF). Then, work dealing with the characterization of liposomes by CE is discussed. CE analysis of liposomes is possible because in many cases the vesicles exhibit an electric charge as mentioned above. Finally, affinity electrophoresis in the broadest sense involving liposomes will be discussed and at the end of this contribution a separate section is devoted to peptides and proteins. It is obvious that these topics overlap in some cases.

2. Liposomes for electrically driven capillary chromatography

When liposomes are used as lipophilic chromatographic phase, two methods are differentiated in the literature according to the arrangement of this phase. In both methods the mobile (aqueous) phase is moving through the separation system by the EOF. In capillary electrochromatography (CEC) the stationary phase is really fixed in the system, either as a packed bed, a monolithic phase, or as coated layer at the inner capillary wall. In EKC the lipophilic phase is suspended in the aqueous mobile phase (or vice versa) in form of micelles, microemulsions or other particles forming a pseudo-stationary phase. These particles are normally electrically charged and move thus with an own electrophoretic velocity under the influence of the applied electric field. With respect to the separation principle being a chromatographic one it is not a pre-requisite that the one phase is fixed, it is essential that they migrate in the aqueous phase with the EOF. The analytes are electrically driven; if the compounds are uncharged they migrate with the EOF. Separation is possible due to the different partitioning of the analytes between the two phases. Note that the separation of charged analytes in these electrically driven systems can be described similarly by taking into account their own electrophoretic migration. In this section we will discuss analyte separation rather than the physico-chemical parameters it is based on; distribution coefficients and binding constants are the topic of the separate Section 4.

2.1. Liposomes as pseudo-stationary phases

Nakamura et al. [9] used liposomes as pseudo-stationary phase in EKC for the separation of hydrophobic compounds. Liposomes consisting of anionic and cationic lipids were prepared by Foley and co-workers [10]. The vesicles were made from *n*-dodecyltrimethylammonium bromide (DTAB) and sodium dodecyl sulphate (SDS). These detergents, either pure or as mixture, form micelles. However, at a mass ratio of 40/60 of DTAB/SDS and at a total surfactant concentration of 1% (w/v) the detergent mixture forms vesicles of about 100 nm diameter, with the cationic groups directed towards the interior, and the anionic groups towards the exterior of the vesicle. The authors compared these vesicles with SDS micelles and mixed micelles formed by SDS and DTAB with respect to detergent ratio, phase

ratio, elution range and selectivity, hydrophobicity, etc. The vesicular systems showed a larger elution window as compared to the micelles.

LUVs formed from two different zwitterionic phospholipids, either with 1-palmitoyl-2-oleoyl-sn-glycero-3-phosphocholine (POPC) or with 1,2-dipalmitoyl-sn-glycerol-3-phosphocholine (DPPC) as main constituent, were prepared by Wiedmer et al. [11] and their retention characteristics were evaluated with corticosteroids as reference compounds. A second, anionic lipid (PS; cardiolipin (CL); phosphatidylglycerol (PG); or phosphatidic acid (PA)) was present at up to 30% in the liposome preparations. Running buffer was 50 mM 2-(*N*-cyclohexylamino)ethanesulfonic acid (CHES) at pH 9. Boric acid buffer was found to be unsuitable due to the interaction of borate with the steroids: they were retained even in the absence of liposomes. Relative migration times, defined as t_m/t_0 (t_m is the migration time of the analyte, t_0 that of an EOF marker) were given; they increased with total lipid concentration and decreased with the POPC/CL ratio. The effect of the anionic head group (from PG, PA, PS or CL, respectively) was investigated at different temperatures. Separation of the corticosteroids increased with increasing negative charge of the vesicles.

Steroid hormones could be separated using liposomes made from POPC and POPC/cholesterol (Ch) (80/20 mol%). The electrophoretic (anionic) mobility of the vesicles with particle diameters of around 120 nm were small (between 2 and $13 \times 10^{-9} \text{ m}^2 \text{ V}^{-1} \text{ s}^{-1}$) and changed with buffer type (at constant ionic strength of 20 mM and 25 °C) [12]. The EOF was dependent on the coating of the capillary. Retention of analytes correlated with the results obtained by monolayer penetration measurements. With similar liposomes (POPC/PS, but no Ch) phenols and steroids were separated [13].

A similar comparison as in ref. [10] was made with three surfactant vesicles and one phospholipid vesicle [14]. The authors related properties like particle diameter, mobility, retention and migration window, separation efficiency and selectivity to those of common MEKC systems with SDS. Two types of surfactant vesicles were formed from non-stoichiometric aqueous mixtures of the oppositely charged and single-tailed surfactants cetyltrimethylammonium bromide (CTAB) and sodium octyl sulfate (SOS) at a 30/70 molar ratio, and of *n*-octyltrimethylammonium bromide (OTAB) and SDS at a 70/30 molar ratio. Other surfactant vesicles consisted of double-tailed bis(2-ethylhexyl)sodium sulfosuccinate (AOT) in 10% MeOH, and phospholipid vesicles were made from POPC/PS in a ratio of 80/20. The vesicles had mean diameters of between 76 and 108 nm, and mobilities of about $35 \times 10^{-9} \text{ m}^2 \text{ V}^{-1} \text{ s}^{-1}$ (with the exception of OTAB/SDS, which exhibited a mobility of only $17 \times 10^{-9} \text{ m}^2 \text{ V}^{-1} \text{ s}^{-1}$). Interestingly, all vesicles were negatively charged, although the OTAB/SDS vesicles were prepared with the cationic surfactant added in excess. The phase ratios of the pseudo-chromatographic systems were between 10^{-2} and 10^{-3} (with surfactant concentrations between 0.5 and 1.8%, w/v). CTAB/SOS vesicles formed spontaneously in aqueous solution. A constant particle size was obtained after 14 h of growth as determined by dynamic light scattering. For a moderately retained analyte (the retention factors were not given)

plate numbers between 60,000 and 130,000 were measured. The same migration order for positional isomers (nitrotoluenes) was observed for the vesicle systems, but it differed from that seen when SDS micelles were used. Interpretation of the retention data based on linear solvation energy relationship (LSER, see Section 4) revealed that hydrogen bond acidity and cohesiveness were the most relevant parameters. In previous work of this group, similar systems (CTAB/SOS at 80/20 mol% and AOT in 10% MeOH) were used to correlate retention factors to P_{OW} (the partition constant between octanol and water) for a number of organic standard compounds, pesticides and organic acids [15]. The results were based on LSER.

The same group investigated the influence of organic solvents added to the BGE on particle size, retention of neutral analytes, methylene and shape selectivity, and based the interpretation of the change in retention on LSER analysis [16]. So-called class I (at 0.5%, v/v) and class II solvents (at up to 15%, v/v) were added to the BGE, consisting of 1.8% (w/v) CTAB/SOS in 10 mM *N*-(2-hydroxyethyl)piperazine-2'-(2-ethanesulfonic acid) (HEPES) buffer at pH 7.2. Class I modifiers, polar organic compounds like alkylpolyols, are absorbed in the vesicle and change thus the partition properties for the analytes. From this class the authors applied 1-butanediol, 1,2,6-hexanetriol, glycidol, and 2-amino-1-butanol. Class II modifiers change physical properties of the bulk liquid phase like the dielectric constant, and affect in this way analyte partition. Solvents like methanol or acetonitrile belong to class II; acetonitrile was chosen in this paper. It was found that all modifiers decrease the methylene selectivity, α_{CH_2} . The methylene selectivity can be derived from the slope of the curves relating the retention factor, k , of a series of homologues versus their carbon number, n_C . For this purpose, alkylphenones are often taken. The according regression can be expressed by

$$\log k = \log \alpha_{CH_2} n_C + \log \beta \quad (1)$$

$\log \beta$ is the intercept of the regression line. It was further found that the shape selectivity is decreased by the class II modifier. Shape selectivity is the selectivity coefficient which relates the retention factors of two positional isomers, 1 and 2, according to k_1/k_2 . The class II modifier acetonitrile, on the other hand, did not affect shape selectivity. Based on LSER analysis of the retention data it was concluded that cohesiveness and hydrogen bond acidity play the major role when acetonitrile was the modifier. With class I solvents cohesiveness is important as well, but hydrogen bond basicity is decisive. In a recent paper [17] the authors compared the effect upon changing the counter-ion of the cationic detergent from bromide to chloride. The size of the vesicles changed from an average diameter of 85 to 96 nm. Class I and class II modifiers had similar effects on elution range, methylene selectivity, and efficiency. LFER analysis suggested a difference in solute-vesicle interaction due to the counter-ion.

The elution range for EKC with particles containing chiral *N*-dodecoxycarbonylvaline (DDCV) was increased by applying mixed vesicles with an oppositely charged detergent, CTAB [18]. The vesicle-based separation system finally consisted of

1.4% (w/v) CTAB/DDCV (30/70 mol%) in 35 mM CHES buffer, pH 8.5. Compared to mixed micelles consisting of the DDCV and SDS, a larger elution range, higher methylene and shape selectivity was observed. Interestingly enantioselectivity was completely lost in the vesicle system compared to the micellar one, indicating a different separation mechanism in both EKC systems.

The aggregation behaviour of a novel detergent, sodium *N*-(4-dodecyloxybenzoyl)-L-valinate (SDLV), which differs from that used in ref. [18] by substitution of the carbonyl by a benzoyl group, was investigated by dynamic light scattering, microscopy, fluorescence probe and surface tension methods [19]. It spontaneously forms vesicles with 30–70 nm diameter in aqueous solutions. It was used as chiral selector for EKC [20]. The atropisomers of binaphthol, binaphthyl diamine and binaphthol phosphate, and the enantiomers of Tröger's base and benzoin were separated in borate buffer (at pH 9.7 and 10.3) with 2–5 mM SDLV.

Retention factors of drugs in liposome systems composed of POPC and PS (in a molar ratio of 80/20, suspended in phosphate buffer of ionic strength 0.05 M at pH 7.4) were compared with different micellar and microemulsion systems with respect to the $\log P_{OW}$ values and membrane permeability [21]. Literature data on the permeability of monolayers of the human intestinal epithelial cell line Caco-2 and of the intestinal segment of rat ileum and rat colon for 20 compounds (including 10 β -blockers) were taken as reference. Although the correlations were not high (the highest correlation coefficient was 0.88) the best correlation with membrane permeability was observed for the liposomal system.

2.2. Immobilized phospholipids as stationary phases

Phospholipids and liposomes have been applied as stationary phase in LC for a long time; see e.g. the recent review article of Wiedmer et al. [2]. For their use in CEC phospholipid layers can be immobilized on the capillary wall where they form a hydrophobic stationary phase. There is no principal disparity between electrokinetic and pressure driven chromatography concerning separation selectivity with regard to neutral analytes; the difference lays in the zone dispersion effects. However, for ionic analytes it is obvious that the selectivity of the two methods differs due to the additional contribution of the electrophoretic migration in CEC.

A method to immobilize liposomes in the capillary for CEC was proposed by Yang et al. [22] who made use of the high affinity avidin/biotin system; first, the silanol groups of the fused silica capillary were reacted with 3-aminopropyltriethoxysilane. The resulting aminopropylsilica surface was treated with glutaraldehyde to obtain an aldehyde-activated surface, to which avidin was coupled. Finally, unilamellar liposomes assembled from PC and 2 mol% biotinylated polyethylene were immobilized to this surface. The vesicles had 40 or 90 nm mean diameter. The smaller vesicles contained ~80, the larger ones ~800 biotinylated polyethylene molecules at the outer surface. The authors argue that repeated coating finally resulted in up to 15 liposome layers on the wall.

Örnkov et al. [23] attached derivatized agarose carrying positively charged quaternary ammonium groups electrostatically to the silica surface simply by rinsing the capillary with the solution. The negatively charged liposomes were then immobilized to the agarose via electrostatic interaction by a subsequent flush. Drugs as analytes were retained due to the stationary phase as concluded from the comparison with their migration in non-coated capillaries. The migration sequence of the analytes was in agreement with their lipophilicity expressed by $\log P_{OW}$.

Cunliffe et al. [24] coated the wall of the silica capillary with 1,2-dilauroyl-sn-glycero-3-phosphocholine (DLPC) in order to prevent protein adsorption in CE. The lipid was not intentionally applied as stationary chromatographic phase. CE of both cationic and anionic proteins resulted in highly efficient separations, indicating a reduction of adsorption, especially for the cationic analytes. However, incomplete protein recovery, together with some tailing of the electrophoretic peaks of the cationic proteins pointed to residual adsorption.

Riekkola and co-workers [25] has published a series of papers describing methodologies to produce immobilized liposome layers for CEC. In the first paper, they presented a simple method for coating the capillaries. LUVs with a diameter of about 100 nm consisting of POPC with different proportions of PS and Ch were prepared as usual by extrusion; they form a bilayer on the silica surface by simple rinsing. The best separation of uncharged steroids and column stability were obtained with anionic POPC/PS (80/20 mol%) liposomes. HEPES buffer turned out to be most favourable for the separation when used in the coating procedure and in the BGE. The favourable role of HEPES was confirmed in ref. [26]. It was shown that hydrophobic interactions between analytes and the negatively charged phospholipid coating (PC/PS) are important for the migration of charged analytes. Other piperazine-based compounds, i.e., *N*-(2-hydroxyethyl)piperazine-*N'*-(2-hydroxypropanesulfonic acid) (HEPPSO), piperazine-*N,N'*-bis(2-ethanesulfonic acid) (PIPES), and piperazine-*N,N'*-bis(hydroxypropanesulfonic acid) (POPSO), at pH 7.4 were evaluated as solution constituents for liposome coating and as buffering compounds for the separation of the analytes; the phospholipid coatings again consisted of PC and PS. The quality of the coating was evaluated via separation of five steroids used as neutral model analytes. Similar to HEPES, addition of small diamines (ethylenediamine, diaminopropane, bis-tris-propane) to the liposome solution improved the coating quality [27] (see Fig. 1). Improved separations were related to an increase in packing density of the anionic phospholipids caused by the linear diamines. It was observed that in contrast to the diamine, buffers like phosphate may have negative effect on coating formation. Finally, it was demonstrated that Ca-ions can most favourably be used as substitute for HEPES for the stabilization of the phospholipid coating [28,29]. Application of Ca^{2+} in the coating procedure as well as its presence in the separation buffer containing 3 mM POPC/PS vesicles (at a ratio of 80/20 mol%) led to an improvement in separation of steroids and phenols. In a recent paper Hautala et al. [30] investigated the stability of the phospholipid layer as a function of the buffer pH used during the coating procedure, and for electrochromatographic separation. The lipo-

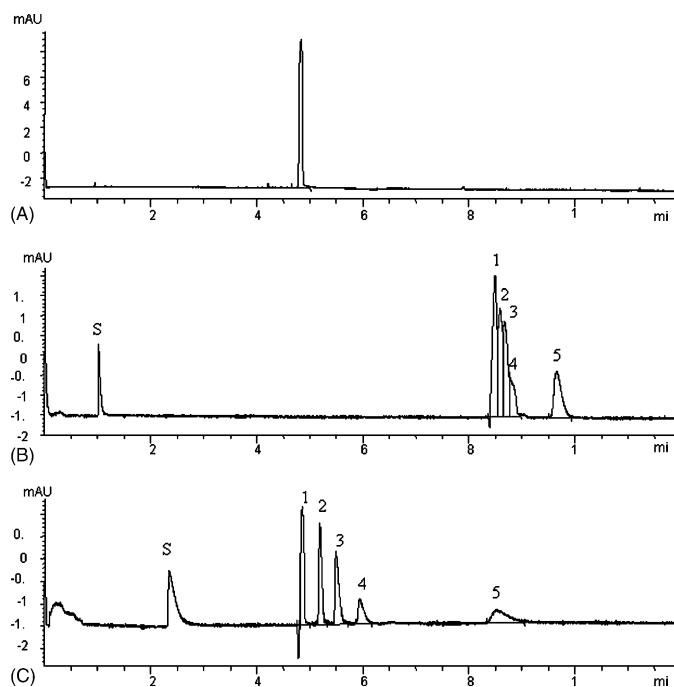


Fig. 1. Effect of the liposome coating on the separation of steroids. BGE in all cases 20 mM Tris, pH 7.4. (A) No coating; (B) PC/PS coating using 10 min preflush with 5 mM 1,3-diaminopropane (DAP) before coating with PC/PS (80/20 mol% 1 mM solution); (C) capillary coating as in (B); but 5 mM of DAP added to the liposome solution. Sample aldosterone (1), androstenedione (2), testosterone (3), 17α -hydroxyprogesterone (4), progesterone (5); voltage 20 kV, capillary length 60/51.5 cm. (S) Indicates a system peak. From ref. [27] with permission.

some solution consisted of 3 mM PC/PS in molar ratio of 80/20; buffer constituent was HEPES. The authors argue that the extent of the attachment of the coating to the fused silica surface is connected to the protonation of the amines of both, the phospholipids and HEPES. The authors found that, as in ref. [28], Ca^{2+} plays an important role in stabilization of the layer. Separation of five steroids was investigated, and relative migration times of the analytes (related to the residence time of an EOF marker) were given. Because the steroids employed were neutral compounds, the migration times can easily be converted into retention factors, k_i . It can be deduced that the k_i values are significantly larger in systems containing Ca^{2+} . The coating was stable at a pH between 4.5 and 8.0. At pH 10.8 the phospholipids leaked out.

From the measured migration time in untreated and in liposome coated capillaries retention factors and free energies of interaction were derived for a number of drugs [31]. The analytes (salicylic acid, acetylsalicylic acid, ketoprofen, warfarin, phenytoin, propranolol) were ionized at the pH 7.5 of the BGE. The capillary was coated with a layer of POPC. The reported capacity (retention) factors were between 0.7 and 5.7. As the phase ratio was unknown, distribution coefficients were not determined. A significant loss in separation selectivity for the liposome-modified capillary, as compared to the uncoated one, was observed and related to the interaction between analyte and stationary phase. A similar investigation was carried out with POPC liposomes not bound to the wall, but introduced into the capillary as a suspension plug [32].

3. Analysis and characterization of liposomes by capillary electrophoresis

A number of papers deal with CE in the context of liposomes but not with analyzing the vesicles explicitly. They describe CE as a method for determining drugs encapsulated in liposomal formulations, mainly by measurements of the concentration of free drug by direct analysis [33–37], and the total concentration after disruption of the liposomes, e.g. by solubilisation with detergents. Stability of the liposomes and drug leakage was determined by direct injection of the formulations as long as drug and vesicles could be resolved.

In one of the first papers dealing with CE of liposomes Roberts et al. [5] investigated the size distribution of vesicles consisting of 1,2-dimyristoyl-sn-glycero-3-phosphocholine (DMPC), dicetylphosphate (DCP), and Ch. A cationic membrane dye, 1,1'-dioctadecyl-3,3',3'-tetramethylindodicarbocyanine, DiI-C₁₈(C₅), served for the detection of the vesicles at 650 nm. The authors related the width of the electrophoretically measured liposome peak to the size distribution measured by laser light scattering. The average particle size was 355 nm. The relatively wide size range (expressed by the standard deviation) as derived from laser light scattering was ± 210 nm. The mean electrophoretic mobility of the anionic vesicles was $39.3 \times 10^{-9} \text{ m}^2 \text{ V}^{-1} \text{ s}^{-1}$ but no values for the distribution of the mobilities of the liposomes are given. The authors related peak dispersion not to longitudinal diffusion; they assumed that the particles are too large as to exhibit a significant diffusional mass transport during the residence time in the capillary. The diffusion coefficient, D , was $1.5 \times 10^{-12} \text{ m}^2 \text{ s}^{-1}$, which is about two to three orders of magnitude smaller than that of, for example, compounds with one benzene ring [38]. This means that, according to the Einstein equation for one-dimensional

diffusion ($\sigma_z = \sqrt{2Dt}$) the spatial peak width σ_z , after the same migration time, t , is by more than one order of magnitude smaller for the liposome than for a small organic molecule; in fact it should be negligible. For the liposome a charge of -821 was calculated, which seemed low taking into account the large number of embedded ionic compounds. However, the number was considered as reasonable due to the non-stoichiometric ratio of cationic and anionic lipid components of the vesicle. The liposomes were lysed upon reaction with the surfactant *n*-octyl- β -D-glucopyranoside, either off-line or in the capillary by injection of plugs of solutions containing liposomes and detergent. Like in the initial liposome preparation spikes were observed in the electropherograms in increasing number and these were accompanied by the disappearance of the liposome peak upon increasing the concentration of the detergent. The spikes were related to aggregates of the liposomes, and to precipitated lipidic particles formed after disruption of the bilayer membrane.

Kawakami et al. [39] analyzed, by CE, the homogeneity of liposomes composed of DPPC and 1,2-distearoyl-sn-glycero-3-phosphoglycerol (DSPG) in a 10/1 molar ratio. The authors related the particle size to migration time. With non-charged UV-absorbing molecules embedded in the membrane, the heterogeneity of the membrane composition of the vesicles of a certain preparation even when monodispersed was derived from the ratio of the UV signals at two different wavelengths. The migration time of the vesicles of about 100 nm diameter made from DPPC/DSPG was measured. The vesicles were most probably unilamellar as they were produced upon extrusion. The migration times showed a discontinuity when the temperature of the CE system was increased [40]. This discontinuity was related to the transition temperature from the gel-like to the liquid crystal phase. It was assumed that softening of the mem-

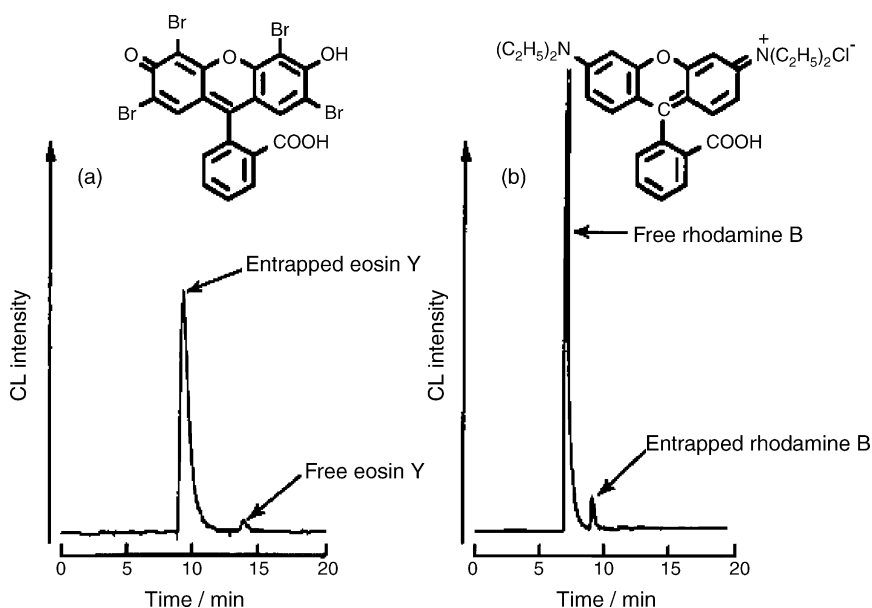


Fig. 2. Electropherograms of liposomes with entrapped dye and free dye. (a) Eosin Y; (b) rhodamine B. SUVs were prepared from DPPC. Conditions: fused silica capillary, 70 cm length, 50 μm I.D.; voltage 15 kV; BGE for separation 10 mM sodium carbonate buffer (pH 9.0); chemiluminescence detection, reagent mixture, 50 mL of 1 mM bis(2,4,6-trichlorophenyl)oxalate (TCPO) acetonitrile solution and 288 μL of 30% (w/w) aqueous H_2O_2 . From ref. [41] with permission.

brane, e.g. by addition of Ch or short-chain lipids, would lead to more elongated liposomes in the electric field during migration, accompanied by a reduced frictional force and a higher mobility. Substitution of DPPC by Ch shifted the discontinuity point of the curve (plotting migration time versus viscosity) to higher viscosity and lower temperature, respectively, which was as expected from the decreased membrane rigidity.

Liposomes made from DPPC and 1,2-dipalmitoyl-sn-glycerol-3-phosphoserine (DPPS) containing dyes (eosin Y or rhodamine B) were analyzed by Tsukagoshi et al. by CE and detected by chemiluminescence upon reaction of the dyes with bis(2,4,6-trichlorophenyl)oxalate (TCPO) and H_2O_2 [41] or peroxyoxalate [42,43] at the capillary outlet. The dyes were trapped in the vesicles during the preparation of the liposomes. The stability of the vesicles and the permeation of the dye could be monitored by the appearance of the peak of the free dye emerging in the electropherograms (see Fig. 2).

With an ingenious approach Arriaga and co-workers [44] were able to measure the size and mobility distribution of individual liposomes. The authors separated multilamellar vesicles composed of PC, PS, PE and Ch in coated capillaries and detected the individual particles by laser-induced fluorescence (LIF) using an Ar-laser (488 nm). The output of the detector photomultiplier was passed through a low pass analog filter with RC of 10 ms, which allowed the detection of the single events (Fig. 3). The particles exhibited an average diameter of 1.1 μm , the standard deviation of the size distribution was 0.2 μm and their size range was between 0.8 and 3 μm . The mobilities of the individual anionic particles were approximately Gaussian distributed and between about 20 and $40 \times 10^{-9} \text{ m}^2 \text{ V}^{-1} \text{ s}^{-1}$, with an average of $30 \times 10^{-9} \text{ m}^2 \text{ V}^{-1} \text{ s}^{-1}$ and a standard deviation of $3 \times 10^{-9} \text{ m}^2 \text{ V}^{-1} \text{ s}^{-1}$. The authors calculated the vesicle volumes to about 1.4 fL; the volume distribution was clearly not Gaussian, it was rather a steep Poisson-like distribution with the maximum number of particles with about 0.2 fL volume (see Fig. 4 in ref. [44]). According to the authors the distribution of the mobility most probably originated from different surface charge densities of the membrane and/or polydispersity of the liposomes (see also ref. [45]).

For liposomes consisting of PC/PG/Ch in various ratios Radko et al. [46] found that the electrophoretic migration was directly related to particle size (ranging from 125 to 488 nm in mean diameter). Investigations were carried out at different ionic strength. Size-dependent migration was a function of κR (κ^{-1} is the thickness of the electric double layer which depends on the ionic strength of the buffer; R is the liposome radius). The mobility of the liposomes thus depends on κR and on the surface charge density, in accordance with the Overbeek–Booth electrokinetic theory. The authors related the size-dependent electrophoretic separation of the liposomes mainly to the relaxation effect caused by the finite relaxation time needed to re-establish the ion cloud upon the movement of an ion.

Wiedmer et al. [13] measured electrophoretic mobilities of liposomes by CE and determined their size by dynamic light scattering. The liposomes were composed from binary mixtures of POPC with CL, PG, PA or PS, and unilamellar vesicles were produced from multilamellar vesicles (lipid concentration about

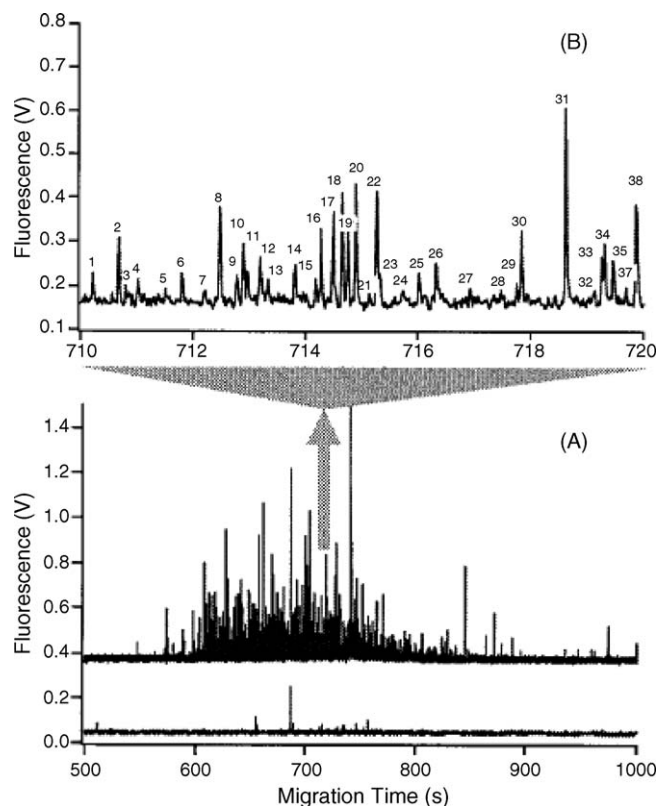


Fig. 3. Electropherograms of a liposome suspension. (A) Top record: electropherogram of the original liposome suspension five-fold diluted (offset +0.15 V). Bottom record: 100-fold dilution of liposomes not containing fluorescein. (B) Expanded migration window from 710 to 720 s in the electropherogram of the five-fold dilution (A, top record). Liposome composition PC, PS, and PEA and Ch in a molar ratio of 47.3/2.3/42.9/7.5. Separation: -200 V cm^{-1} in 250 mM sucrose, 10 mM HEPES, pH 7.5 in a 50 μm I.D. poly(acryloylaminopropanol)-coated capillary. Fluorescence detection: Ar-laser, 20 mW, 488 nm excitation, $535 \pm 17 \text{ nm}$ band-pass, 1000 V PMT bias. Data acquisition: 50 Hz. From ref. [44] with permission.

3–4 mM) in the usual way by extrusion. The mobilities of the anionic particles were about the same for the same ratio between the second lipid and POPC; in a 50 mM CHES buffer with pH 9 mobilities were about $40 \times 10^{-9} \text{ m}^2 \text{ V}^{-1} \text{ s}^{-1}$. They increased with increasing concentration of PS. Particle diameters were independent of composition, namely about 110–120 nm. A given liposome preparation migrated significantly slower in borate buffer as compared to other buffers with the same pH of 9.0.

The electrophoretic mobilities of liposomes (consisting of PC, PA and Ch) with a pH gradient between the lumen and the outer solution were studied by Phayre et al. [47]. The particle diameter was between 130 and 170 nm (as measured by dynamic laser light scattering). The pH difference between the luminal solution (pH_i) and the outside buffer (pH_o) was 1.4 units with the higher pH either inside or outside. These liposomes were compared with vesicles having the same pH of 7.4 on both sides of the membrane (Fig. 4). A significant difference in mobility was found between all three types of vesicles. Their mobilities were in a range between 29 and $37 \times 10^{-9} \text{ m}^2 \text{ V}^{-1} \text{ s}^{-1}$ and decreased in the sequence (pH_i/pH_o): $8.8/8.8 > 7.4/7.4 > 7.4/8.8 > 8.8/7.4$. The mobilities could not be related to the different degree of ion-

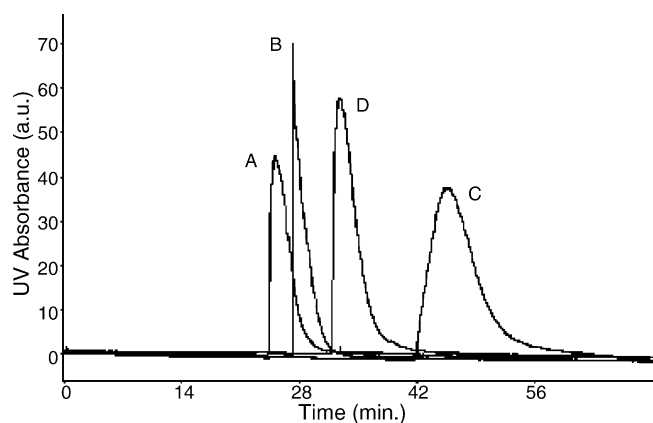


Fig. 4. Electropherograms of liposomes with different pH interiors and exteriors: (A) 8.8 in, 8.8 out; (B) 7.4 in, 7.4 out; (C) 8.8 in, 7.4 out; (D) 7.4 in, 8.8 out. Liposome made from PC and PA (10:1 molar ratio), and 20% (mol/mol) Ch. Liposome diameters between 130 and 170 nm. Capillary 62/77 cm length 50 μ m I.D., coated with BRIJ35. BGE: 2 mM tricine, 15 mM potassium sulfate titrated to pH 7.4 or 8.8 with 1 M sodium hydroxide, 0.001% (w/v) BRIJ 35 added. Voltage –25 kV; UV detection at 214 nm. From ref. [47] with permission.

ization due to acid–base equilibria. It was concluded that more sophisticated models were needed, taking the membrane as electrical capacitor on the one hand, and considering the relaxation effect of ion migration, on the other hand.

In continuation of previous work, Hayes and co-worker [48] investigated the discrepancy between the electrophoretic behaviour of liposomes under various experimental conditions and that predicted by electrokinetic theories. In extension of classical theories for rigid, spherical colloidal particles the variation of ion densities and electric potentials within the ion atmosphere normal to the surface of the large particle were considered together with the deformation of the liposomes to spheroid particles with prolate shape. However, the predicted mobilities were always smaller than those found experimentally, although the shape of the curves depicting the reduced mobility as function of κR agreed with the theory. The authors related these deviation to the unique properties of the liposomes, namely to their deformability and their susceptibility to field-induced polarization. In their most recent work [49] these authors improved the theoretical prediction of electromigration of colloids, taking into account multipole effects, deformability, polarisability and mobile surface charges.

4. Distribution coefficients and binding constants

Distribution coefficients between the lipophilic phospholipid vesicles and the aqueous phase can be determined by CE in the same way as with MEKC or MEEKC. As described in Section 2.1, in a number of papers Foley and co-workers [10,14–18] related $\log k$ to $\log P_{OW}$ values and applied LSER to interpret the interactions of the solutes with the liposomes. Khaledi and co-workers [50] made an investigation of the factors that are responsible for partitioning of analytes between the aqueous phase and vesicles formed from dihexadecylphosphate (DHP), an anionic double-chain surfactant. The authors applied LSER based on the descriptor values of 41 uncharged test solutes. The

LSER model quantifies the contribution of individual interactions on the retention factor, k , according to

$$\log k = vV + bB + aA + sS + eE + C \quad (2)$$

V is the McGowan volume, B the hydrogen-bond acceptor basicity, A the hydrogen-bond donor acidity, S the dipolarity/polarisability, and E is the excess molar refraction. The coefficients v , b , a , s and e are relative measures for the interaction of the analytes with the pseudo-phase compared to the aqueous phase. v is a measure for the difference in cohesive energy between the aqueous and the pseudo-stationary phase, b for the H-bond donor strength, a for the H-bond acceptor strength, s for the dipolarity/polarisability and e for the interaction of the pseudo-stationary phase with n - or π -electrons of the analytes. C is the regression constant which is given by the phase ratio.

The results were compared with analyses using SDS and sodium dodecyl phosphate (SDP) with respect to $\log P_{OW}$. The authors pointed to the shortcomings of taking $\log P_{OW}$ values to describe bio-partitioning of drugs, because n -octanol is a bulk phase, whereas a membrane displays a structured environment. Therefore, it might be assumed that partitioning into a membrane would better correlate with partitioning into micelles than into a bulk liquid. However, interestingly the opposite was observed: $\log k$ values from the higher structured DHP vesicles correlate better with $\log P_{OW}$ values than with $\log k$ from micelles. A detailed analysis of the LSER results shows that size and hydrogen bond acceptor strength play the major role in partitioning between water and the SUVs. Analysis of the Gibbs free energy of transfer for the individual functional groups of the solutes from the aqueous phase into the vesicular phase shows that the energy associated with cavity formation is the main contributor. The surprising result of the better correlation of the $\log k$ values of lipid bilayer membranes with $\log P_{OW}$ than with $\log k$ values of SDS micelles was also found in liposome EKC with 1,2-dipalmitoyl-sn-glycero-3-phosphoglycerol (DPPG)/DPPC and DPPG/DPPC/Ch vesicles [51]. In continuation of this work LSER was applied to interpret the retention data of neutral solutes in a system containing vesicles formed from a cationic double-chain surfactant, dihexadecyldimethylammonium bromide [52]. The vesicles were dispersed in deionised water (no buffer was used for EKC). Particles with 50 nm average diameter were formed, with the bromide ions predominantly attached electrostatically at the vesicle surface. This was concluded from their average charge, which was only 118, compared to 17,500 charges calculated from the number of surfactants per vesicle. The free energy of transfer of a functional group, R , from water to the pseudo-stationary phase, expressed as

$$\Delta\Delta G = -RT \ln \left(\frac{k_{\phi-R}}{k_{\phi}} \right) \quad (3)$$

was derived as well. Here $k_{\phi-R}$ is the retention factor of the substituted benzene and k_{ϕ} that of benzene. It could be demonstrated that the charge of the head group is most relevant for the interactive characteristics of vesicles.

Burns and Khaledi [53] measured the capacity (retention) factors for a number of neutral and charged analytes in sys-

tems consisting of liposomes made from DPPC, DPPG and Ch with about 40 nm diameter at pH 7.5; the partition coefficient was derived from the retention factor and the phase ratio. The latter was calculated from the partial specific volume of the surfactant, the phospholipid concentration and the critical aggregation concentration. The logarithm of the partition coefficients of the 18 investigated monosubstituted benzenes (all neutral) ranged between 1.05 and 2.99. The data obtained by liposome EKC were compared with those predicted by two methods based on quantitative structure-partition relationship (QSPR). The first method relates the partition coefficients from the liposome system to those from water/*n*-octanol. The second method uses descriptors for LSER. The good agreement between calculated and measured data illustrates that the migration properties of analytes in EKC can indeed be predicted. In addition, EKC is a fast and sensitive method with low consumption of chemicals and solvents allowing for the determination of the partition coefficients in multi-analyte mixtures. For 26 basic drugs the retention factors were determined in systems containing phospholipid vesicles made from PS, PC, PG and Ch at different ratios [54]. Buffers were HEPES, CHES, 2-(*N*-morpholino) ethanesulfonic acid (MES), 3-(cyclohexylamino)-1-propanesulfonic acid (CAPS) and phosphate with different ionic strength, pH was 7.0 or 7.4. It was found that the retention of the cationic analytes with the negatively charged liposomes is governed by electrostatic interactions, and the ionic strength plays a dominant role at given pH. Retention data showed low correlation with log P_{OW} values. It should be mentioned that the dipolarity and polarisability of the solvation environment associated with such SUVs made from PG, PC and Ch was investigated with a series of di-*n*-alkyl-*p*-nitroanilines as solvatochromic π^* indicators in combination with size exclusion methods and photon correlation spectroscopy [55].

Khaledi and co-worker [56] also investigated the effect of the pH on the distribution of basic drugs (tetracaine, nefopam, lisocain) between the aqueous phase and negatively charged liposomes in a quantitative way by EKC. The liposomes consisted of PC, PG and Ch. Partitioning of the neutral and the cationic form, both analyte species being in acid–base equilibria, between the two phases was considered. From the retention data and based on fundamental thermodynamics the distribution coefficients of the species, and their particular fractions as a function of the pH were derived. The curves have the typical sigmoid shapes. Partition coefficients were between 46 and 1406 M^{-1} for the cations, and between 20 and 360 M^{-1} for the neutral solutes. Moreover, the authors were able to derive, from the retention data, the shifts in pK_a of the solutes caused from their interaction with the lipid bilayer. When compared to water, the pK_a values changed by between 0.05 and 0.47 units.

Interactions between cationic liposomes commercially employed for drug delivery and a fluorescein conjugated 2'-*O*-methyl-phosphorothioate (Me-PTh) antisense oligonucleotide were studied and binding constants were derived from the change of the mobility of the oligonucleotide upon modifying the liposome concentration in the BGE [57]. The antisense oligonucleotide was taken up from HeLa cells in a liposome

concentration dependent manner and interfered specifically with mRNA of an aberrant luciferase reporter gene. As a result of this interaction, luciferase activity was restored. That way, the concentration of delivered antisense oligonucleotide as well as its corresponding gene expression was determined for two liposome formulations (Lipofectamine and Escort).

Liposomes were chosen as models for the affinity of drugs towards low density lipoprotein (LDL) [58]. Total binding affinities (" nK values") of verapamil and propranolol for liposomes were determined by frontal analysis. nK was calculated from C_t , the total drug concentration, from C_u , the unbound drug concentration, and from L_t , the total liposome concentration according to $nK = (C_t - C_u)/C_u L_t$. Frontal analysis by CE was carried out by co-incubation of liposomes and drug in a physiological buffer, injection of a plug of this solution, electrophoresis in the same buffer, and detection of the drug zone by UV. The height of the trapezoidal peak was taken as a measure for the unbound drug. A number of liposomes with different composition were investigated; they consisted of POPC, PLPC (1-palmitoyl-2-linoleoyl-sn-glycero-3-phosphocholine), DLPC and 1-palmitoyl-sn-glycero-3-phosphocholine (mono-PPC). Significant differences in the nK values were found. They varied within more than one order of magnitude with values between $8.5 \times 10^7\text{ M}^{-1}$ and $103 \times 10^7\text{ M}^{-1}$ for verapamil and $12 \times 10^7\text{ M}^{-1}$ and $178 \times 10^7\text{ M}^{-1}$ for propranolol. The increase in the negative charge of the phospholipids was found more relevant for the ligand-binding affinity than the acyl-chain structure. The binding affinities as function of the liposome composition (size, surface charge) point to the great significance of the electrostatic interactions in binding of the basic drugs. It seems that liposomes bind the drugs unspecifically as in the case of LDL. The results are taken to demonstrate the suitability of liposomes as models to explain the difference of drug binding between LDL and oxidized LDL.

Marques and Schneider [59] proposed a liposome system to bind DNA in a sequence specific manner. For this purpose the authors embedded di-alkyl peptide nucleic acid amphiphiles (PNAAs) in the membrane of liposomes that consisted of 1,2-distearoyl-sn-glycero-3-phosphocholine (DSPC) and Ch. Peptide nucleic acids (PNAs) are synthetic nucleic acid analogues which form duplexes and triplexes with complementary single and double stranded DNA, respectively. The final amount of PNAA within the membrane was determined via UV absorption. Such PNA liposomes were incubated with complementary single strand DNA oligomers. Hybridization of the components was assessed by CE. Free DNA showed a sharp peak, whereas PNA liposomes rendered a broad signal with similar mobility. Samples incubated with complementary DNA showed both signals. The broad peak, however, shifted its mobility, which strongly indicated duplex formation. From the reduced area of the DNA peak it was derived that almost all PNA formed a duplex with complementary 10-mers of DNA. A single mismatch within this sequence yielded no binding at all and longer oligomers showed greatly diminished binding to PNA liposomes. The sequence-specific binding of these liposomes and its possible application as biosensing tag in analytical devices was demonstrated.

5. Work related to proteins and peptides

The first paper describing the application of liposomes in a manner as micelles or oil droplets are used in MEKC or MEEKC, respectively, was published about 10 years ago [4]. Conceptually, the liposomes were to serve as models for biological membranes like in LC where they are immobilized on gels. In their paper the authors added liposomes consisting of PC (and cholate) to the BGE (25 mM phosphate, pH 7.4) and separated several charged analytes in a coated capillary after application of an electric field. They assumed that the mobility of both the EOF and the liposomes was negligible. Increased retention of the analytes was related to their interaction with the vesicles. In accordance with results obtained by immobilized-liposome chromatography, two octapeptides, the one with two cysteines replaced by serines with respect to the other, were separated with better resolution in the presence of the liposomes.

Apolipoproteins constitute the protein moiety of lipoprotein particles. Liposomes were used as models for lipoproteins such as very low-density lipoprotein (VLDL) or LDL in an affinity electrophoretic approach to study the interaction of apolipoproteins with lipids [60]. The unilamellar liposomes consisted of DMPC and were about 100–120 nm in diameter. The number of copies of apolipoprotein apo CIII (Mr 8.8 kDa) and its derived peptides (2.1–4.5 kDa) bound to a single liposome and the binding strength was derived by an equation which relates the change of the mobility of these ligands to the concentration of the liposomes in the BGE. This change is illustrated in Fig. 5 showing the electropherogram of apo CIII at five different liposome concentrations. Two assumptions were made: non-cooperative binding between apo CIII and the liposome, and the equality of the mobilities of the complex and the free liposome. The binding constant for apo CIII was $22 \times 10^3 \text{ M}^{-1}$ and those of the peptides were by factors of 2 to 3 lower, in agreement with data obtained by other methods. The number of analytes bound per vesicle was 1350 for apo CIII, and between 470 and 5200 for the peptides.

Tsukagoshi et al. [61] presented an immunoassay using eosin Y containing liposomes as a labelling reagent for human serum albumin (HSA). After introduction of a thiol group onto HSA via *N*-succinimidyl 3-(2-pyridyldithio) propionate as described by Carlsson et al. [62] the resulting HSA derivative was enabled to bind labeled liposomes covalently. That protein–liposome conjugate was then added to a definite amount of ordinary analyte HSA and subsequently incubated with antibody-immobilized glass beads to perform a competitive immunoassay. Since an excess of protein was used, HSA separated in a glass beads-bound and a free section. The reactant solution, consisting of free HSA (labeled and unlabeled), was applied to a CE-chemiluminescence detection system to remove compounds that might perturb the chemiluminescence and to detect the liposomes, respectively. At the tip of the capillary the liposomes were destroyed by organic solvents which contained the chemiluminescence reagent. In this way a chemiluminescence signal was induced by the vesicles. Based on the competitive binding reaction of the two HSA species to the glass beads, the amount of labeled HSA indicated a relationship to that of analyte HSA.

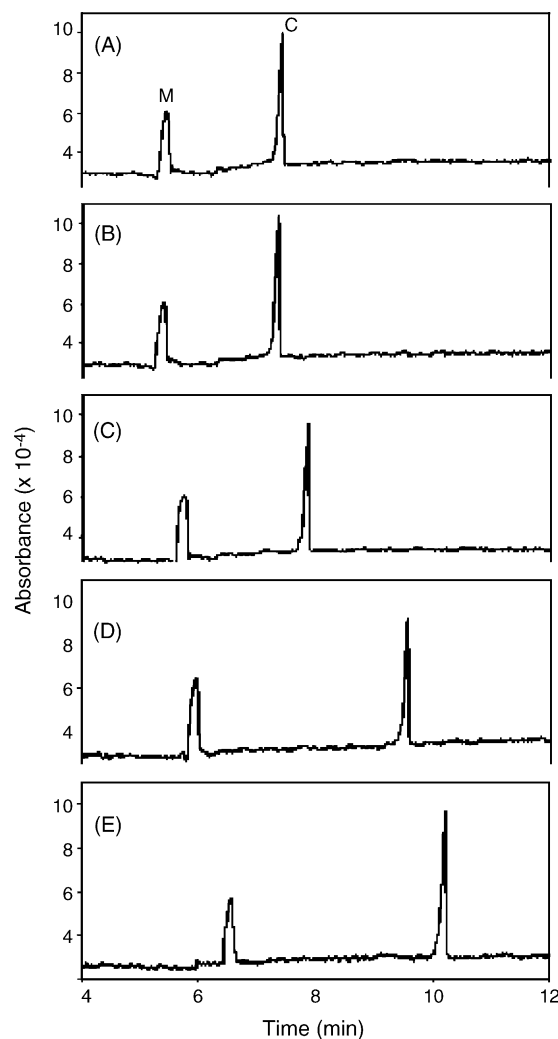


Fig. 5. Electropherograms of apolipoprotein apo CIII at different vesicle concentrations. C, apo CIII; M, internal marker. Vesicle concentrations: (A) 0; (B) 2.1×10^{-6} ; (C) 1.1×10^{-5} ; (D) 2.1×10^{-5} ; and (E) $2.1 \times 10^{-4} \mu\text{M}$ DMPC vesicle in phosphate-saline buffer at pH 7.4. From ref. [60] with permission.

Basic proteins (lysozyme, cytochrome *c*, ribonuclease A, and α -chymotrypsinogen A) were separated in accordance with their electrophoretic mobilities by zone electrophoresis in capillaries coated with a phospholipid layer consisting of POPC in acidic [63] or neutral [64] BGEs. The same phospholipid was also used as a carrier. Coating was a condition to obtain protein peaks, as it suppressed adsorption onto the wall. Since the EOF was reduced upon coating, no significant change in the electrophoretic behaviour of the proteins was observed indicating only minor interactions between the proteins and the vesicles in solution. With the same phospholipid layer, resolution of three peptides (angiotensin I, II and III) was found to increase with increasing concentration of the phospholipids [64], indicating a chromatographic interaction of the separands with the stationary phase.

Tachibana et al. [65] proposed to insert membrane proteins into the liposomes and to determine the binding behaviour of ligands by electrochromatography. In this way they derived the binding constants between a cell wall precursor model pep-

tide $\text{Me}(\text{CH}_2)_8\text{CO-Gly-L-Ala-d-D-Glu-Lys}(\text{Ac})\text{-D-Ala-D-Ala}$ and vancomycin.

Riekkola and co-workers [66] used lysozyme, bound to the phospholipid coating, as chiral agent. The interaction of lysozyme with the lipid layer led to strong immobilization of the protein in the capillary. The layer was stabilized when the capillary wall was first coated with 1-(4-iodobutyl)-1,4-dimethylpiperazin-1-ium iodide (M1C4). The preparation of the chiral stationary phase was carried out simply by serially rinsing with the solutions containing M1C4, the liposomes, and the protein. The attached liposomes were responsible for the stereoselectivity; this was supported by the finding that the protein was not needed in the BGE for chiral separation of D- and L-tryptophan.

Bo and Pawliszyn [67] studied the dynamic process of conjugate formation between four standard proteins and vesicles consisting of PC and PC/PS (80/20 mol%) by capillary isoelectric focusing (CIEF) with whole-column imaging detection (WCID). Stable conjugates between the PC vesicles and trypsin inhibitor, β -lactoglobulin B (two conjugates), and phosphorylase b could be separated from the native proteins due to the pI -shift of the conjugates. Trypsinogen, on the other hand, showed an unchanged CIEF profile, which was explained by a very weak interaction with PC vesicles. Using PC/PS vesicles, the conjugates of all four proteins had lower pI than their native forms

resulting from the acidic PS. PC/PS vesicles exhibited multiple conjugates with trypsin inhibitor (six peaks), β -lactoglobulin B (four peaks), and phosphorylase b (three peaks). This finding was explained by multiple sites interaction of the proteins with the PC/PS vesicles. The conjugates were measured at different incubation times (up to 90 min) to determine the final interaction equilibrium. The CIEF profile of trypsin inhibitor is shown in Fig. 6. In a similar paper [68] the authors investigated the phospholipids–protein interactions of seven standard proteins with PC vesicles at different PC concentration, incubation time, and incubation temperature by measuring the protein profiles with CIEF-WCID.

Receptor proteins were attached via their his_6 -tag to liposomes [69]. For this purpose a lipid containing nitrilotriacetic acid (NTA) as head group was incorporated in the bilayer of liposomes consisting of POPC, PE and Ch and a short polyethylene glycol (PEG) chain for stabilisation. A Ni^{2+} –NTA complex was generated at the liposome surface, to which, in turn, the tagged proteins were bound. The two steps of complex formation could be monitored by the shift of the electrophoretic peak of the vesicle (the lumen was filled with a fluorescence dye for detection). The complex between liposome and protein was stable but was destroyed upon addition of EDTA, which removes the Ni ion and thus the receptor protein from the liposome, as evidenced by a shift of the peak to the original position.

6. Conclusion

Electrically driven chromatography with liposomes is a valuable tool to measure interactions between lipid membranes and a large variety of ligands. It needs only minute amounts of sample. The liposomes can be applied as pseudo-stationary phases in the electrically driven separation system in a simple manner, namely as stable charged colloidal or sub-colloidal constituents of the BGE.

Liposomes, attached to the wall of the separation capillary as a bilayer, form a true stationary phase in a CEC system. Some aspects should be taken into consideration concerning this methodology, independent of whether it is pressure or electrokinetically driven. The one is the slow kinetics of mass transfer in the mobile phase within the open tube due to the low diffusion coefficients in liquids (which are five orders of magnitude lower than in gases). This requires low migration velocities in order to avoid excessive peak broadening contributed from the mass transfer term. The second is the small phase ratio resulting from the thin layer of the stationary phase and the relatively large volume of the bulk mobile phase. The latter problem, which seems typical for this methodology, can be illustrated by the data published in ref. [22]. For a phase with as much as five liposome layers the amount of assembled lipid in a capillary of 40 cm length and 75 μm inner diameter is 12 nmol. The phase ratio is therefore, as small as about 10^{-3} . High partition coefficients are thus needed to obtain favourable retention factors, which should exceed values of say 1 or 2. If the retention factors are too low, and if the selectivity coefficients are not very high, a useful resolution will not be achieved. If, e.g. the selectivity coefficient is 1.1, and a low retention factor of 0.1 is assumed,

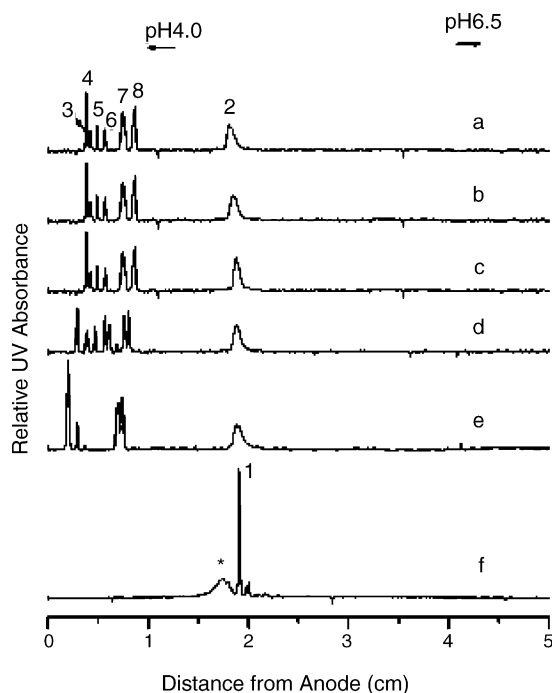


Fig. 6. CIEF profile of conjugates between liposome (PC/PS, 80/20 mol%) with trypsin inhibitor in dependence of incubation time: (a) 90 min; (b) 60 min; (c) 30 min; (d) 15 min; (e) 5 min; (f) native protein. Sample solution: 0.25% methyl cellulose, 4% pharmalytes, 10.7 mM trypsin inhibitor; 250 mM PC/PS (80/20 mol%). Catholyte, 100 mM NaOH, anolyte, 100 mM H_3PO_4 . (*) Denotes degradation product of the protein. Peak 1, native protein. Peaks 3–8 PC/PS–trypsin inhibitor conjugates. UV detection at 280 nm; applied voltage 500 V for 2 min, then maintained at 3000 V; focusing time 8 min. From ref. [67] with permission.

baseline resolution of 1.5 for two peaks of the same height could be achieved only if the plate number is 600,000, which is not trivial. Most systems described in the literature deliver only around 100,000 plates or less in practice. This example illustrates the limits of the CEC method. Note that here neutral analytes are considered, which are driven only by the EOF. Nevertheless, it has to be pointed out that open tubular electrochromatography has high potential with respect to separation efficiency due to the plug-like velocity profile of the ionic analytes as well as of the EOF. Taylor dispersion, as occurs in open tubes due to the parabolic velocity profile of the hydrodynamic flow, is absent.

Migration data (retention factors or electrophoretic mobilities) can elegantly be used to derive thermodynamic data like binding constants, partition coefficients or free energies of transfer. This is an interesting methodology when interactions of biomembranes with ligands like drugs, peptides, proteins or other biopolymers should be mimicked.

For the analytic characterization of the vesicles their different electrophoretic velocities when migrating in the electric field can be utilised. It should be noted that there is no direct relation between mobility and size of the vesicles. No simple theory can describe the relation between these two parameters. However, physical properties like mobilities, diffusion coefficients or charge numbers, and other characteristics such as membrane stability can be determined in an easy manner.

Acknowledgement

This work was supported by the Austrian Science Foundation (Project P15667).

References

- [1] A. Gliozzi, A. Relini, P.L.-G. Chong, J. Membr. Sci. 206 (2002) 131.
- [2] S.K. Wiedmer, M.S. Jussila, M.-L. Riekkola, TrAC 23 (2004) 562.
- [3] R.L. Owen, J.K. Strasters, E.D. Breyer, Electrophoresis 26 (2005) 735.
- [4] Y. Zhang, R. Zhang, S. Hjerten, P. Lundahl, Electrophoresis 16 (1995) 1519.
- [5] M.A. Roberts, L. Locascio-Brown, W.A. MacCrehan, R.A. Durst, Anal. Chem. 68 (1996) 3434.
- [6] U. Schnabel, C.-H. Fischer, E. Kenndler, J. Microcolumn Sep. 9 (1997) 529.
- [7] A. Gomez-Hens, J. Manuel Fernandez-Romero, TrAC 24 (2005) 9.
- [8] S.P. Radko, A. Chrambach, J. Chromatogr. B 722 (1999) 1.
- [9] H. Nakamura, I. Sugiyama, A. Sano, Anal. Sci. 12 (1996) 973.
- [10] M. Hong, B.S. Weekley, S.J. Grieb, J.P. Foley, Anal. Chem. 70 (1998) 1394.
- [11] S.K. Wiedmer, J.M. Holopainen, P. Mustakangas, P.K.J. Kinnunen, M.-L. Riekkola, Electrophoresis 21 (2000) 3191.
- [12] S.K. Wiedmer, M.S. Jussila, J.M. Holopainen, J.-M. Alakoskela, P.K.J. Kinnunen, M.-L. Riekkola, J. Sep. Sci. 25 (2002) 427.
- [13] S.K. Wiedmer, J. Hautala, J.M. Holopainen, P.K.J. Kinnunen, M.-L. Riekkola, Electrophoresis 22 (2001) 1305.
- [14] R.J. Pascoe, J.P. Foley, Electrophoresis 24 (2003) 4227.
- [15] W.L. Klotz, M.R. Schure, J.P. Foley, J. Chromatogr. A 962 (2002) 207.
- [16] R. Pascoe, J.P. Foley, Electrophoresis 23 (2002) 1618.
- [17] S.A. Schuster, J.P. Foley, J. Sep. Sci. 28 (2005) 1399.
- [18] R.J. Pascoe, A.G. Peterson, J.P. Foley, Electrophoresis 21 (2000) 2033.
- [19] A. Mohanty, J. Dey, Langmuir 20 (2004) 8452.
- [20] A. Mohanty, J. Dey, J. Chromatogr. A 1070 (2005) 185.
- [21] E. Örnkvist, J. Gottfries, M. Erickson, S. Folestad, J. Pharm. Pharmacol. 57 (2005) 435.
- [22] Q. Yang, X.-Y. Liu, J. Miyake, H. Toyotama, Supramol. Sci. 5 (1998) 769.
- [23] E. Örnkvist, S. Ullsten, L. Soderberg, K.E. Markides, S. Folestad, Electrophoresis 23 (2002) 3381.
- [24] J.M. Cunliffe, N.E. Baryla, C.A. Lucy, Anal. Chem. 74 (2002) 776.
- [25] J.T. Hautala, M.V. Linden, S.K. Wiedmer, S.J. Ryhänen, M.J. Säily, P.K.J. Kinnunen, M.-L. Riekkola, J. Chromatogr. A 1004 (2003) 81.
- [26] S.K. Wiedmer, M. Jussila, R.M.S. Hakala, K.-H. Pystynen, M.-L. Riekkola, Electrophoresis 26 (2005) 1920.
- [27] S.J. Varjo, J.T. Hautala, S.K. Wiedmer, M.L. Riekkola, J. Chromatogr. A 1081 (2005) 92.
- [28] J.T. Hautala, S.K. Wiedmer, M.-L. Riekkola, Anal. Bioanal. Chem. 378 (2004) 1769.
- [29] M.V. Linden, S.K. Wiedmer, R.M. Hakala, M.L. Riekkola, J. Chromatogr. A 1051 (2004) 61.
- [30] J.T. Hautala, S.K. Wiedmer, M.L. Riekkola, Electrophoresis 26 (2005) 176.
- [31] G. Manetto, M.S. Bellini, Z. Deyl, J. Chromatogr. A 990 (2003) 281.
- [32] G. Manetto, M. Silvana Bellini, Z. Deyl, J. Chromatogr. A 990 (2003) 205.
- [33] D. Chen, D.L. Cole, G.S. Srivatsa, J. Pharm. Biomed. Anal. 22 (2000) 791.
- [34] N. Griese, G. Blaschke, J. Boos, G. Hempel, J. Chromatogr. A 979 (2002) 379.
- [35] P. Perjesi, T. Kim, A.D. Zharikova, X. Li, T. Ramesh, J. Ramasubbu, L. Prokai, J. Pharm. Biomed. Anal. 31 (2003) 929.
- [36] A.H. Malek, M.G. Khaledi, Electrophoresis 24 (2003) 1054.
- [37] M.J. Orchard, I.P. Collin, M. Bushell, Chromatographia 50 (1999) 181.
- [38] B. Maichel, B. Gaš, E. Kenndler, Electrophoresis 21 (2000) 1505.
- [39] K. Kawakami, Y. Nishihara, K. Hirano, J. Colloid Interface Sci. 206 (1998) 177.
- [40] K. Kawakami, Y. Nishihara, K. Hirano, Langmuir 15 (1999) 1893.
- [41] K. Tsukagoshi, Y. Okumura, R. Nakajima, J. Chromatogr. A 813 (1998) 402.
- [42] K. Tsukagoshi, H. Akasaka, R. Nakajima, T. Hara, Chem. Lett. (1996) 467.
- [43] K. Tsukagoshi, Y. Okumura, H. Akasaka, R. Nakajima, T. Hara, Anal. Sci. 12 (1996) 869.
- [44] C.F. Duffy, S. Gafoor, D.P. Richards, H. Admadzadeh, R. O'Kennedy, E.A. Arriaga, Anal. Chem. 73 (2001) 1855.
- [45] S.P. Radko, M. Stastna, A. Chrambach, J. Chromatogr. B 761 (2001) 69.
- [46] S.P. Radko, M. Stastna, A. Chrambach, Anal. Chem. 72 (2000) 5955.
- [47] A.N. Phayre, H.M.V. Farfano, M.A. Hayes, Langmuir 18 (2002) 6499.
- [48] M.D. Pysher, M.A. Hayes, Langmuir 20 (2004) 4369.
- [49] M.D. Pysher, M.A. Hayes, Langmuir 21 (2005) 3572.
- [50] A.A. Agbodjan, H. Bui, M.G. Khaledi, Langmuir 17 (2001) 2893.
- [51] S.T. Burns, A.A. Agbodjan, M.G. Khaledi, J. Chromatogr. A 973 (2002) 167.
- [52] A.A. Agbodjan, M.G. Khaledi, J. Chromatogr. A 1004 (2003) 145.
- [53] S.T. Burns, M.G. Khaledi, J. Pharm. Sci. 91 (2002) 1601.
- [54] J.M. Carrozzino, M.G. Khaledi, Pharm. Res. 21 (2004) 2327.
- [55] J.M. Carrozzino, E. Fuguet, R. Helburn, M.G. Khaledi, J. Biochem. Biophys. Methods 60 (2004) 97.
- [56] J.M. Carrozzino, M.G. Khaledi, J. Chromatogr. A 1079 (2005) 307.
- [57] J. McKeon, M.G. Khaledi, J. Chromatogr. A 1004 (2003) 39.
- [58] Y. Kuroda, Y. Watanabe, A. Shibukawa, T. Nakagawa, J. Pharm. Biomed. Anal. 30 (2003) 1869.
- [59] B.F. Marques, J.W. Schneider, Langmuir 21 (2005) 2488.
- [60] E.D. Breyer, S. Howard, N. Raje, S. Allison, R. Apkarian, W.V. Brown, J.K. Strasters, Anal. Chem. 75 (2003) 5160.
- [61] K. Tsukagoshi, H. Akasaka, Y. Okumura, R. Fukaya, M. Otsuka, K. Fujiwara, H. Umehara, R. Maeda, R. Nakajima, Anal. Sci. 16 (2000) 121.
- [62] J. Carlsson, H. Drevin, R. Axen, Biochem. J. 173 (1978) 723.

- [63] D. Corradini, G. Mancini, C. Bello, *J. Chromatogr. A* 1051 (2004) 103.
- [64] D. Corradini, G. Mancini, C. Bello, *Chromatographia* 60 (2004) S125.
- [65] K. Tachibana, Y. Shimojo, T. Fukuzawa, Kokai Tokkyo Koho, Japan Science and Technology Agency, Japan, 2005, 15pp. (in Japanese).
- [66] T. Bo, S.K. Wiedmer, M.-L. Riekkola, *Electrophoresis* 25 (2004) 1784.
- [67] T. Bo, J. Pawliszyn, *Electrophoresis* 27 (2006) 852.
- [68] T. Bo, J. Pawliszyn, *Anal. Biochem.* 350 (2006) 91.
- [69] G. Bilek, L. Kremser, D. Blaas, E. Kenndler, *Electrophoresis*, submitted for publication.

Gerhard Bilek¹
Leopold Kremser¹
Dieter Blaas^{2*}
Ernst Kenndler¹

¹Institute for Analytical Chemistry,
University of Vienna,
Vienna, Austria

²Max F. Perutz Laboratories,
Vienna Biocenter,
Medical University of Vienna,
Vienna, Austria

Received February 17, 2006

Revised April 14, 2006

Accepted May 11, 2006

Research Article

Capillary electrophoresis of liposomes functionalized for protein binding

CE enabled assessing the attachment of hexa-histidine-tagged proteins to functionalized phospholipid liposomes. The liposomes were made of 1-palmitoyl-2-oleoyl-*sn*-glycero-3-phosphocholine, phosphatidyl-ethanolamine, cholesterol and distearoyl-glycero-3-phosphoethanolamine-*N*-methoxy(polyethylene glycol) in a molar ratio of 29:26:40:5. The unilamellar vesicles, which had an average diameter of 170 nm, were labelled by inclusion of FITC-dextran for fluorescence detection. CE was carried out in poly(vinyl alcohol) (PVA)-coated capillaries at 25°C with a BGE consisting of Tris-HCl (50 mM, pH 8.0). For conjugation of the liposomes with the proteins (soluble synthetic receptor fragments with molecular mass of 60 and 70 kDa, respectively), Ni²⁺ was implanted into the vesicle surface by an anchor lipid containing a nitrilotriacetate acid (NTA) group as complexation agent for the metal ions. The difference in surface charge enabled the separation of the different species of interest by CE: plain vesicles, vesicles functionalised with Ni-NTA, vesicle–protein complexes and the species formed upon removal of the Ni-ions by complexation with EDTA. Loss of the Ni-ions resulted in the release of the proteins and the reappearance of the plain Ni-free NTA-liposome species in the electropherograms.

Keywords: Capillary electrophoresis / Liposomes / Proteins / Surface modification / Vesicles
DOI 10.1002/elps.200600087

1 Introduction

Liposomes can be made with a lipid composition similar to that of plasma membranes or of the membranes of cell organelles, and proteins with a suitable anchor can be inserted to create membranes closely resembling that of their natural counterparts. The defined composition of the system allows avoiding interference of many other components present in natural cellular membranes. This makes liposomes an attractive model for studying interactions of receptors with substances of biochemical, biological or medical interest like drugs, receptor ligands or adhesion molecules in the context of the membrane.

Correspondence: Professor Ernst Kenndler, Institute for Analytical Chemistry, University of Vienna, Währingerstr. 38, A-1090 Vienna, Austria

E-mail: ernst.kenndler@univie.ac.at

Fax: +43-1-4277-9523

Abbreviations: **Ch**, cholesterol; **DOGS-NTA**, 1,2-dioleoyl-*sn*-glycero-3-[(*N*-(5-amino-1-carboxypentyl)iminodiacetic acid)succinyl]; **DLS**, dynamic light scattering; **DSPE-PEG**, 1,2-distearoyl-*sn*-glycero-3-phosphoethanolamine-*N*-[methoxy(polyethylene glycol)-750]; **FL**, fluorescence; **LUV**, large unilamellar vesicle; **MLV**, multilamellar vesicle; **NTA**, nitrilotriacetic acid; **PE**, L- α -phosphatidyl-ethanolamine; **POPC**, 1-palmitoyl-2-oleoyl-*sn*-glycero-3-phosphocholine; **PVA**, poly(vinyl alcohol); **SEC**, size-exclusion chromatography

From the analytical point of view, it is advantageous that liposomes form stable suspensions in aqueous media and move in an electric field. This makes them appealing targets for CE. Many parameters influence the electrophoretic mobility of these vesicles. Liposomes composed of neutral and zwitterionic constituents were considered to be uncharged in BGEs of a pH within the analyte's isoelectric pH range [1]. However, in most cases they exhibit electric charges. For this reason, they can be analyzed by CE, and they proved useful as anionic pseudostationary phases in EKC ([2–22]; for recent reviews see [23, 24]. It was found that, besides the pH, the kind of the electrolytes [6, 25] and its ionic strength [5, 18], and the preparation procedure of the vesicles influences the electrophoretic properties of the particles [23, 26]. If their electrophoretic mobility is affected upon attachment of ligands, this change can be used to assess, or even quantify, the interaction in a form of ACE. This can be realised either under equilibrium or under nonequilibrium conditions, in the latter case given that the kinetic off-rate is low as compared to the time of the electrophoretic analysis.

* Dieter Blaas, E-mail: dieter.blaas@meduniwien.ac.at.

The present work describes the first step in the development of an analytical procedure based mainly on CE to mimic the interaction of viruses with their receptors anchored in biomembranes, with liposomes used as a model. The intention of using PEG-conjugated lipids was to stabilize the vesicle membrane in order to prevent attachment at the capillary wall and to avoid inadvertent vesicle aggregation. Normally, proteins are attached to the liposomal surface by covalent coupling *via* amino or thiol groups [27]. Here we investigate the coordinative binding of a protein, *via* an appended His₆-tag, to the surface of liposomes with an incorporated Ni-nitrilotriacetate acid (NTA)-carrying lipid. A similar approach was used for a frequency surface acoustic waveguide device [28] after preparation of a modified phospholipid bilayer on a silica surface. Here we monitor by CE the interaction between a protein and large unilamellar vesicles (LUVs) in homogeneous solution. Due to the anticipated relatively strong binding (for a His₆-tagged antibody fragment, the complex constant is in the 10⁷ M⁻¹ range [28]), we selected nonequilibrium conditions.

2 Materials and methods

2.1 Chemicals

1-Palmitoyl-2-oleoyl-*sn*-glycero-3-phosphocholine (POPC), L- α -phosphatidyl-ethanolamine (PE), cholesterol (Ch), 1,2-dioleoyl-*sn*-glycero-3-[(N-(5-amino-1-carboxypentyl)iminodiacetic acid)succinyl] (DOGS-NTA), used as Ni salt, and 1,2-distearoyl-*sn*-glycero-3-phosphoethanolamine-*N*-[methoxy(polyethylene glycol)-750] ammonium salt (DSPE-PEG), were all obtained from Avanti Polar Lipids (Alabaster, AL, distributor Instruchemie B.V., The Netherlands). HCl and chloroform (both analytical grade) were from E. Merck (Darmstadt, Germany), Tris and FITC-dextran from Sigma (Milwaukee, WI). The Latex beads used as size standards for size-exclusion chromatography (SEC) were from Polysciences (Warrington, PA). The protein carrying a His₆-tag at its C-terminus was from the Vienna Biocenter (Austria).

2.2 Preparation of multilamellar vesicle (MLV) stocks

POPC, PE, Ch, DOGS-NTA-Ni and DSPE-PEG were dissolved in chloroform to produce five separate lipid stocks with a concentration of 10 mg/mL each [29]. These stock solutions were combined at the desired ratio in a 50 mL pointed flask. The final volume of the mixture was approximately 1 mL. By the aid of a rotary evaporator, the organic solvent was removed under vacuum resulting in a

thin lipid film at the wall of the flask. To ensure uniform deposition of the phospholipids, bottom settings were redissolved twice in 1.5 mL chloroform followed by immediate evaporation. The last evaporation was run for at least 4 h to guarantee a well-dried lipid layer without any traces of solvent [30]. Subsequently, the lipid film was suspended in 2 mL of 50 mM Tris-HCl (pH 8.0). FITC-dextran (70 kDa, 2 mM) was added to label the vesicles. After a hydration period of 30–60 min at 65°C in a water bath, MLVs were produced by 4–7 freeze/thaw cycles; the lipid suspension was frozen in liquid nitrogen and thawed at 65°C in a water bath [31, 32]. The suspension was vortexed between each cycle. Finally, the freshly prepared MLVs were stored in the dark, under N₂ atmosphere, at –20°C (<http://www.avantilipids.com>, 2005).

2.3 Preparation of LUVs by extrusion

The extruder (Mini-Extruder, Avanti Polar Lipids) was equipped with two polycarbonate filters. In imitation of a native cell system, filters with a pore diameter of 400 nm were chosen, accepting the corresponding disadvantage of a higher vesicle-heterogeneity. MLVs were loaded into one of the two syringes, and the apparatus was fully assembled prior to insertion into the heating block. Liposomes were extruded at elevated temperature (>60°C) in order to avoid agglomeration caused by rigid biomembranes. In this way, it was ensured that all vesicle compounds exceeded their phase transition temperature and reached a liquid-crystal state, while the suspension was passed 19 times across the pore channels [33]. The resulting unilamellar vesicles were stored in the dark under N₂ at 4°C (<http://www.avantilipids.com>, 2005).

2.4 Purification and isolation *via* SEC

A Sephacryl S-1000 column (30 cm × 1 cm) was used to separate the vesicles from free FITC-dextran and other low-molecular-weight impurities and byproducts by SEC. The column was equilibrated with 50 mM Tris-HCl (pH 8.0) at 250 μ L/min. The void volume was determined with fluorescent latex beads (200 nm diameter; 120 μ L of a 1:100 dilution of the stock). The vesicle suspension (120 μ L) was then applied and fractions of 300 μ L were collected at 250 μ L/min [34]. The vesicles eluted at the void volume as determined fluorimetrically, using a 96-well plate reader (Wallac 1420 VICTOR V, PerkinElmer, Finland; Software: Wallac 1420 Manager Version 2.0). The parameters were set to 485 nm (excitation) and 535 nm (emission). The fractions were also measured by UV spectroscopy at 280 nm (Hitachi U-2000 spectrophotometer) to confirm the results of the fluorescence (FL) determinations [35].

2.5 Dynamic light scattering (DLS)

DLS measurements were carried out after purification of the liposomes with SEC. The average vesicle diameter was estimated using a Zetasizer (Malvern Nano-ZS, Malvern instruments, UK). For an appropriate concentration, the liposome suspensions were diluted with 50 mM Tris-HCl (pH 8.0) prior to the measurements [36–38].

2.6 CE

CE was performed using two different instruments. One of them was a homemade apparatus equipped with an LIF detector (Ar-laser, Laser-Physics, Reliant 50S-489, 50 mW, λ_{em} 488 nm) [39]. The other was an automated HP3D instrument (Agilent, Waldbronn, Germany) coupled to an external FL-detector (ZETALIF Evolution, Pico-metrics, Ramonville, France) equipped with an Ar-laser (model 163-M12, 25 mW; Spectra-Physics, Mountain View, CA). A poly(vinyl alcohol) (PVA)-coated capillary (Agilent) with an id of 75 μ m was used for the homemade instrument; it was positioned in still air at room temperature ($\sim 25^\circ\text{C}$) without thermostating and had a length of 30.0 cm (effective length 21.5 cm). High voltage was applied by the use of a power supply unit (Type HNC 20.000, Heinzinger Electronic; Germany). Experiments were performed at a constant voltage of -5 kV, with the anode placed at the detector side of the capillary; the resulting current was about 21 μ A. Samples were applied by hydrodynamic injection at the cathodic side of the capillary by lifting the sample vial by 3 cm for 12 s. For FL detection, the emitted light was focused by a microscopic lens system and passed through a filter with a cut-off wavelength of 500 nm. Light intensity was measured with a photomultiplier (Hamamatsu H5785, Shimokanzo, Japan). Data collection was done with DataApex software (Prague, Czech Republic).

An untreated fused-silica capillary (Composite Metal Services) with an id of 75 μ m, a total length of 73.0 cm and an effective length of 58.0 cm was used with the automated HP3D instrument. The capillary was thermostated at 20°C . The applied voltage was $+25$ kV, with the FL-detector placed at the cathodic side of the capillary; the resulting current was about 35 μ A. Sample injection was performed by applying a pressure of 25 mbar for 10 s. Data acquisition and evaluation of the FL-signal was carried out using Agilent ChemStation Plus software.

For all experiments, Tris-HCl 50 mM (pH 8.0), filtered through a 0.20 μ m cellulose acetate filter, was used as BGE. The mobility of the analytes was determined using that of the internal standard (fluorescein) as reference. Prior to each measurement, the capillaries were rinsed with BGE.

3 Results and discussion

3.1 Conditions for the production of liposomes stable for CE

The electrophoretic properties of liposomes are strongly dependent on their composition and the manner how they are produced. In the present work, several lipids, buffer compositions, different fluorescence dyes and extrusion parameters were tested and modified in order to obtain reproducible electropherograms from the liposome. In initial experiments, the vesicles were made of POPC and Ch (65:35 mol%) only, and were labelled by incorporation of pure fluorescein (2 mM dissolved in 50 mM borate buffer pH 7.5). However, it turned out that both, the lipid composition and the nature of the fluorescent dyes were unfavorable. As observed with SEC, incorporated fluorescein was not fully retained by liposomes. Even such a purification of stained vesicles in succession showed free dye, suggesting its release.

Increasing the amount of Ch as described in [33] and addition of PE as further lipid led to liposomes with improved stability; the ratio of the lipids used was 27:25:48 mol% (POPC:PE:Ch). In addition, borate buffer was substituted by Tris-HCl (50 mM, pH 8.0), because, according to the recommendation of the supplier, borate is not well-suited for use in PVA-coated capillaries. Despite advanced lipid compositions, liposomes were still leaky for incorporated fluorescein, as mentioned above. Therefore, coumarin 6, a lipophilic dye, and FITC-dextran were tested. Both dyes have approximately the same fluorescence characteristics as fluorescein ($\lambda_{em}/\lambda_{ex}$ of 494/518 nm). However, presumably because it destabilized the membranes, irreproducible traces were obtained upon CE of liposomes stained with coumarin 6, which tends to insert into the lipid bilayer. In contrast, FITC-dextran was found to be well-retained in the aqueous core of the vesicle. Liposomes produced in this manner were still not suited to render peaks in CE. Thus, a phospholipid conjugated with PEG (DSPE-PEG, see Fig. 1) was added during liposome production to stabilise the membrane. Finally, to allow for attachment of His₆-tagged proteins, DOGS-NTA, a lipid derivatised with NTA (Fig. 1), was also added. The composition of the liposomes used in our studies is as given below in the individual sections.

3.2 Characterization of particle size

Before determining the particle size distribution by DLS, the liposome samples were purified by SEC. As expected, the liposomes were eluted with the void volume (controlled by polystyrene particles). From each sample, at least three DLS measurements were carried out. The results refer to vesicles consisting of POPC, PE, Ch and

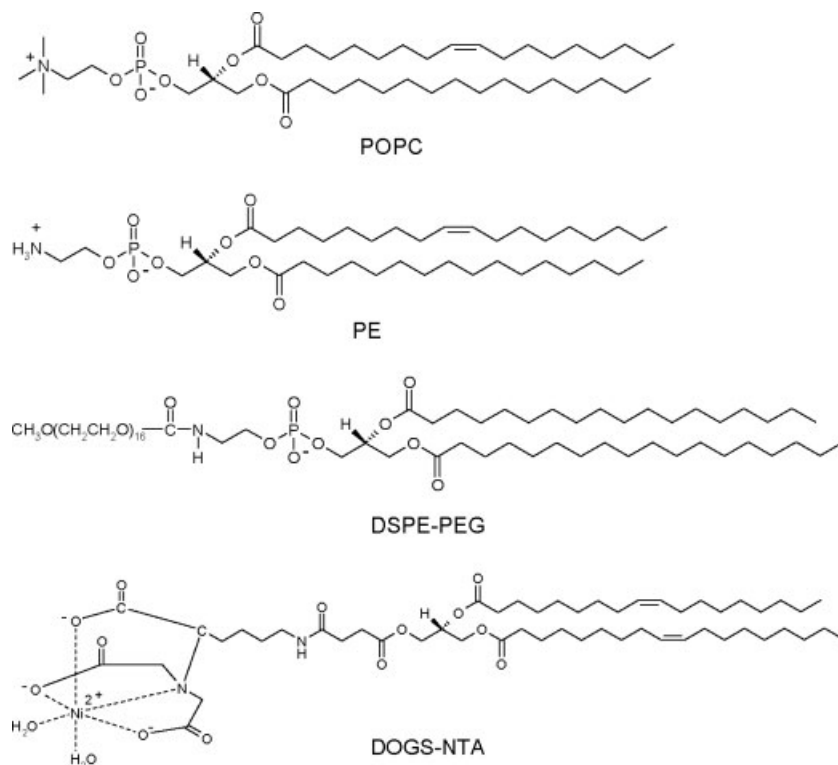


Figure 1. Structural formulae of the constituents of the liposomes investigated in this communication. For PE, the main fatty acids present in the natural product, palmitic and oleic acid are depicted.

DSPE-PEG (29:26:40:5 mol%). DLS gave an average particle diameter \bar{z} of 170.5 nm (it varies for three independent measurements with an SD of 0.6 nm), with a particle size distribution of 65.3 nm. This value is the SD, σ , of the curve depicting the relative frequency of a particular size class *versus* the size class, or, in other words, it is the square root of the second moment of the distribution function. The polydispersity index, PDI, defined as $PDI = (\sigma/\bar{z})^2$, is 0.15. According to this value, the Cumulants algorithm, representative for hypothetical monomodal distributions, was chosen to calculate respective vesicle diameters. For a critical comparison of different algorithm for particle size distribution determination of liposomes see [40].

3.3 CE of liposomes

The following types of liposomes were analyzed: (i) liposomes grafted with DSPE-PEG to increase stability; (ii) Ni-NTA-implanted liposomes (also DSPE-PEG-grafted); (iii) liposomes with the Ni-ions removed from the latter species upon reaction with EDTA. All vesicles were labelled with FITC-dextran dissolved in the aqueous vesicle core. In order to reduce the background fluorescence, SEC was carried out before CE; this step removes the excess dye.

3.3.1 PEG-grafted liposomes

As mentioned above, our attempts at analyzing liposomes consisting of POPC, PE and Ch by CE failed. The results were not reproducible, neither by using untreated nor PVA-coated fused-silica capillaries. Therefore, we decided to stabilize the liposomes by grafting them with DSPE-PEG. This is a lipid consisting of two distearoyl chains, and to which a PEG chain is linked. As the distearoyl groups become part of the membrane, the hydrophilic PEG protrudes from the surface of the liposome, makes it more hydrophilic and reduces aggregation. Figure 2 shows a typical electropherogram of PEG-grafted liposomes (POPC:PE:Ch:DSPE-PEG 29:26:40:5 mol%) using LIF detection at 488/520 nm. The concentration of the liposomes in this sample is given very roughly due to the many procedures applied for their preparation and purification; we assume the concentration given as the lipid content being in the 10^{-4} M range. Fluorescein (2 nM) was added as internal standard prior to each measurement. Note that no neutral marker was used to indicate the (very low) EOF, because even concomitant injection of the marker at the detector end would lead to very long residence times. The time axis of the electropherograms was normalised by the aid of the internal standard to count for variations, e.g. due to the changing EOF.

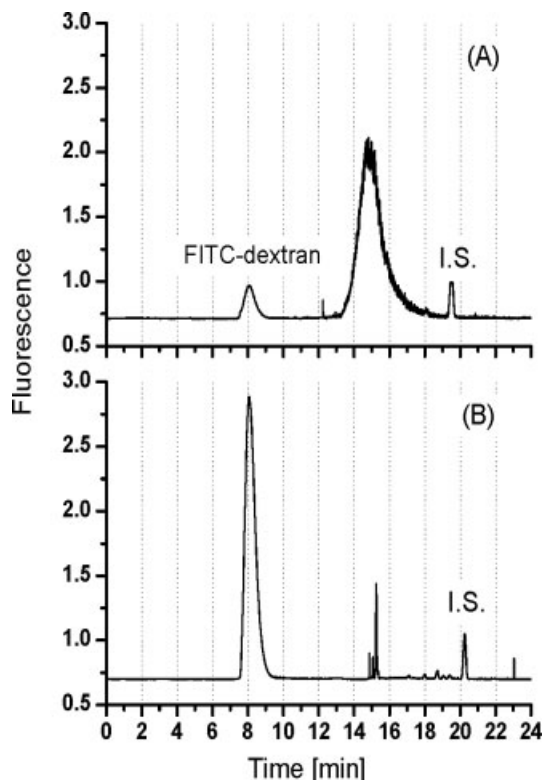


Figure 2. Electropherograms of (A) Ni-NTA-implanted liposomes (lipid ratio POPC:PE:Ch:DSPE-PEG DOGS-NTA-Ni²⁺ = 29:26:40:5.5 mol%, FL-labelled with FITC-dextran); and (B) of liposomes disintegrated by heat treatment (80°C, 15 min) in the presence of 10 mM SDS. IS, internal standard (fluorescein). CE conditions: bare fused-silica capillary, id 75 μ m, total length 73 cm (effective length 58.0 cm). BGE: Tris-HCl, 50 mM, pH 8.0. Constant voltage: +20 kV, current: 35 μ A. Injection by pressure (25 mbar for 10 s) at the anodic side. Temperature, 20°C; fluorescence detection at 488 nm excitation wavelength and 520 nm cut-off.

In most cases, liposomes consisting of POPC, PE and Ch have negative charge, although they consist of either zwitterionic (POPC, PE) or uncharged (Ch) constituents [1, 2, 6, 41]. The present liposomes possess additional negative charges from the phosphate group of DSPE-PEG. The peak assigned to the liposomes is relatively broad in the time domain (Fig. 2A), indicating heterogeneity. However, if we consider the mobility distribution of the species forming this peak, it is surprisingly narrow. Taking the peak in Fig. 2, we can calculate the average mobility derived from the apex as $24.6 \times 10^{-9} \text{ m}^2 \text{V}^{-1} \text{s}^{-1}$. The width of this peak (expressed by its SD) in mobility units is as small as $1.0 \times 10^{-9} \text{ m}^2 \text{V}^{-1} \text{s}^{-1}$, which is only about 4% of the average mobility. This means that 99% ($\pm 3\sigma$) of all particles possess mobilities within $\pm 3 \times 10^{-9} \text{ m}^2 \text{V}^{-1} \text{s}^{-1}$ or within 12% of the average value.

An additional indication for the heterogeneity of the vesicle population can be followed from the seemingly large noise of the peak signal, which is much stronger than that of the baseline (see Fig. 2A). This stronger signal fluctuation is not originating from the detector, but is most probably the result of the numerous vesicle species which are resolved only in part. It is noteworthy in this context that Arriaga *et al.* [42] were able to detect single MLVs with a very fast detector after separation by CE. These vesicles exhibited a similar mobility distribution than those depicted in Fig. 2.

In Fig. 2B, the electropherogram resulting after destruction of the vesicles by heating the sample at 80°C for 15 min is shown. The liposome peak in Fig. 2A has disappeared, and a large peak of the released FITC-dextran arises. This peak has nearly the same corrected area as the initial liposome peak (they differ by only 10%). The three small peaks in the migration range around 15 min are impurities of FITC-dextran.

It is informative to calculate the approximate volume and mass of the vesicles. Taking a particle radius of roughly 100 nm, the volume of a single vesicle is about $4 \times 10^{-15} \text{ cm}^3$. If we assume a density of 1 g/cm³, because the main part of the vesicle is water, a mass of $4 \times 10^{-15} \text{ g}$ follows. The volume of the bilayer, calculated from the surface of the vesicle and the bilayer thickness of 5 nm, is then $\sim 6 \times 10^{-16} \text{ cm}^3$, and its mass roughly $5 \times 10^{-16} \text{ g}$. Thus, the lipids contribute only about 12% to the mass of the entire vesicle.

3.3.2 Ni²⁺-implanted liposomes

In order to allow for binding of a His-tag to the vesicle surface, PEG-grafted liposomes containing Ni²⁺-saturated DOGS-NTA (ratio POPC:PE:Ch:DSPE-PEG:DOGS-NTA = 26:24:40:5:5 mol%) were produced. In the DOGS-NTA molecule (see Fig. 1), the lipid group 1,2-dioleoyl is linked to NTA, a well-known metal-chelating agent. The lipophilic DOGS is imbedded in the membrane, and the NTA-group is exposed to the solvent. The compound occupies four of the six available coordination sites of a Ni-ion (see Fig. 1).

An electropherogram of these Ni-NTA-implanted liposomes (also in an estimated concentration in the 10^{-4} M range, related to the total lipid content) is shown in Fig. 3. A peak similar to the solely PEG-grafted liposomes (Fig. 2) is observed. However, the Ni-NTA-containing liposomes exhibit a shorter migration time; accordingly, these vesicles have a higher average mobility ($29.5 \times 10^{-9} \text{ m}^2 \text{V}^{-1} \text{s}^{-1}$). This is not unexpected because the Ni-NTA lipid should introduce one additional negative

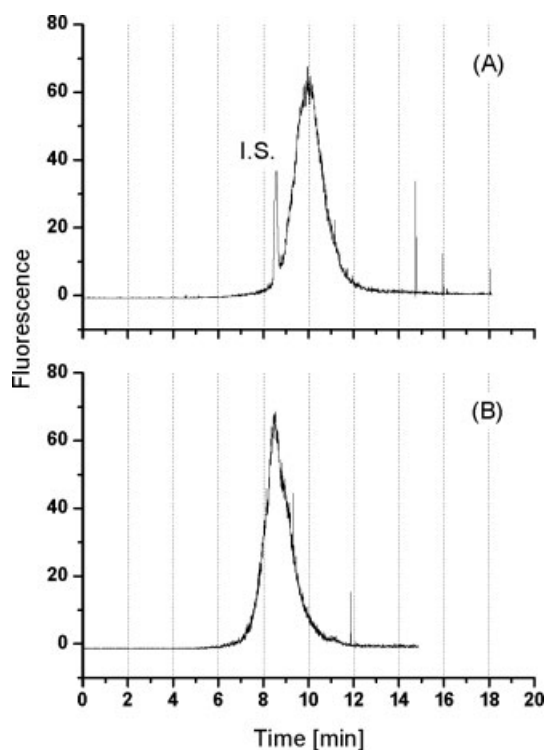


Figure 3. Electropherograms of (A) Ni^{2+} -NTA-implanted liposomes (ratio POPC:PE:Ch:DSPE-PEG:DOGS-NTA- Ni^{2+} = 26:24:40:5:5 mol%, FL-labelled with FITC-dextran); (B) after addition of EDTA (10 mM) to the liposome sample. CE conditions: PVA capillary, id 75 μm , total length 30 cm (effective length 21.5 cm). BGE: Tris-HCl 50 mM, pH 8.0. Constant voltage: -5 kV , current: 21 μA . Hydrodynamic injection at the cathodic side (lifting the inlet by 3 cm for 12 s). Temperature, 25°C ; fluorescence detection at 488 nm excitation wavelength and 500 nm cut-off.

charge. It was observed that the Ni-NTA-containing particles became more heterogeneous than the PEG-grafted liposomes; the SD of the mobilities increased from $1 \times 10^{-9}\text{ m}^2\text{V}^{-1}\text{s}^{-1}$ to $1.4 \times 10^{-9}\text{ m}^2\text{V}^{-1}\text{s}^{-1}$ (see Table 1).

The number of lipid molecules in the bilayer (with a mass of $5 \times 10^{-16}\text{ g}$ per vesicle, see above) is about 3×10^5 (taking 1000 Da as an approximate molecular weight of the lipid). Taking into account that the DOGS-NTA contributes 5% to the total lipid in the bilayer, it can be estimated that each vesicle contains roughly 15 000 DOGS-NTA molecules and consequently the same number of Ni-ions.

The logarithm of the equilibrium binding constants of the complexation reaction between Ni^{2+} and (free) NTA and EDTA are 11.3 and 18.4, respectively (both as anions at ionic strength of 0.1 M) [43]. EDTA will thus remove the Ni-ions, and two negative charges will be added for each

removed Ni^{2+} at the vesicle surface. Since half of the Ni^{2+} is at the inner leaflet of the vesicle and not accessible for the EDTA, roughly 7500 Ni-ions are complexed and consequently 15 000 negative charges will be added per vesicle. Thus, the electrophoretic mobility of the liposome should increase upon addition of EDTA.

This change in mobility can indeed be observed by CE as shown in Fig. 3. Addition of an excess of EDTA leads to a shift of the liposome peak towards shorter migration time (*i.e.* higher mobility). The peak now overlaps with the peak of the internal standard. Removal of the Ni^{2+} resulted in an increase in average mobility by $4.1 \times 10^{-9}\text{ m}^2\text{V}^{-1}\text{s}^{-1}$ to $33.6 \times 10^{-9}\text{ m}^2\text{V}^{-1}\text{s}^{-1}$ (Table 1). The spread remained the same, namely $1.5 \times 10^{-9}\text{ m}^2\text{V}^{-1}\text{s}^{-1}$ or 5%, expressed by the SD.

3.4 Interaction of His-tagged proteins with Ni-implanted liposomes

The NTA-group at the membrane surface occupies four coordination sites of the Ni-ions (Fig. 1). The remaining two sites (normally occupied by two water molecules in aqueous solutions) are accessible for histidines, as are present, *e.g.* in the His₆-tag genetically appended to recombinant proteins for the sake of easy purification.

It should be mentioned that nonequilibrium conditions were used for the binding experiments due to the anticipated relatively large complex constant. It was assumed that it is in the range of 10^7 M^{-1} as reported for a His₆-tagged antibody fragment [28]. Because the concentration of the present reactants are in the 10 μM range, we anticipate sufficient stability of the complex formed by incubation, at least within the CE run. Therefore, we reacted the compounds prior to the measurement instead of adding one reactant to the BGE as in case of equilibrium affinity electrophoresis.

Ni-NTA-containing liposomes were thus incubated with proteins possessing a His₆-tag on the C-terminus of the polypeptide chain. Incubation was simply carried out by mixing the components at room temperature 30 min prior to injection. The proteins were products obtained within the frame of our investigations on virus–receptor interactions. Both proteins were synthetic soluble receptor fragments. Protein1 consists of 540 amino acids and has a molecular mass of approximately 60 kDa, protein2 has 620 amino acids with a molar mass of 70 kDa.

The electropherogram measured after incubation of Ni-NTA-containing liposomes (total lipid concentration range 10^{-4} M) with protein1 (34 μM) is shown in Fig. 4. It can be clearly seen that incubation resulted in a huge shift in migration indicating the attachment of the protein to the

Table 1. Average mobility, μ , of the different liposomes measured from the apex of the electrophoretic peaks and mobility distribution of the species forming the peaks expressed as the SD calculated from the electrophoretic peak widths

Liposome	$\mu^a)$	μ Distri- bution ^{b)}	μ Distri- bution (%)	From Fig.
PEG-grafted	24.6	± 1.0	4	–
PEG-grafted after addition of EDTA	24.7	± 1.1	4	–
PEG-grafted/DOGS-NTA-Ni	29.6	± 1.3	5	3
PEG-grafted/DOGS-NTA-Ni	29.4	± 1.5	5	4
PEG-grafted/DOGS-NTA-Ni	29.4	± 1.2	3	5
PEG-grafted/DOGS-NTA-Ni + His ₆ protein1 (60 kDa)	19.3	± 0.9	3	4
PEG-grafted/DOGS-NTA-Ni + His ₆ protein2 (70 kDa)	26.9	± 1.0	3	5
PEG-grafted/DOGS-NTA-Ni after addition of EDTA	33.6	± 1.5	5	3
PEG-grafted/DOGS-NTA-Ni after addition of EDTA	33.4	± 1.3	4	5
PEG-grafted/DOGS-NTA-Ni + His ₆ protein1 (60 kDa) after addition of EDTA	33.4	± 2.1	7	4
PEG-grafted/DOGS-NTA-Ni + His ₆ protein2 (70 kDa) after addition of EDTA	34.8	± 1.9	5	5

As reference value 33.8 ± 0.1 ($n = 5$) was used for the determination of the mobility of fluorescein, taken as the internal standard. The relative error in the measurement of the mobility (expressed by the SD, $n = 5$, was $0.2\text{--}0.4 \times 10^{-9} \text{ m}^2\text{V}^{-1}\text{s}^{-1}$).

a) ($\ln 10^{-9} \text{ m}^2\text{V}^{-1}\text{s}^{-1}$); measured from peak apex.

b) ($\ln 10^{-9} \text{ m}^2\text{V}^{-1}\text{s}^{-1}$); measurement in triplicate.

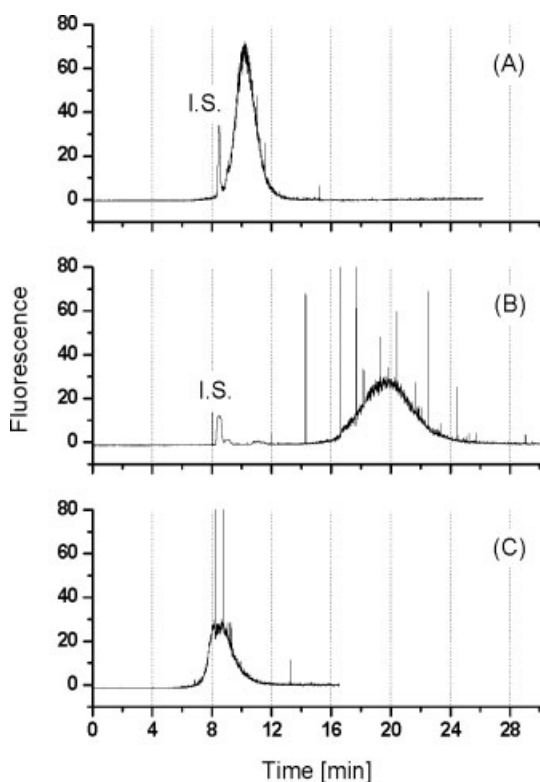


Figure 4. Electropherograms of (A) Ni^{2+} -NTA-containing liposomes, (B) liposomes as in (A) but incubated with $33.8 \mu\text{M}$ protein1 possessing a His₆-tag; (C) liposomes as in (B) after addition of EDTA (20 mM). Liposomes were produced with a lipid ratio POPC:PE:Ch:DSPE-PEG-DOGS-NTA- $\text{Ni}^{2+} = 26:24:40:5:5$ mol%, FL-labelled with FITC-dextran. CE conditions as in Fig. 3.

liposomes. Indeed, the mobility of the liposomes changes by nearly 1/3 from 29.4 to $19.3 \times 10^{-9} \text{ m}^2\text{V}^{-1}\text{s}^{-1}$ (Table 1). Formation of a liposome–protein complex was evidenced by the addition of EDTA. As seen in Fig. 4, in the presence of EDTA, a peak of Ni^{2+} -free NTA-liposome (see Fig. 3) reappeared. The peaks had in fact the same mobility: 33.6 versus $33.4 \times 10^{-9} \text{ m}^2\text{V}^{-1}\text{s}^{-1}$, see Table 1.

By the same means, complex formation between Ni^{2+} -NTA-containing liposomes and protein2 ($7.4 \mu\text{M}$) was assessed by CE (see Fig. 5). Incubation of the liposomes (the average mobility as derived from this Fig. is $29.4 \times 10^{-9} \text{ m}^2\text{V}^{-1}\text{s}^{-1}$) with the protein gave rise to a shift of the liposome peak to a higher migration time corresponding to a reduction in average mobility to $26.9 \times 10^{-9} \text{ m}^2\text{V}^{-1}\text{s}^{-1}$. As in Fig. 4, treatment of the complex with EDTA reconstituted the DOGS-NTA-containing but Ni^{2+} -free liposome with an average mobility of $34.8 \times 10^{-9} \text{ m}^2\text{V}^{-1}\text{s}^{-1}$.

Although there is clear evidence for specific binding of the proteins *via* their His-tags to Ni-NTA of the liposomes, the question arises whether unspecific binding of the protein to the lipid membrane has an effect on the electrophoretic properties of the vesicles. To clarify this aspect, solely PEG-grafted liposomes (not containing Ni-NTA) were incubated under the same conditions with the protein and the mixture analyzed by CE. The result is shown for protein2 in Fig. 6. Indeed, no change in mobility is observed (the mobilities differ by only $0.1 \times 10^{-9} \text{ m}^2\text{V}^{-1}\text{s}^{-1}$). Although the peak in Fig. 6B seems narrower, this is not

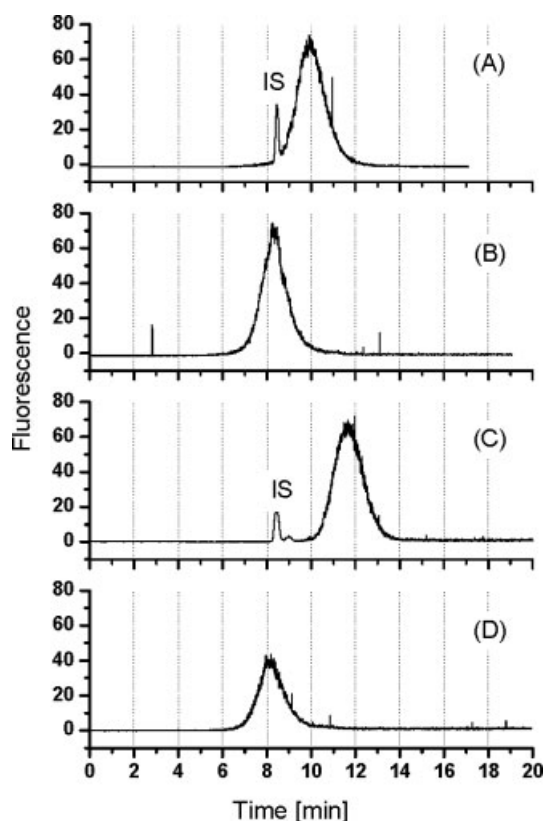


Figure 5. Electropherograms of (A) Ni^{2+} -NTA-containing liposomes, (B) liposomes as in (A) after the addition of 10 mM EDTA, (C) liposomes as in (A) but incubated with 7.4 μM protein2 possessing a His₆-tag; (D) liposomes as in (C) but after the addition of EDTA (20 mM). Liposomes were produced with a lipid ratio POPC:PE:Ch:DSPE-PEG:DOGS-NTA- Ni^{2+} = 26:24:40:5:5 mol%, FL-labelled with FITC-dextran. CE conditions as in Fig. 3.

confirmed when the calculated peak widths are compared. Expressed in mobility, both peaks have a spread of $0.8 \times 10^{-9} \text{ m}^2\text{V}^{-1}\text{s}^{-1}$ (given as SDs in 0.6 of the height). It is obvious that this result is not a direct confirmation of the absence of unspecific binding, but it corroborates that, even when present, it does not influence the mobility significantly. This is in clear contrast to the results found when the protein decorates the liposome by specific attachment.

Finally, the less probable influence of EDTA on the electrophoretic property of the vesicles is briefly discussed. In order to prove this effect, again solely PEG-grafted liposomes (not containing Ni-NTA) were incubated with EDTA (10 mM) and the mobilities before and after incubation were measured. The result is also given in Table 1. It was found that (as expected) EDTA does not affect the mobilities (24.6 vs. 24.7, both in $10^{-9} \text{ m}^2\text{V}^{-1}\text{s}^{-1}$) within the measuring error: SD was $0.3 \times 10^{-9} \text{ m}^2\text{V}^{-1}\text{s}^{-1}$, $n = 5$.

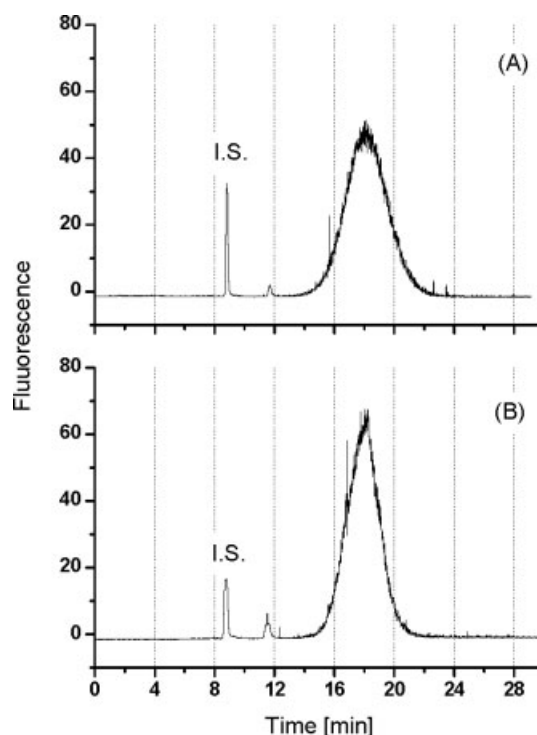


Figure 6. Electropherograms of (A) PEG-grafted liposomes (lipid ratio POPC:PE:Ch:DSPE-PEG = 29:26:40:5 mol%, FL-labelled with FITC-dextran); and (B) liposomes as in (A) after incubation with 5.9 μM protein2. CE conditions as in Fig. 3.

4 Concluding remarks

CE is well-suited to monitor the binding of proteins to liposomes. It enables the assessment of specific protein-liposome interaction, especially by the shift in the electrophoretic mobility. The method paves the way to study the interaction between liposome-attached proteins and their ligands, mimicking the situation prevailing at the surface of natural cell membranes. The method has a number of advantages. In addition to the well-known high speed of analysis and large flexibility in system modification, it is especially the low consumption of analytes, carriers and modifiers which is often a large benefit in bioanalysis. In many cases, analytes are available only in minute amounts; carriers and modifiers are expensive and/or not simply obtainable. As a major advantage, the system works in homogeneous solution, which can approximate physiological conditions. Interactions between the reactants are not hindered by steric restrictions, in contrast to most immunoassays involving the attachment of one analyte to a plastic surface.

The technique appears particularly promising for binding experiments based on the interaction of ligands with a membrane protein. The latter can be produced in a sol-

uble form, i.e. without its hydrophobic membrane anchor, and subsequently being attached to the lipid bilayer via a genetically appended hexa-His tag. Interactions of these protein-carrying liposomes with ligands that modify the migration behavior of the liposomes in the electric field can then be monitored by CE easily and with great sensitivity.

This work was supported by the Austrian Science Foundation (Project P15667). The authors thank Jari Hautala and Marja-Liisa Riekkola (University of Helsinki) for helpful suggestions for liposome stabilization and Andreas Wagner (Polymun Scientific, Vienna) for the possibility to carry out the DLS measurements.

5 References

- [1] Zhang, Y., Zhang, R., Hjertén, S., Lundahl, P., *Electrophoresis* 1995, 16, 1519–23.
- [2] Roberts, M. A., Locascio-Brown, L., MacCrehan, W. A., Durst, R. A., *Anal. Chem.* 1996, 68, 3434–3440.
- [3] Hong, M., Weekley, B. S., Grieb, S. J., Foley, J. P., *Anal. Chem.* 1998, 70, 1394–1403.
- [4] Pascoe, R. J., Peterson, A. G., Foley, J. P., *Electrophoresis* 2000, 21, 2033–42.
- [5] Radko, S. P., Štastná, M., Chrambach, A., *Anal. Chem.* 2000, 72, 5955–5960.
- [6] Wiedmer, S. K., Holopainen, J. M., Mustakangas, P., Kinnunen, P. K. J., Riekkola, M.-L., *Electrophoresis* 2000, 21, 3191–3198.
- [7] Agbodjan, A. A., Bui, H., Khaledi, M. G., *Langmuir* 2001, 17, 2893–2899.
- [8] Wiedmer, S. K., Hautala, J., Holopainen, J. M., Kinnunen, P. K. J., Riekkola, M.-L., *Electrophoresis* 2001, 22, 1305–1313.
- [9] Burns, S. T., Khaledi, M. G., *J. Pharm. Sci.* 2002, 91, 1601–1612.
- [10] Burns, S. T., Agbodjan, A. A., Khaledi, M. G., *J. Chromatogr. A* 2002, 973, 167–76.
- [11] Pascoe, R., Foley, J. P., *Electrophoresis* 2002, 23, 1618–27.
- [12] Peng, X., Sternberg, E., Dolphin, D., *Electrophoresis* 2002, 23, 93–101.
- [13] Wiedmer, S. K., Jussila, M. S., Holopainen, J. M., Alakoskela, J.-M. et al., *J. Sep. Sci.* 2002, 25, 427–437.
- [14] Agbodjan, A. A., Khaledi, M. G., *J. Chromatogr. A* 2003, 1004, 145–53.
- [15] Manetto, G., Silvana Bellini, M., Deyl, Z., *J. Chromatogr. A* 2003, 990, 205–214.
- [16] Pascoe, R. J., Foley, J. P., *Electrophoresis* 2003, 24, 4227–40.
- [17] Tsukagoshi, K., *Bunseki Kagaku* 2003, 52, 1–13.
- [18] Carrozzino, J. M., Khaledi, M. G., *Pharm. Res.* 2004, 21, 2327–35.
- [19] Dey, J., Mohanty, A., Roy, S., Khatua, D., *J. Chromatogr. A* 2004, 1048, 127–32.
- [20] Pysher, M. D., Hayes, M. A., *Langmuir* 2004, 20, 4369–4375.
- [21] Carrozzino, J. M., Khaledi, M. G., *J. Chromatogr. A* 2005, 1079, 307–16.
- [22] Mohanty, A., Dey, J., *J. Chromatogr. A* 2005, 1070, 185–92.
- [23] Wiedmer, S. K., Jussila, M. S., Riekkola, M.-L., *TrAC* 2004, 23, 562–582.
- [24] Wiedmer, S. K., Jussila, M., Hakala, R. M. S., Pystynen, K.-H., Riekkola, M.-L., *Electrophoresis* 2005, 26, 1920–1927.
- [25] Bilek, G., Kremser, L., Blaas, D., Kenndler, E., *J. Chromatogr. B* 2006, 841, 38–51.
- [26] Gomez-Hens, A., Manuel Fernandez-Romero, J., *TrAC* 2005, 24, 9–19.
- [27] Torchilin, V. P., Weissig, V., Martin, F. J., Heath, T. D., New, R. C., in: Weissig, V. (Ed.), *Liposomes*, Oxford University Press, Oxford 2003.
- [28] Gizeli, E., Glad, J., *Anal. Chem.* 2004, 76, 3995–4001.
- [29] Rappolt, M., Vidal, M. F., Kriechbaum, M., Steinhart, M. et al., *Eur. Biophys. J.* 2003, 31, 575–585.
- [30] De Maria, P., Filippone, P., Fontana, A., Gasbarri, C. et al., *Colloids Surf. B* 2005, 40, 11–18.
- [31] Traikia, M., Warschawski, D. E., Recouvreux, M., Cartaud, J., Devaux, P. F., *Eur. Biophys. J.* 2000, 29, 184–195.
- [32] Corradini, D., Mancini, G., Bello, C., *Chromatographia* 2004, 60, S125–S132.
- [33] Patty, P. J., Frisken, B. J., *Biophys. J.* 2003, 85, 996–1004.
- [34] Ingebrigtsen, L., Brandl, M., *Pharmaceutics* 2002, 3, 1–7.
- [35] Kawakami, K., Nishihara, Y., Hirano, K., *J. Colloid Interface Sci.* 1998, 206, 177–180.
- [36] Schurtenberger, P., Hauser, H., *Biochimica* 1984, 778, 470–480.
- [37] Hunter, D. G., Frisken, B. J., *Biophys. J.* 1998, 74, 2996–3002.
- [38] Käsbauer, M., Lasic, D. D., Winterhalter, M., *Elsevier* 1997, 86, 153–159.
- [39] Kremser, L., Konecni, T., Blaas, D., Kenndler, E., *Anal. Chem.* 2004, 76, 4175–4181.
- [40] Vorauer-Uhl, K., Wagner, A., Borth, N., Katinger, H., *Cytometry* 2000, 39, 166–71.
- [41] Kessler, R., Manz, H. J., *Electrophoresis* 1990, 11, 979–80.
- [42] Duffy, C. F., Gafoor, S., Richards, D. P., Admadzadeh, H. et al., *Anal. Chem.* 2001, 73, 1855–1861.
- [43] Seel, F., *Grundlagen der analytischen Chemie: unter besonderer Berücksichtigung der Chemie in wäßrigen Systemen*, Verlag Chemie, Weinheim 1979.

Mimicking Early Events of Virus Infection: Capillary Electrophoretic Analysis of Virus Attachment to Receptor-Decorated Liposomes

Gerhard Bilek,^{†,‡} Leopold Kremser,[†] Jürgen Wruss,[‡] Dieter Blaas,[‡] and Ernst Kenndler^{*,†}

Institute for Analytical Chemistry, University of Vienna, A-1090 Vienna, Austria, and Max F. Perutz Laboratories, Vienna Biocenter, Medical University of Vienna, Vienna, Austria

The attachment of human rhinovirus serotype 2 to an artificial cell membrane was followed by capillary electrophoresis. The cell membrane was mimicked by liposomes (average diameter of about 190 nm) containing a lipid with a nitrilotriacetic acid (NTA) group. This group, in the presence of Ni^{2+} ions, served as anchor for the his_6 -tags of recombinant derivatives of the very-low-density lipoprotein (VLDL) receptor comprising either modules 1, 2, and 3 (V123) or five tandem copies of module 3 (V33333). We demonstrate by capillary electrophoresis with laser induced fluorescence detection of the liposomes that the minor receptor group rhinovirus HRV2 binds specifically to the receptor-decorated vesicles; the major receptor group rhinovirus HRV14, which uses a different receptor for cell binding, does not attach to the liposomes.

The very first event in virus infection is the specific attachment of the virion to structures at the host cell membrane, which are termed “virus receptors”, neglecting the fact that their original function lies in cell–cell interaction and/or metabolism of the cell. Viruses have adapted to exploit these molecules for their proper benefit. The membrane of eukaryotic cells is complex and contains many different proteins attached to or embedded in the lipid bilayer. This complicates the analysis of virus binding to specific receptors in their biological context. A simpler system, mimicking the cell membrane with its physicochemical properties but containing only one type of protein at the time, can be realized with liposomes. These vesicles can be made to carry the proteins of choice attached by various means like insertion via hydrophobic transmembrane sequences, binding via covalently linked lipids, or by making use of noncovalent attachment of the proteins to suitable functional groups connected to chemically modified lipids. Based on the latter concept, in the present work, we established a model for the interaction between a minor group human rhinovirus (HRV) and its cognate receptors, members of the low-density lipoprotein receptor family, and used capillary electrophoresis (CE) for its analysis.

Modeling of virus attachment was carried out in different steps, as depicted schematically in Figure 1. First, liposomes were

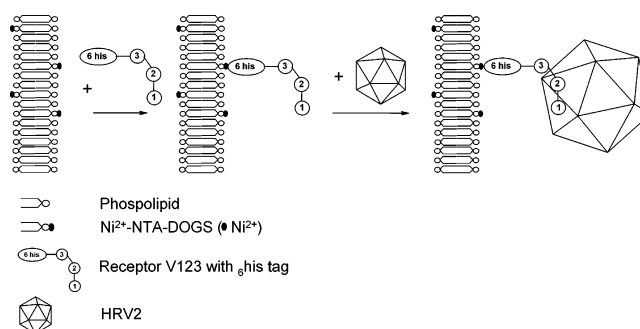


Figure 1. Schematic representation of the attachment of HRV2 to the liposome membrane. A ternary adduct is formed from the Ni^{2+} –NTA–implanted liposome, receptor construct V123, and HRV2. A part of the liposome bilayer is shown that contains the NTA–lipid with complexed Ni^{2+} ions. The receptor construct binds via its his_6 -tag to the membrane surface by complexation with the Ni^{2+} ions. Finally, HRV2 binds biospecifically to the liposome surface via the modules of the receptor construct. The average diameter of the liposomal vesicles is about 190 nm, their bilayer thickness is about 5 nm, and HRV2 diameter is about 30 nm. Note that the MBP fused to the N-terminus of the receptor is depicted.

prepared from standard lipids including nitrilotriacetate (NTA)-modified dioleoyl-glycerol complexed with Ni^{2+} -ions. A recombinant soluble receptor construct containing a hexa-histidine tag (his_6 -tag) at its C-terminus was then attached via the Ni^{2+} –NTA–lipid to the liposome surface. As a result, a receptor-decorated vesicle was formed modeling the cell membrane. Finally, virus was attached to these receptor-decorated vesicles via biospecific interaction. All individual steps were followed by CE via laser-induced fluorescence (LIF) detection of a fluorescent dye dissolved in the aqueous vesicle core of the liposomes.

EXPERIMENTAL SECTION

Instrumentation. CE with LIF detection was carried out with a homemade instrument consisting of an Ar-laser (Reliant 50S-489, 50 mW, Laser-Physics), a high voltage power supply unit (HNC 20.000, Heinzinger Electronic, Germany), and an optical bench where the fluorescence light was focused by a microscopic lens system and passed through a cutoff filter (500 nm) before reaching the photomultiplier (Hamamatsu H5785, Shimokanzo, Japan). Data were collected with the DataApex software (Prague, Czech Republic). A PVA-coated capillary (30.0/21.5 cm length, 75 or 100 μm inner diameter (ID); Agilent, Waldbronn, Germany) was used with the detection window placed at the anodic side of

* To whom correspondence should be addressed. E-mail: ernst.kenndler@univie.ac.at.

[†] University of Vienna.

[‡] Medical University of Vienna.

the instrument. The capillary was positioned in still air at room temperature ($\sim 25^\circ\text{C}$) without thermostating. The background electrolyte for the CE analysis of the liposomes consisted of tris-(hydroxymethyl)-aminomethan (Tris)/HCl (50 mmol L^{-1} , pH 8.0). Experiments were performed at a constant voltage of -5 kV ; the resulting current was about $21\text{ }\mu\text{A}$. Samples were applied by hydrodynamic injection at the cathodic side of the capillary by lifting the sample vial by 3 cm for 12 s .

CE with UV detection was performed with an automated HP3D instrument (Agilent) equipped with a diode array UV-vis detector ($190\text{--}600\text{ nm}$). An untreated fused-silica capillary ($68.0/59.5\text{ cm}$ length, $75\text{ }\mu\text{m}$ ID; Composite Metal Services Ltd.) was used and thermostated at 20°C . The separation buffer was prepared by adjusting boric acid (100 mmol L^{-1}) with NaOH to pH 8.3 and adding SDS to 10 mmol L^{-1} . The applied voltage was $+20\text{ kV}$, with the UV detector placed at the cathodic side of the capillary; the resulting current was about $25\text{ }\mu\text{A}$. Samples were injected by 25 mbar pressure for 10 s .

The average vesicle diameter and the size-distribution of purified liposome preparations were determined by using dynamic light scattering on a Zetasizer (Malvern Nano-ZS, Malvern instruments, U.K.). The suspensions of the liposomes were diluted with 50 mM Tris-HCl (pH 8.0) to a concentration appropriate for the measuring range of the instrument. This is described in more detail in ref 1.

The Ni concentration of the liposomes was determined by atomic absorbance spectroscopy (AAS) using a 4100 ZL instrument (Perkin-Elmer) with a transverse heated graphite atomizer in the stabilized temperature platform furnace technique and Zeeman-effect background correction (longitudinal). A Ni hollow cathode lamp (25 mA , slit 0.2 mm , wavelength: 232.0 nm) was used. Sample volume was $20\text{ }\mu\text{L}$; analyses were performed without chemical modifiers. The organic matrix was dry ashed in the graphite tube with air at 500°C . For the individual steps of analysis, the following temperatures were applied: ashing, 500°C , pyrolysis, 1100°C , atomization, 2400°C , cleaning, 2450°C . Ar flow was 250 mL min^{-1} .

Reagents. Liposomes were made from 1-palmitoyl-2-oleoyl-*sn*-glycero-3-phosphocholine (POPC), 1- α -phosphatidylethanolamine (PE), cholesterol (Ch), the ammonium salt of 1,2-distearoyl-*sn*-glycero-3-phosphoethanolamine-*N*-[methoxy(polyethyleneglycol)-750] (DSPE-PEG), and the Ni^{2+} salt of 1,2-dioleoyl-*sn*-glycero-3-[(*N*-(5-amino-1-carboxypentyl) iminodiacetic acid) succinyl] (Ni^{2+} -NTA-DOGS), all obtained from Avanti Polar Lipids (Alabaster, AL, distributor Instruchemie B.V., Netherlands). HCl, NaOH, boric acid, and chloroform (p.a.) were from E. Merck (Darmstadt, Germany). Tris and fluorescein isothiocyanate (FITC)-dextran (70 kDa) were from Sigma (Milwaukee, WI). Fluorescence latex beads used as standards in size exclusion chromatography (SEC) were from Polysciences (Warrington, PA).

The major group rhinovirus HRV14 and the minor group rhinovirus HRV2 were grown in HeLa H1 suspension culture and purified as described elsewhere.² The virus concentration and the purity of the virus were monitored by CE.³ The virus stock solutions were at 5.7 mg/mL (HRV2) and 1.3 mg/mL (HRV14).

Two recombinant soluble receptor constructs, derived from the human very low-density lipoprotein receptor (VLDLR), were expressed and purified as described.⁴ Both were expressed and used for all experiments as fusion proteins, carrying at their N-terminus the maltose-binding protein (MBP) and at their C-terminus a his₆-tag. V123 comprises the first three ligand binding modules of VLDLR, and V33333 is an artificial concatemer of five copies of the third module of VLDLR. They exhibit different functional affinity (avidity) toward HRV2.^{5,6} The concentration of the respective receptor stock solutions was 8 mg/mL for V123 and 2 mg/mL for V33333.

SEC was carried out on a Sephacryl S-1000 column from GE Healthcare, Uppsala, Sweden.

Procedures. Multilamellar vesicle (MLV) suspensions were prepared by dissolving POPC, PE, Ch, DSPE-PEG, and Ni^{2+} -NTA-DOGS in chloroform to produce separate lipid stocks with a concentration of 10 mg/mL each. These chloroform stocks were combined in a 50 mL pointed flask at a ratio of POPC:PE:Ch:DSPE-PEG: Ni^{2+} -NTA-DOGS = $26:24:40:5:5$ [mol %] to produce Ni^{2+} -NTA implanted vesicles with PEG grafting as described in ref 1. Briefly, the organic solvent of the final mixture (approximately 1.5 mL) was removed under vacuum by the aid of a rotary evaporator. To ensure uniform deposition of the lipids as a thin film, the bottom settings were redissolved twice in 1.5 mL of chloroform followed by immediate evaporation. The last evaporation was conducted for at least 4 h to ensure complete removal of traces of the solvent. Subsequently, the lipid film was hydrated in 2.5 mL of 50 mmol L^{-1} Tris-HCl (pH 8.0), containing $70\text{ }\mu\text{mol L}^{-1}$ FITC-dextran to label the vesicles. After $30\text{--}60\text{ min}$ at 65°C in a water bath, MLVs were produced by $3\text{--}6$ freeze/thaw cycles; the lipid suspension was frozen in liquid nitrogen, thawed at 65°C in a water bath, and vortexed to peel off the lipid film. To avoid oxidation, freshly produced MLVs were gassed with N_2 before storing them at -20°C in the dark.

To form large unilamellar vesicles (LUVs) that better mimic the cell surface, MLVs were passed through two polycarbonate filters with a pore diameter of 400 nm by the aid of an extruder (Mini-Extruder, Avanti Polar Lipids) at 65°C to prevent aggregation of the rigid lipid membranes. Under this condition, all lipids are above their phase transition temperature and in a liquid-crystal state. The suspension was passed 21 times through the filters. The resulting LUVs were stored under N_2 atmosphere at 4°C in the dark.

Vesicles were separated from free FITC-dextran and other low-molecular weight contaminants by SEC, using a Sephacryl S-1000 column ($30\text{ cm} \times 1\text{ cm}$). The column was equilibrated with 50 mM Tris-HCl (pH 8.0), and its void volume was determined at $250\text{ }\mu\text{L/min}$ with fluorescent latex beads (200 nm diameter; $120\text{ }\mu\text{L}$ of a $1:100$ dilution of the stock). Next, the LUV suspension ($120\text{ }\mu\text{L}$) was applied, and SEC was carried out with the same mobile phase at the same flow rate; fractions of $300\text{ }\mu\text{L}$ were collected. The liposomes eluted with the void volume as deter-

(1) Bilek, G.; Kremser, L.; Blaas, D.; Kenndler, E. *Electrophoresis* **2006**, *27*, 3999–4007.

(2) Kienberger, F.; Zhu, R.; Moser, R.; Blaas, D.; Hinterdorfer, P. *J. Virol.* **2004**, *78*, 3203–3209.

(3) Okun, V. M.; Ronacher, B.; Blaas, D.; Kenndler, E. *Anal. Chem.* **1999**, *71*, 2028–2032.

(4) Ronacher, B.; Marlovits, T. C.; Moser, R.; Blaas, D. *Virology* **2000**, *278*, 541–550.

(5) Moser, R.; Snyers, L.; Wruss, J.; Angulo, J.; Peters, H.; Peters, T.; Blaas, D. *Virology* **2005**, *338*, 259–269.

(6) Okun, V. M.; Moser, R.; Ronacher, B.; Kenndler, E.; Blaas, D. *J. Biol. Chem.* **2001**, *276*, 1057–1062.

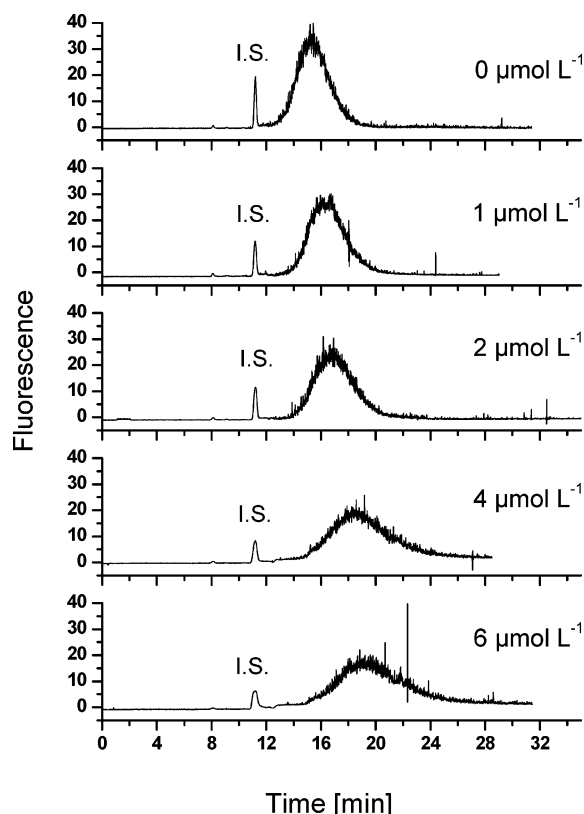


Figure 2. Electropherograms of liposomes containing Ni^{2+} -NTA-carrying lipid, incubated with increasing concentration of V33333 (between 1 and $6 \mu\text{mol L}^{-1}$). Liposome composition: POPC:PE:Ch:DSPE-PEG: Ni^{2+} -NTA-DOGS = 26:24:40:5:5 mol %, FL-labeled with FITC-dextran ($70 \mu\text{mol L}^{-1}$). Ni^{2+} -NTA concentration (5% of total lipid) accessible for receptor binding in the incubation mixture is $1.8 \mu\text{mol L}^{-1}$. I.S. internal standard (fluorescein), 2 nmol L^{-1} . CE-conditions: PVA capillary, 30 cm/21.5 cm length, ID $75 \mu\text{m}$. BGE: Tris-HCl, 50 mM, pH 8.0. Voltage, -5 kV ; current, $21 \mu\text{A}$. Hydrodynamic injection at the cathodic side (lifting the inlet by 3 cm for 12 s). Temperature 25°C ; fluorescence detection at 488 nm excitation wavelength and 500 nm cutoff.

mined by fluorimetry, using a 96-well plate reader (Wallac 1420 VICTOR V, Perkin-Elmer, Finland) set at 485 nm excitation and 535 nm emission wavelength. Fractions were also subjected to UV spectrometry at 280 nm (Hitachi U-2000 spectrophotometer) to confirm the location of the peak.

RESULTS AND DISCUSSION

Receptor-Decorated Liposomes. VLDL-receptors are mosaic proteins that most probably evolved from single modules and building blocks. Their ligand-binding domains at the N-terminus are composed of various numbers of ligand binding repeats or type A modules, each about 40 amino acids in length, among them 6 cysteines that are all engaged in disulfide bridges. VLDLR has 8 ligand binding repeats. V33333 is a synthetic soluble receptor construct; it is a concatemer of five copies of module 3 of VLDLR fused to MBP. The complete receptor construct (including MBP) consists of 620 amino acids and has a molecular mass of 67 439 Da. As it possesses a 6 histidine tag, it binds to Ni^{2+} -NTA of the NTA-DOGS lipid present in the liposome membrane. The resulting vesicles can be considered a simplified model of a cell with epitopes for viral attachment. For decoration with the receptor

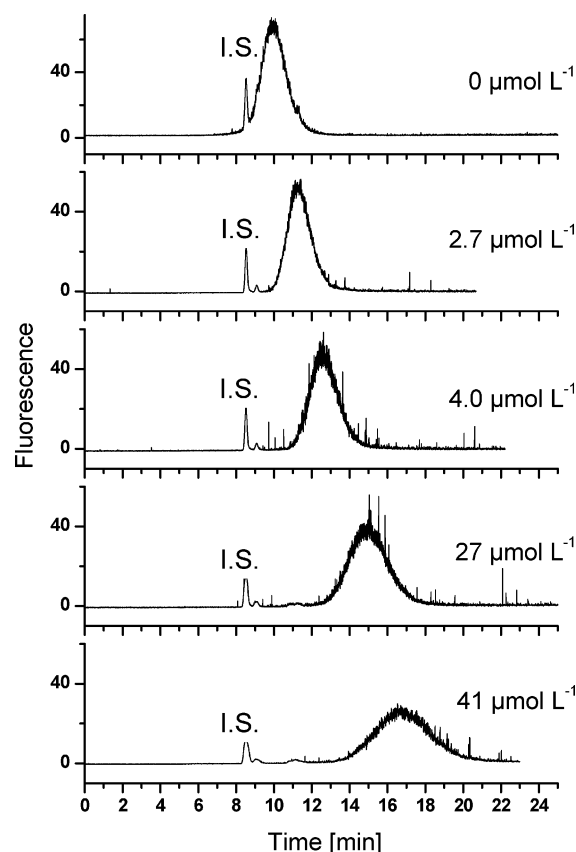


Figure 3. Electropherograms of Ni^{2+} -NTA-lipid containing liposomes after incubation with increasing concentrations of V123 (between 2.7 and $41 \mu\text{mol L}^{-1}$). Ni^{2+} -NTA concentration (5% of total lipid) accessible for receptor binding in the incubation mixture is $2.0 \mu\text{mol L}^{-1}$. Liposome composition and CE conditions are as in Figure 2.

constructs, the Ni^{2+} -NTA-implanted liposomes were reacted with V33333 with increasing concentrations (between 1 and $6 \mu\text{mol L}^{-1}$), and the resulting products were analyzed by CE-LIF. The electropherograms are shown in Figure 2. It can be seen that a typical, relatively broad liposome peak is obtained, which gradually shifts to longer migration time with increasing V33333 concentration in the reaction mixture. The change in the mobility clearly demonstrates attachment of the receptors to the liposome surface; the broadening of the peak with increasing receptor concentration is most probably due to heterogeneity resulting from a mixture of liposomes carrying different numbers of receptors.

Similarly, another recombinant soluble receptor construct, V123, was attached to the functionalized liposomes. This fragment consists of the first three modules of VLDLR. V123 encompasses 535 amino acid residues with a total molecular mass of 59122 Da. As V33333, V123 is fused to MBP and carries a C-terminal his₆-tag. The electropherograms obtained upon incubation of the Ni^{2+} -NTA-functionalized liposomes at increasing concentrations of V123 are depicted in Figure 3. The liposome suspension had approximately the same concentration as in the experiments described for V33333. Again, upon addition of increasing amounts of V123 (from 2.7 to $68 \mu\text{mol L}^{-1}$), a gradual shift of the liposome peak was observed. The plateau of its mobility at the higher concentrations of the receptor in the incubation mixture (Figure 4) indicates that saturation with the receptor occurs above $\sim 35 \mu\text{mol L}^{-1}$. Saturation was not attained with V33333, as the

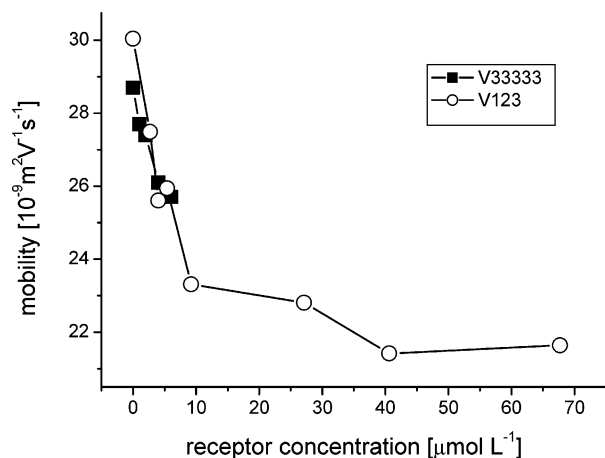


Figure 4. Mobilities of the liposomes (as measured at the apex of the peaks shown in Figures 2 and 3) at different concentrations of the recombinant receptor fragments V123 and V33333, respectively, in the incubation mixture with the Ni^{2+} -NTA-carrying vesicles. The mobilities were typically reproducible within $1 \times 10^{-9} \text{ m}^2 \text{ V}^{-1} \text{ s}^{-1}$, according to a relative standard deviation of about 4% (for 3–5 measurements).

concentration of the available stock solution was lower than that of V123 (see Experimental Section).

The Ni^{2+} -concentration in the samples was determined by AAS (note that the Ni-NTA-containing lipid contributed only 5% of total lipid). The Ni^{2+} concentration as obtained after size exclusion chromatography of the liposomes was estimated to about $16 \mu\text{mol L}^{-1}$. Consequently to dilution upon addition of V33333, the final Ni^{2+} concentration was thus $3.6 \mu\text{mol L}^{-1}$. Because one-half of the NTA is located at the inner face of the liposome and is thus not accessible, roughly $1.8 \mu\text{mol L}^{-1}$ of the Ni^{2+} -NTA is available for complex formation with the his₆-tagged receptor (for concentrations of the components in the other binding experiments, see figure legends). It is remarkable that the receptor concentration required to reach the plateau of the binding curve is considerably higher. Several causes can be responsible for this effect. The most probable reason is the dissociation of the Ni^{2+} -NTA/receptor complex; the equilibrium dissociation constant of the binding reaction between Ni^{2+} -NTA and a his₆ tag is about 10^{-5} – $10^{-6} \text{ mol L}^{-1}$.^{7–9} As this is within the concentration range of the analytes in the incubation mixture, an excess of receptor fragment is needed to shift the equilibrium toward the complex.

Virus Attachment to Receptor-Decorated Liposomes.

When free in solution, V33333 binds to HRV2, as demonstrated by using CE in our previous papers.^{10,11} We determined the composition of the V33333–HRV2 complex at saturation with 12 receptors per virion. However, interaction of the virus with the cell surface does not involve soluble receptors but rather receptors that are firmly anchored within the membrane. In the present

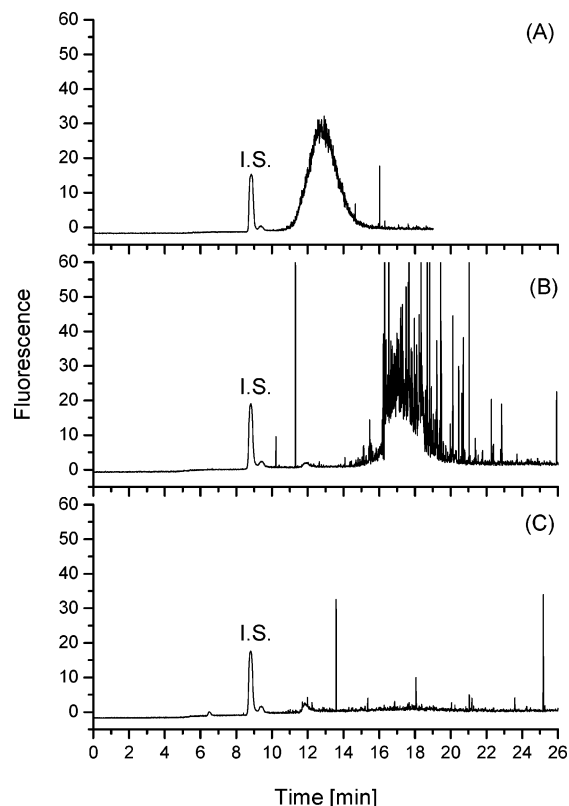


Figure 5. Electropherograms of (A) liposomes decorated with V33333, (B) liposomes as in (A), incubated with HRV2, and (C) liposomes carrying HRV2 as in (B), after 40 min sonication. Liposome composition and CE conditions are as in Figure 2. Incubation condition (in $100 \mu\text{L}$): (A) Ni^{2+} -NTA:V33333 = 1.6:7.4 ($\mu\text{mol L}^{-1}$); (B) and (C) Ni^{2+} -NTA:V33333:HRV2 = 1.6:7.4:0.059 ($\mu\text{mol L}^{-1}$).

paper, we investigated the interaction of rhinoviruses with receptor fragments present on the liposome surface. This allows free diffusion within the plane of the lipid bilayer and thus mimics much better in vivo conditions than, for example, surface plasmon resonance methodology or any other assay in which one of the components, receptor or virus, is firmly attached to a solid support. Therefore, several membrane-attached receptors might be recruited by an individual virion.

Incubation of the virus with the V33333-decorated liposome results in electropherograms exhibiting a change of the vesicle peak (Figure 5). Both migration time and shape of the liposome signal were completely changed. The vesicles emerged considerably later, and the peaks were partly covered with a large number of spikes (compare Figure 5A with B). The spikes suggest that clusters of vesicles are formed with virions bridging two or more liposomes. As previously observed for plain liposomes,¹ the peak together with the spikes completely disappeared upon sonication (Figure 5C), indicating that the vesicles had been destroyed.

As for V33333, upon incubation of V123-decorated vesicles for 30 min with HRV2, the liposomal peak disappeared and a large number of spikes emerged within the region of the expected position of the vesicles carrying virus (Figure 6B). This provides evidence that complexes had indeed been formed (compare to the vesicles with attached V33333 carrying virus, Figure 5B). Additional evidence for the presence of liposome-bound virus comes from the following experiment; a sample of the putative virus-carrying vesicle was incubated with 20 mM EDTA for several

- (7) Khan, F.; He, M.; Taussig, M. J. *Anal. Chem.* **2006**, *78*, 3072–3079.
- (8) Nieba, L.; Nieba-Axmann, S. E.; Persson, A.; Hamalainen, M.; Edebratt, F.; Hansson, A.; Lidholm, J.; Magnusson, K.; Karlsson, A. F.; Pluckthun, A. *Anal. Biochem.* **1997**, *252*, 217–228.
- (9) Lata, S.; Reichel, A.; Brock, R.; Tampe, R.; Piehler, J. *J. Am. Chem. Soc.* **2005**, *127*, 10205–10215.
- (10) Nicodemou, A.; Petsch, M.; Konecni, T.; Kremser, L.; Kenndler, E.; Casasnovas, J.; Blaas, D. *FEBS Lett.* **2005**, *579*, 5507–5511.
- (11) Konecni, T.; Kremser, L.; Snyers, L.; Rankl, C.; Kilar, F.; Kenndler, E.; Blaas, D. *FEBS Lett.* **2004**, *568*, 99–104.

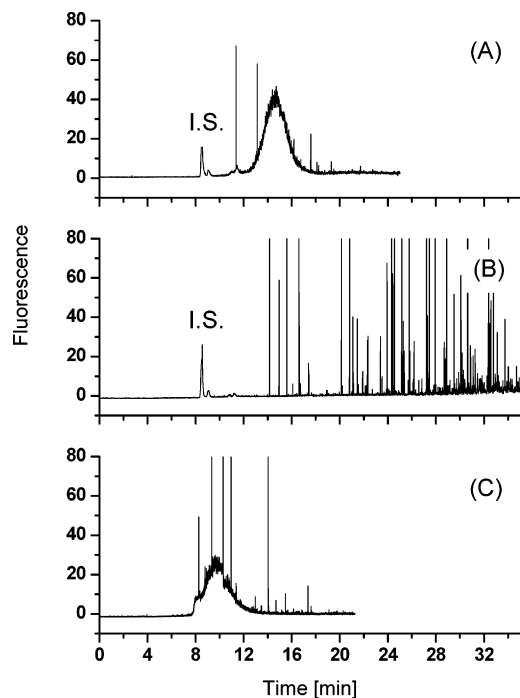


Figure 6. Electropherograms of (A) V123-decorated liposomes: Ni^{2+} -NTA-implanted liposomes incubated with V123; (B) V123-decorated liposomes as in (A), incubated with HRV2; (C) HRV2 was bound to V123-decorated liposomes as in (B), and then EDTA was added. Liposome composition and CE conditions are as in Figure 2. Incubation conditions (total incubation volume: 50 μL): (A) Ni^{2+} -NTA:V33333 = 2.0:13.5 ($\mu\text{mol L}^{-1}$); (B) Ni^{2+} -NTA:V33333:HRV2 = 2.0:13.5:0.053 ($\mu\text{mol L}^{-1}$).

minutes to destroy the Ni^{2+} -NTA complex (the binding constant of the Ni^{2+} -EDTA complex is about 7 orders of magnitude larger than that of the Ni^{2+} -NTA complex) and thus to displace the receptor from the liposome surface. As expected, the signal corresponding to bare liposome was re-established after treatment of the vesicles with EDTA (Figure 6C), thus confirming that the spikes indeed correspond to aggregates of liposomes bridged by receptor-bound virions. The signal of the recovered liposomes was slightly reduced as compared to that of the original sample because of dilution.

Taken together, our data indicate that virus becomes attached to the vesicles via the biospecific reaction with the receptor fragment. Nevertheless, more experiments were carried out to exclude any unspecific interactions. For this purpose, we investigated, by CE, whether the liposome peak changed upon addition of virus to vesicles not carrying receptor. As a further control, binding of a major group virus to receptor-decorated liposomes was assessed. As major group viruses use intercellular adhesion molecule 1, ICAM-1, as a receptor for cell entry and do not bind VLDLR, binding to the liposome could originate only from unspecific interactions.

HRV2 Binding to VLDLR-Decorated Liposomes Is Specific. First, we incubated HRV2 with Ni^{2+} -NTA-implanted liposomes lacking receptors. CE analysis showed no shift of the liposome peak within the reproducibility of the measurements (data not shown). This result cannot fully exclude unspecific interactions because binding of the virus to the liposomes might not affect the electrophoretic mobility. However, it makes it clear that the shift of receptor-decorated liposome peak upon incubation

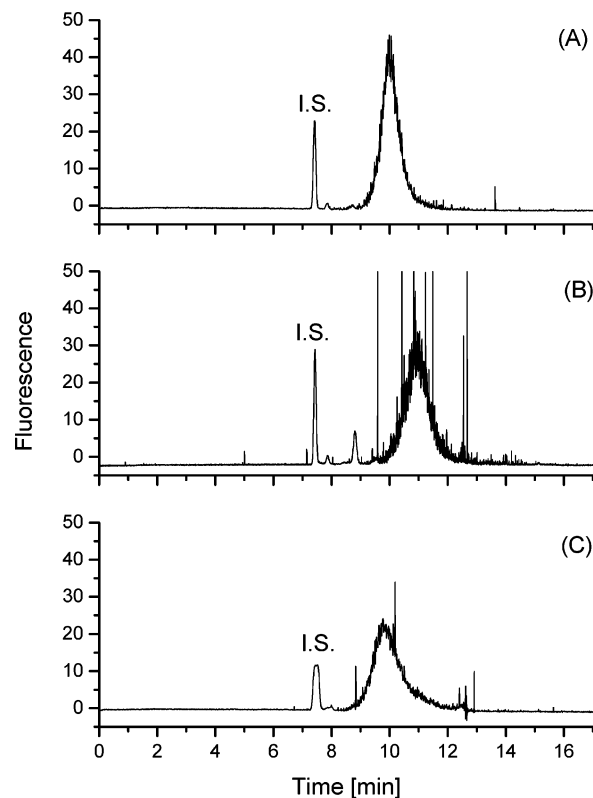


Figure 7. Electropherograms of V33333-decorated liposomes, after incubation with the minor group virus HRV2 and the major group virus HRV14, respectively. (A) V33333-decorated liposomes; (B) liposomes as in (A), after incubation with HRV2 for 1 h; (C) liposomes as in (A), after incubation with HRV14 for 1 h. I.S. fluorescein 0.7 nmol L^{-1} . PVA capillary 30.0/21.5 cm length, ID 100 μm . BGE: 50 mM Tris-HCl, pH 8.0. Incubation conditions (total incubation volume: 10 μL): (A) Ni^{2+} -NTA:V33333 = 0.7:7.4 ($\mu\text{mol L}^{-1}$); (B) V33333-decorated liposome as in (A), incubated with 0.067 $\mu\text{mol L}^{-1}$ HRV2; (C) V33333-decorated liposome as in (A), incubated with 0.061 $\mu\text{mol L}^{-1}$ HRV14.

with HRV2 (Figure 5) must be caused by the virus attaching via the receptor.

As pointed out above, in contrast to the minor group virus HRV2, major group viruses such as HRV14 do not bind members of the LDLR-family. This latter serotype was thus selected as a control. Indeed, HRV14 did not form any complex with V33333, as confirmed by CE with UV absorbance detection. When compared to the electrophoretic peaks of free V33333, free HRV14, and HRV2, the peak of HRV2 disappeared upon incubation with the receptor construct, and a peak corresponding to the V33333-virus complex was noticed. No such effect was seen for HRV14. Both virus and receptor peaks remained unchanged when the mixture of the components was analyzed (data not shown).

Thus, V33333-decorated liposomes were incubated with the respective HRV serotypes, and the incubation mixtures were analyzed by CE. All experiments were carried out with the same vesicle and receptor concentrations in the incubation solutions, and all data were acquired in one and the same series (this is relevant because it was observed that the liposomes from different preparations can possess slightly different electrophoretic properties). As expected, HRV2 shifted the liposome peak toward longer migration times (compare Figure 7A with B), and some spikes indicate the formation of virus-liposome clusters. In contrast, addition of the major group virus left the liposome peak nearly

unaffected (compare Figure 7A and C). Within the 95% confidence limit, the two peaks exhibit the same mobility (of $26.5 \times 10^{-9} \text{ m}^2 \text{ V}^{-1} \text{ s}^{-1}$, standard deviation $0.5 \times 10^{-9} \text{ m}^2 \text{ V}^{-1} \text{ s}^{-1}$, compare these data with the mobility of $24.4 \times 10^{-9} \text{ m}^2 \text{ V}^{-1} \text{ s}^{-1}$ of the HRV2-carrying liposomes in Figure 7B). This result is additional proof that the shift of the receptor-decorated liposome peak, upon addition of HRV2, does not originate from unspecific interactions, but results from the specific binding of virus to receptor-carrying liposomes.

CONCLUSIONS

CE was successfully applied to assess the specific attachment of HRV2 to receptor-decorated liposomes. Two recombinant soluble fragments of the VLDL receptor, V33333 and V123, fused to maltose binding protein and carrying a C-terminal his₆-tag, were attached to liposomes via a Ni²⁺-NTA-conjugated lipid used as a component of the liposome bilayer establishing a model of the cell membrane. The liposomes were labeled with an FL dye, dissolved in the aqueous vesicle core, thus enabling CE with LIF detection. Attachment of the virus was detected by a change of the electrophoretic mobility of the liposome, indicated by a shift of the vesicle peak. This shift was related to the biospecific interaction of the virus with the receptors. No change in the

mobility of the V33333-decorated liposomes was observed with a major group virus that uses ICAM-1 instead of members of the LDLR-family for infection. This allows the conclusion that the binding of HRV2 to these receptor-carrying liposomes is specific and represents a valid model for the attachment of the virus to the cell membrane. It also shows that a fragment of a natural receptor (V123) and an artificial receptor (V33333) behave similarly with respect to their promoting liposome binding of the virus, allowing one to extrapolate our findings to the *in vivo* situation. Further work will be conducted to analyze the next steps in virus infection that occur in the endosome such as structural changes of the virion and release of the genomic RNA.

ACKNOWLEDGMENT

This work was supported by the Austrian Science Foundation (projects P15667 and P19365). We thank Irene Goesler for the preparation of the viruses, and I. Steffan and M. Leodolter for the AAS measurements.

Received for review September 14, 2006. Accepted November 17, 2006.

AC061728M

Victor U. Weiss
Gerhard Bilek
Angela Pickl-Herk
Dieter Blaas*
Ernst Kenndler

Max F. Perutz Laboratories,
Medical University of Vienna,
Vienna Biocenter (VBC), Vienna,
Austria

Received February 20, 2009

Revised March 24, 2009

Accepted March 25, 2009

Research Article

Mimicking virus attachment to host cells employing liposomes: Analysis by chip electrophoresis

Electrophoresis on a chip increasingly replaces electrophoresis in the capillary format because of its speed and containment of the sample within a disposable cartridge. In this paper we demonstrate its utility in the analysis of the interaction between a virus and a liposome-anchored receptor, mimicking viral attachment to host cells. This became possible because detergents, obligatory constituents of the BGE for capillary electrophoretic separation of the virus, were not necessary in the chip format. Separations were carried out in sodium borate buffer, pH 8.3. Liposomes and virus were both labeled for laser-induced fluorescence detection at $\lambda_{\text{ex}}/\lambda_{\text{em}}$ 630/680 nm. Free virus and virus-receptor complexes were resolved from virus attached to receptor-decorated liposomes in the absence of additives or sieving matrices within about 30 s on commercially available microfluidic chips.

Keywords:

Chip electrophoresis / Fluorescence labeling / Human rhinovirus / Liposome / Very-low-density lipoprotein receptor
DOI 10.1002/elps.200900108

1 Introduction

Human rhinoviruses (HRVs), main causative agents of the common cold, bind different cell surface receptors for infection. HRV2 belongs to the minor group of HRVs that recognize members of the low-density lipoprotein receptor family [1]. The ligand-binding domain of these receptors is composed of various numbers of modules of about 40 amino acid residues in length and arranged in tandem that differently contribute to ligand binding [2]. In order to better understand the structural basis of ligand recognition, recombinant concatemers of module 3 of the very-low-density lipoprotein receptor (VLDLR) have been used in a

number of studies [3–5]. As a result, it is now clear that up to five modules within a single receptor molecule can attach to five icosahedral-symmetry-related binding sites around one vertex of the viral capsid [6, 7].

Attachment of viruses to cells can be mimicked *in vitro* by using receptor-carrying liposomes [8, 9]. In previous work we used electrophoresis in coated fused-silica capillaries to monitor this process. Attachment of HRV2 to fluorescent unilamellar liposomes decorated with maltose-binding protein (MBP)-V33333, a his₆-tagged receptor consisting of five repeats of module 3 of human VLDLR and expressed as a fusion with MBP, resulted either in a shift of the liposome peak or in its disappearance; concomitantly, a large number of spikes were observed, which we attributed to aggregates [10].

Detergents proved essential in preventing aggregation of viral particles in CE with fused-silica capillaries, independent of whether bare or coated [11]. However, work with liposomes precludes the use of surfactants. A solution to this problem was our finding that chip electrophoresis rendered neat virus peaks even in the absence of detergents for reasons that are not fully clear to us. We assume that it might be related to the much shorter residence time in the chip compared with the capillary. However, we first used chip electrophoresis for the analysis of complex formation of virus with different soluble concatemers of module 3 [12, 13]. In the present paper the recombinant

Correspondence: Professor Ernst Kenndler, Max F. Perutz Laboratories, Medical University of Vienna, Inst. Med. Biochem., Vienna Biocenter (VBC), Dr. Bohr Gasse 9/3, A-1030 Vienna, Austria

E-mail: ernst.kenndler@univie.ac.at

Fax: +43-1-4277-9616

Abbreviations: DOGS-NTA, 1,2-dioleoyl-*sn*-glycero-3-[*N*-(5-amino-1-carboxypentyl) iminodiacetic acid)succinyl] (nickel salt); FL, fluorescence; HRV, human rhinovirus; MBP, maltose-binding protein; PEG750PE, 1,2-distearoyl-*sn*-glycero-3-phosphoethanolamine-*N*-[methoxy (polyethylene-glycol)-750] (ammonium salt); POPC, 1-palmitoyl-2-oleoyl-*sn*-glycero-3-phosphocholine; spin SEC, spin size exclusion chromatography; v-r, virus-receptor; v-r-l, virus-receptor-liposome; VLDLR, very-low-density lipoprotein receptor

*Additional corresponding author: Professor Dieter Blaas
E-mail: dieter.blaas@medunivie.ac.at

his₆-tagged MBP-V3333 molecules were attached to the membrane *via* 1,2-dioleoyl-*sn*-glycero-3-[(*N*-(5-amino-1-carboxypentyl) iminodiacetic acid)succinyl] (nickel salt) (DOGS-NTA). In order to follow the binding of the virus to the membrane, we then employed fluorescence (FL) detection of both virus and liposomes. For this purpose virus was labeled within its protein coat with the amine-reactive dye Cy5, whereas liposomes were visualized *via* encapsulation of Atto 637 (free acid form) in their aqueous core. We here demonstrate the utility of chip electrophoresis for the assessment of the interaction of virus with receptor-decorated liposomes.

2 Materials and methods

2.1 Chemicals

Sephadex G50 (DNA grade) and Cy5 were obtained from Amersham Bioscience (Little Chalfont, England). Cy5 was dissolved in DMSO (>99.9%, Sigma Aldrich, Steinheim, Germany) to yield a 25 mM stock solution. Atto 637 (in free acid form) was obtained from Fluka (Buchs, Switzerland). Boric acid (99.99%) was from Sigma Aldrich. Sodium hydroxide (>97%) was from E. Merck (Darmstadt, Germany). Water was doubly distilled from a quartz apparatus. 1-Palmitoyl-2-oleoyl-*sn*-glycero-3-phosphocholine (POPC), 1,2-distearoyl-*sn*-glycero-3-phosphoethanolamine-*N*-[methoxy (polyethyleneglycol)-750] (ammonium salt) (PEG750PE) and DOGS-NTA were from Avanti Lipids (Alabaster, AL, USA) and purchased *via* Instruchemie (Delfzijl, The Netherlands). DOGS-NTA was already loaded with nickel ions upon delivery and was incorporated into liposomes as such.

2.2 Biological materials

Preparation and purification of HRV2 and assessment of purity and concentration were carried out as described previously [14, 15]. A 5 μ L aliquot of HRV2 at 9.5 mg/mL (1.1 μ M) in 50 mM sodium borate, pH 7.4 was employed in all chip electrophoresis experiments. The model receptor consisted of four copies of ligand-binding module 3 of human VLDLR arranged in tandem; it was fused to MBP at its N-terminus and carried a his₆-tag at its C-terminus (MBP-V3333) [4]. The working solution was at 2.0 mg/mL (32 μ M) in TBSC buffer (20 mM Tris-HCl, 150 mM NaCl, 20 mM CaCl₂, pH 7.5).

2.3 Instrumentation

Chip electrophoresis was carried out on the Agilent 2100 Bioanalyzer system applying commercially available DNA chips (Agilent Technologies, Waldbronn, Germany). DNA chips, produced from soda lime glass, allow analysis of up to

12 samples *per* chip. Analytes were monitored *via* FL, employing both excitation wavelengths of the instrument produced by a light-emitting diode (λ_{max} = 470 nm) and a red laser (λ_{max} = 630 nm); chips were thermostated to 30°C during analysis. Data were collected with the Agilent 2100 Expert software. Prior to use BGE and sample buffer were centrifuged for 10 min on a tabletop centrifuge (5415D, Eppendorf, Hamburg, Germany). The same centrifuge was employed for spin size exclusion chromatography (spin SEC).

2.4 Buffers

Electrophoretic separations were carried out in 100 mM boric acid adjusted to pH 8.3 with 3 M NaOH. BGE was prepared daily to attain the EOF values around 5×10^{-8} m²/Vs. BGE was diluted with bidistilled water to 80 mM boric acid concentration (sample buffer; BGE0.8) and to 50 mM boric acid concentration (labeling buffer; BGE0.5).

2.5 Chip handling

DNA chips were handled as described previously [12, 13]. In short, chip channels were filled with 12 μ L BGE on the Chip Priming Station by the application of pressure (20 s, 1 mL syringe volume, upper syringe clip position, position C of the base plate) from the BGE outlet well. Twelve microliters of Cy5 containing sample buffer (62.5 nM dye concentration) were applied to the ladder well for adjustment of the instrument optics and 12 μ L BGE to the remaining two wells marked “G”. Six microliters of the samples were applied to the remaining wells. After the removal of the chip, electrodes were cleaned with the Electrode Cleaning Chip (filled with 380 μ L doubly distilled water). The script (defining all operational steps of the chip analysis) that is normally employed for DNA analysis was modified to positive polarity mode for both sample injection to the separation channel and electrophoretic analysis. The injection voltage was set to 1300 V, the separation voltage to 800 V (approx. 19 kV/m).

2.6 Production of multilamellar vesicles

Lyophilized lipids were dissolved in chloroform at 10 mM each prior to mixing in a round-bottom flask in the molar ratio of POPC:PEG750PE:DOGS-NTA = 18:1:1. Chloroform was added to about 3.0 mL; the solvent was evaporated and the resulting lipid film was dried for at least 3 h under a stream of nitrogen. The dry film was hydrated in 1.7 mL BGE0.5 or BGE0.5 containing 11 μ M Atto 637 (free acid form) to obtain FL liposomes. The flask was rotated at room temperature for at least another 3 h and vortexed several times. The multilamellar vesicle suspension was kept overnight at 4°C for maturation and either extruded to produce large unilamellar vesicles or stored at –40°C.

Assuming that all lipids were incorporated into liposomes, the calculated total lipid concentration was 7.1 mM including, 0.4 mM DOGS-NTA for unstained liposomes, and 5.9 mM, including 0.3 mM DOGS-NTA for FL liposomes.

2.7 Extrusion

To produce vesicles of defined size, the multilamellar vesicle suspension was sequentially extruded through two overlaid polycarbonate filters with pore sizes of 400, 200 and 100 nm by using a Mini-Extruder (Avanti Lipids) placed on a heating block pre-warmed to 50°C. The suspension was passed 35 times through each couple of filters [16, 17].

2.8 Virus labeling

HRV2 was labeled by mixing 5 μ L virus stock with 4.5 μ L BGE0.5 and 0.5 μ L 25 mM Cy5 in DMSO (approximate 2.2×10^3 -fold molar excess of dye over virus). Incubation was carried out overnight under light protection at ambient temperature. Low-molecular-weight material was removed from the labeled virus on spin columns; filters from Corning Spin-X centrifuge tubes (cellulose acetate membrane, pore size 0.45 μ m, obtained from Sigma Aldrich) were filled with Sephadex G50 swelled in BGE0.5 (slurry corresponding to 900 μ L settled material in total, applied consecutively in two 450 μ L portions). The column was spun dry on a table-top centrifuge; the labeling mix was applied and the elution was started *via* spinning for 1 min at 800 rcf. The column was washed with 20 μ L of BGE0.5 *via* spinning (1 min, 800 rcf) and the total recovered eluate (30 μ L) was subjected to the same procedure on a fresh spin column (washing with 15 μ L). The final main fraction contained 5.25 pmoles (*i.e.* 115 nM) HRV2. Only 6% of the total virus remained on the columns and was recovered upon additional washings with 20 μ L buffer, each.

2.9 Liposome purification

Non-encapsulated Atto 637 was removed from the FL-labeled liposomes *via* spin SEC on G50 Sephadex columns as above, but equilibrated in bidistilled water. Ten microliters of liposome suspension were applied followed by elution at 800 rcf (1 min). The column was then rinsed with 20 μ L BGE0.5 (1 min, 800 rcf) and the total eluted material was collected.

2.10 Sample preparation for chip electrophoresis

Cy5-labeled HRV2 was diluted 1:21, the receptor stock solution 1:9 and the liposomes 1:10.5, all with BGE0.8. Note that FL-labeled liposomes were about 3.6 times less concentrated. Atto 495 was added as fluorescent EOF

marker ($\lambda_{\text{ex}} = 495$ nm; 3.0 μ M final concentration). The final concentration of labeled HRV2 was 5.6 nM with the receptor being present in approximately 50-fold molar excess (based on a stoichiometry of 12 receptor molecules binding one virion). The DOGS-NTA in the outer liposomal membrane was in excess over receptor between 1.3- (labeled liposomes) and 5.4-fold (unlabeled liposomes). Samples were prepared by mixing constituents in the sequence receptor, liposomes and labeled HRV2—followed by 20 min incubation at ambient temperature under light protection.

3 Results and discussion

The experimental conditions were selected such as to enable recording of free virus as well as receptor-decorated liposomes and to obtain clear indications for virus attachment to the vesicles. The present chip electrophoresis setup relies on FL detection; therefore, the aqueous core of the liposomes was filled with Atto 637 ($\lambda_{\text{ex}} = 635$ nm) and the virus was rendered fluorescent by reaction of Cy5 ($\lambda_{\text{ex}} = 649$ nm) with the capsid proteins. This allowed for monitoring within the instrument-specific 630 nm channel.

It is evident that separation is governed by the mobility of the analytes and that of the EOF, whereby the mobility of the liposomes might depend on their size (and certainly on their composition) and that of the virus is affected by the chemical modification of its capsid upon labeling [18]. Moreover, the mobility of virus and liposomes presumably changes upon reaction with receptor fragments. Electrophoresis in the micro-device has the invaluable advantage that no detergent is needed (which would most probably disintegrate the liposomes). However, in general its separation performance is lower than that of the classical capillary format.

3.1 Liposomes

The employed liposomes consisted of POPC, PEG750PE and DOGS-NTA in 18:1:1 molar ratio and were extruded consecutively through filters of 400, 200 and 100 nm pore size. Samples representative of the corresponding size ranges taken after each extrusion step were analyzed by chip electrophoresis (Fig. 1). When measuring at the apex of the peaks, the largest vesicles (400 nm size) exhibited a clearly longer migration time when compared with the smaller ones (200 and 100 nm) that were barely distinguishable. Note that longer migration times correspond to higher electrophoretic mobility, as the anionic particles are swept by the EOF toward the cathodic end of the channel. The liposomes with smaller diameter were apparently more homogenous, as they gave narrower peaks. Signal fluctuations within the sample zones of the larger-sized liposomes most likely result from many slightly different species. Atto 637 was not completely removed by spin SEC; however, it did not interfere as it was sufficiently resolved from the

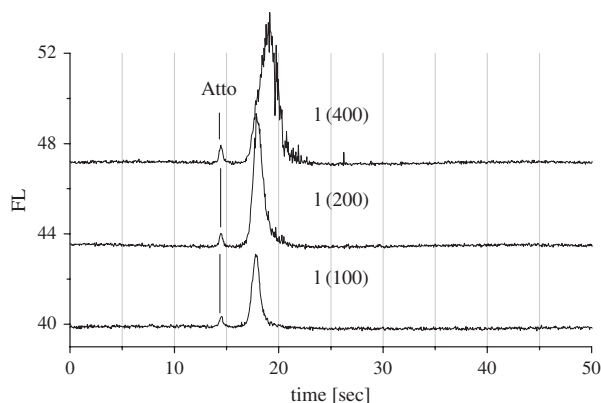


Figure 1. Chip electrophoresis of liposomes, l, from the same preparation but serially extruded through filters with 400, 200 and 100 nm pore size. The liposomes were FL labeled by inclusion of an aqueous solution of Atto 637 into the vesicle core. Total lipid concentration approximately 190 μ M. BGE, 100 mM boric acid adjusted to pH 8.3 with 3 M NaOH. Sample buffer was BGE diluted to 80 mM boric acid concentration. Separations were carried out at 800 V (approx. 19 kV/m). FL signal recorded at $\lambda_{\text{ex}}/\lambda_{\text{em}}$ 630/680 nm (arbitrary units).

liposome peaks. The reproducibility of the migration times, expressed by the standard deviation of the mean as determined on three different days by using five different chips (two samples *per* chip, ten samples in total) was 2.1%.

3.2 Virus–receptor–liposome complex

For the following binding experiments liposomes extruded through 200 nm pore size filters were used. To allow for decoration with his₆-tagged receptors, liposomes were made to contain about 5% DOGS-NTA. In the present work we used MBP-V3333, a receptor fragment consisting of four repeats of module 3 of human VLDLR arranged in tandem and expressed with MBP at its N-terminus and a his₆-tag at its C-terminus. Figure 2A shows the electropherogram of Atto 637-filled liposomes (l), Fig. 2B that of liposomes decorated with MBP-V3333 receptor (l+r). Binding of the receptor *via* its his₆-tag to the DOGS-NTA in the membrane does not significantly change the migration behavior of the liposomes. However, a significantly different electropherogram was obtained after incubation with virus (Fig. 2C). Assuming a final lipid concentration of 190 μ M with 4.8 μ M of DOGS-NTA being accessible at the outer leaflet, the molar excess of the DOGS-NTA groups over receptor was 1.3-fold (see Section 2). However, even when the DOGS-NTA-groups in the membrane are in excess over the his₆-tags, receptor binding is not expected to be quantitative because the dissociation constant is in the 10^{−6} M range [19], which is within the same order as the analyte concentrations. Therefore, a peak attributed to virus bound to soluble receptor fragments, indicated as virus–receptor complex (v–r) was recorded as well (Fig. 2C). It has a slightly longer migration time than the peak ascribed to a contaminant, c, present in all virus preparations and also becoming labeled with amino-

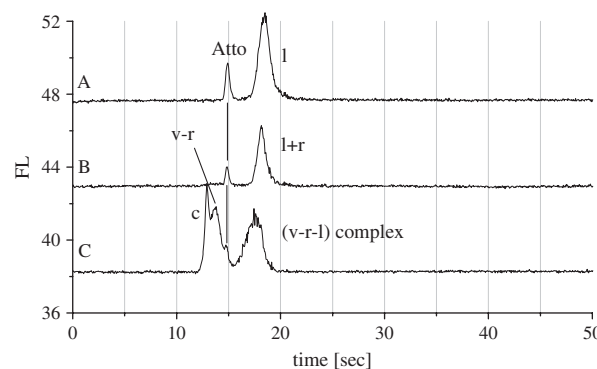


Figure 2. Chip electrophoresis of FL liposomes, l, upon incubation with receptor, r, and Cy5-labeled HRV2, v. (A) Atto 637-labeled liposomes, (B) Liposomes as in (A) after decoration with receptor; (C) Electropherogram obtained after incubation of the receptor-decorated liposomes with HRV2 resulting in binding of virus (v–r–l complex). Sample buffer, BGE, separation conditions and FL detection as with Fig. 1; c, contaminant of the virus preparation.

reactive dyes [20]. The liposome peak is shifted to a shorter migration time with concomitant zone broadening. This peak corresponds to the DOGS-NTA-doped liposomes, decorated with receptor and carrying receptor-attached virus (v–r–l). There is an increase in noise, which probably reflects heterogeneous species, either liposomes carrying various numbers of virions or liposomes aggregated *via* bridging, mediated by single or multiple virions.

To explicitly demonstrate the attachment of labeled HRV2 to our receptor-decorated model membrane, we repeated our experiments with unlabeled liposomes. This approach allowed us to follow exclusively the signal of labeled HRV2. Figure 3A depicts an electropherogram of labeled HRV2 that comigrates with the contaminant c (v+c). Incubation of the virus with MBP-V3333 yields a peak with increased migration time corresponding to (v–r), see Fig. 3B. After incubation of v–r with unlabeled liposomes (Fig. 3C), a third peak, identical to (v–r–l) in Fig. 2 was seen together with excess of v–r. Not only the position but also the apparent noisiness of the peaks was identical upon application of stained and unstained liposomes (compare Figs. 2C and 3C). However, for unstained liposomes the employed total lipid concentration for complex formation was about 3.6 times higher than in experiments with FL-labeled vesicles. Therefore, the ratio between DOGS-NTA-groups and his₆-tagged receptors was about 5.4 as compared with the ratio of 1.3 in the experiment shown in Fig. 2. As a consequence, less free v–r were recorded. This suggests that v–r complexes do not dissociate significantly from the liposomes during electrophoresis.

3.3 Is HRV–liposome binding specific?

In order to exclude direct interaction between virus and liposomes in the absence of receptor, virus and DOGS-NTA-doped liposomes were incubated. Figure 4 shows that virus (and the contaminant, v+c) and liposomes (l) migrate

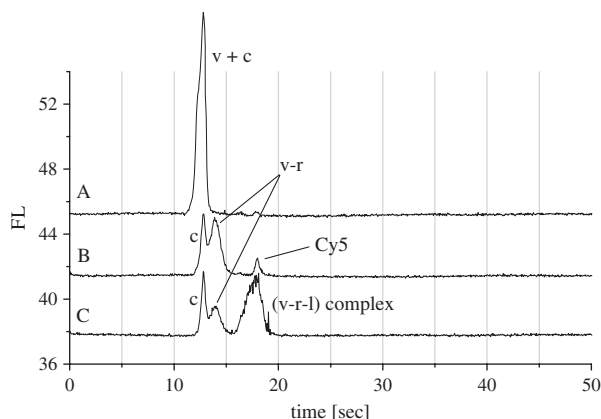


Figure 3. Shift of the labeled HRV2 peak upon subsequent incubation with receptor and unlabeled liposomes. Electropherogram of (A) HRV2 comigrating with the contaminant of the virus preparation; (B) upon incubation with soluble receptor fragments; (C) after incubation of (B) with liposomes. Sample buffer, BGE, separation conditions and FL detection as with Fig. 1; c, contaminant resulting from the virus preparation; small excess of Cy5 is also detected.

identically regardless of whether analyzed separately (A and B) or as a mixture (C). Taken together, these results prove that specific interaction between receptor-decorated liposomes and virus can be monitored by chip electrophoresis in very short times.

4 Concluding remarks

Chip electrophoresis was employed to study the early steps in viral infection by using a liposome-based system. Liposomes as model membranes and a rhinovirus were detected on-chip upon FL labeling. The electrophoretic separation was carried out in a buffer solution without detergent; this is a clear advantage over CE where such additives are mandatory for reproducible analysis of virus. However, detergents disrupt liposomes. Only the conditions of chip electrophoresis allowed for the preservation of the components and the analysis of both components and their interaction products. Liposomes were functionalized *via* incorporation of DOGS-NTA, allowing for decoration with soluble his₆-tagged recombinant receptor fragments. Receptor-carrying liposomes, in turn, were able to specifically bind HRV2. The individual analytes and liposome-bound virus appear as baseline-resolved peaks in the electropherograms; the latter is clearly distinguished from the peaks of their constituents.

This analytic system constitutes a starting point for the investigation of the early infection steps of non-enveloped viruses, which are still not fully understood. These include interactions of the viral capsid with a receptor anchored in a lipid membrane followed by the transfer of the viral genome into the cytosol. Indeed, we are currently investigating RNA release into receptor-decorated liposomes on acidification of within late endosomes. Furthermore, we are in the process of comparing the receptor-binding parameters of the mono-

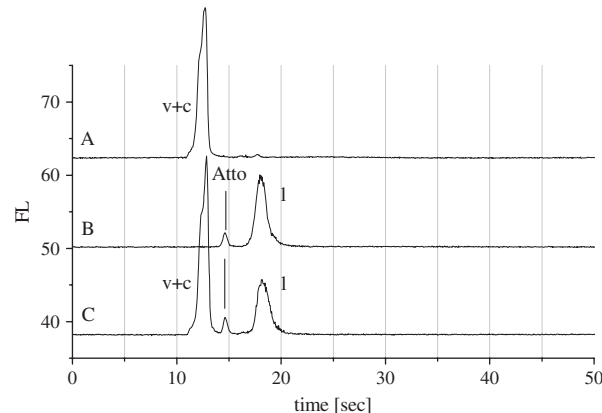


Figure 4. Binding of HRV2 to liposomes depends on the receptor. Electropherograms obtained for (A) HRV2, (B) liposomes and (C) for both analytes after incubation in the absence of receptor. Concentrations as in Fig. 2 and separation conditions as in Fig. 1.

nitrilo-triacetate lipid used in this report with a Tris-nitrilo-triacetate lipid in order to limit dissociation of the receptor from the liposome membrane. These findings will be the subjects of forthcoming publications. Collectively, using a HRV as a model system, our experiments set the stage to make the first step in this process accessible to rapid analysis by chip electrophoresis.

This work was supported by the Austrian Science Foundation (Project P19365). The authors thank Agilent Technologies GmbH, Waldbronn, for support and Irene Goesler for virus preparation.

The authors have declared no conflict of interest.

5 References

- [1] Vlasak, M., Roivainen, M., Reithmayer, M., Goesler, I., Laine, P., Snyers, L., Hovi, T. *et al.*, *J. Virol.* 2005, **79**, 7389–7395.
- [2] Blacklow, S. C., *Curr. Opin. Struct. Biol.* 2007, **17**, 419–426.
- [3] Konecni, T., Kremser, L., Snyers, L., Rankl, C., Kilar, F., Kenndler, E., Blaas, D., *FEBS Lett.* 2004, **568**, 99–104.
- [4] Moser, R., Snyers, L., Wruss, J., Angulo, J., Peters, H., Peters, T., Blaas, D., *Virology* 2005, **338**, 259–269.
- [5] Wruss, J., Runzler, D., Steiger, C., Chiba, P., Köhler, G., Blaas, D., *Biochemistry* 2007, **46**, 6331–6339.
- [6] Verdaguer, N., Fita, I., Reithmayer, M., Moser, R., Blaas, D., *Nat. Struct. Mol. Biol.* 2004, **11**, 429–434.
- [7] Querol-Audi, J., Konecni, T., Pous, J., Carugo, O., Fita, I., Verdaguer, N., Blaas, D., *FEBS Lett.* 2009, **583**, 235–240.
- [8] Bubeck, D., Filman, D. J., Hogle, J. M., *Nat. Struct. Mol. Biol.* 2005, **12**, 615–618.
- [9] Bilek, G., Kremser, L., Blaas, D., Kenndler, E., *Electrophoresis* 2006, **27**, 3999–4007.
- [10] Bilek, G., Kremser, L., Wruss, J., Blaas, D., Kenndler, E., *Anal. Chem.* 2007, **79**, 1620–1625.

- [11] Kremser, L., Blaas, D., Kenndler, E., *Electrophoresis* 2004, 25, 2282–2291.
- [12] Weiss, V. U., Kolivoska, V., Kremser, L., Gas, B., Blaas, D., Kenndler, E., *J. Chromatogr. B* 2007, 860, 173–179.
- [13] Kolivoska, V., Weiss, V. U., Kremser, L., Gas, B., Blaas, D., Kenndler, E., *Electrophoresis* 2007, 28, 4734–4740.
- [14] Okun, V. M., Ronacher, B., Blaas, D., Kenndler, E., *Anal. Chem.* 1999, 71, 2028–2032.
- [15] Hewat, E. A., Neumann, E., Conway, J. F., Moser, R., Ronacher, B., Marlovits, T. C., Blaas, D., *EMBO J.* 2000, 19, 6317–6325.
- [16] Patty, P. J., Frisken, B. J., *Biophys. J.* 2003, 85, 996–1004.
- [17] Hope, M. J., Nayar, R., Mayer, L. D., Cullis, P. R., in: Gregoriadis, G. (Ed.), *Liposome Technology*, 2nd Edn., vol. 1, CRC Press, Boca Raton, FL, 1993, pp. 124–139.
- [18] Kremser, L., Petsch, M., Blaas, D., Kenndler, E., *Anal. Chem.* 2004, 76, 7360–7365.
- [19] Dorn, I. T., Neumaier, K. R., Tampe, R., *J. Am. Chem. Soc.* 1998, 120, 2753–2763.
- [20] Okun, V., Ronacher, B., Blaas, D., Kenndler, E., *Anal. Chem.* 2000, 72, 2553–2558.

9.2 Zusammenfassung der Dissertation (deutsch / englisch)

- Abstract (deutsch) -

Der virale Genomtransfer im Infektionszyklus von nicht-umhüllten Viren ist bisher nur ansatzweise erforscht. Diese Arbeit soll zum besseren Verständnis des Transfermechanismus beitragen und bedient sich des humanen Rhinoviruses (HRV) als Repräsentant dieser Viren. Diese enthalten ein 7 kb RNA-Genom, verkapselt in einer ikosaedrischen Proteinhülle – dem Kapsid. Um die Wirtszelle zu infizieren, muss das Genom durch die endosomale Membran in das Zytoplasma befördert werden. Die essentiellen viralen und zellulären Elemente für den Transfer sollen mit dieser Arbeit - in einem *in-vitro* Ansatz - detektiert werden.

Anstelle von lebenden Zellen mit nativen Rezeptoren fanden Liposome als Modellzelle Einsatz. Die Liposome wurden mit rekombinanten Rezeptorfragmenten bestückt, die dem „very low-density lipoprotein“ Rezeptor entstammten. Über ihr C-terminales His6-Tag konnten sie an ein Nickel-komplexierendes Lipid der Liposomoberfläche gebunden werden. Nach der spezifischen Bindung von HRV Serotyp 2 (HRV2) an diese Rezeptoren der Liposomoberfläche war der resultierende Komplex für eine potentielle Infektion präpariert; er wurde daher „Lipofektosom“ genannt. Die Eignung dieses Modells konnte mittels Kapillarelektrophorese (CE) und Transmissions-Elektronenmikroskopie (TEM) bestätigt werden. Der Nachweis des Genomtransfers erfolgte mit einem revers-transkribierenden (RT) PCR System.

Die Parameter für die korrekte Assemblierung des Lipofektosoms wurden mittels CE mit laser-induzierter Fluoreszenz-Detektion und TEM-Visualisierung optimiert. Letztere Technik ermöglichte Screening von Proben im schwach sauren Medium zur Feststellung der Bedingungen für den vollständigen RNA-Transfer.

Um das Eindringen des RNA-Genoms in das Innere des liposomalen Kompartiments zu bestimmen, wurde ein Protokoll zur RT hinsichtlich seiner Anwendung im Lipofektosom adaptiert. Dadurch konnte anhand eines Lipofektosoms gezeigt werden, dass mit dem Auslösen der Infektion die virale RNA vom Kapsid in das Liposom migrierte; dort konnte sie tatsächlich via RT und PCR detektiert werden. Die Dichtheit des liposomalen Kompartiments stellte eine Grundvoraussetzung für das Funktionieren des verkapselten RT-Kits dar; man kann es somit als Nano-Reaktionscontainer betrachten.

Zusammenfassend wurde gezeigt, dass die hier entwickelte *in-vitro* Methode geeignet ist, den RNA-Transfer nicht-umhüllter Viren zu detektieren. Diese Arbeit demonstrierte am Beispiel des Genomtransfers von HRV2, dass komplexe Infektionsprozesse in diskrete und simple Einzelprozesse aufgelöst werden können.

- Abstract (English) -

Viral genome transfer through cellular membranes is a crucial process in the course of early infection events of non-enveloped viruses. It is the aim of this work to contribute to a better understanding of this mechanism taking human Rhinoviruses as typical representative of this virus type. They contain an RNA genome of about 7 kb in an icosahedral protein capsid, which needs to be transferred through the endosomal membrane to infect the host cell. This work aimed at detecting *in-vitro* the essential viral and cellular elements for proper genome transfer.

Instead of using natural cells with native receptors, the liposome-based model used a nickel chelating lipid for attaching His6-tagged receptor constructs, derived from the very low-density lipoprotein receptor (VLDLR). Upon specific binding of HRV2, the assembly was primed for infection, and thus called “lipofectosome”. The suitability of this model was confirmed by capillary electrophoresis (CE) and transmission electron microscopy (TEM). Finally, proper genome transfer could be demonstrated by a reverse transcription (RT) PCR assay.

Parameters for assembly were optimized by CE with laser-induced fluorescence (LIF) detection and TEM imaging. The latter technique enabled screening of samples kept in moderately acidic environment to identify conditions for entire RNA release.

To confirm the ingress of released RNA into the liposomal compartment, an RT protocol was adapted to allow for its application within lipofectosomes. It was shown that upon triggering infection, lipofectosomes transferred the RNA from within the virion into the interior of the vesicle; their viral RNA was detected via RT and PCR. Since liposomes served here as leak-tight compartment to carry out RT, they can be considered as nano-reaction containers.

In conclusion, a system to monitor *in-vitro* the RNA transfer of non-enveloped viruses was invented. This work shows that even complex infection pathways can be resolved to discrete and plain processes, such as the genome transfer.

9.3 Curriculum Vitae

Gerhard Bilek (Mag.)

diploma – genetics and microbiology

date of birth24th June 1980**address**

Arndtstrasse 53 /16, 1120 Vienna

marital status

unmarried

nationality

Austria

e-Mail

bilek.gerhard@gmx.net

**Education**2006 – 2009
(1030 Vienna)

Ph.D. dissertation: Max F. Perutz laboratories, university of Vienna;
work group: infection biology (Prof. D. Blaas, Prof. E. Kenndler)
*"Functionalized Liposomes as a Model to Reveal Cell-Surface
Associated Events of the Human Rhinovirus Infection-Pathway"*

2005 – 2006
(1090 Vienna)

Diploma thesis: department of analytical chemistry and nutrition
science, university of Vienna
work group: capillary separation science (Prof. Ernst Kenndler)
"Mimicking Cell Attachment of Human Rhinovirus 2 by Liposomes"

2003 – 2004
(Rome, Italy)

Erasmus: Università Roma 3
*"Effects of Microtubule-interfering agents with Focus on Induction
and Progress of Apoptosis in Cancer Cells"*

2000 – 2006
(1030 Vienna)

Study: biology – genetics and microbiology, university of Vienna;

1999 – 2000
(1210 Vienna)

Military service: Van Swieten Kaserne

1994 – 1999
(1170 Vienna)

School with university-entrance diploma for **chemical engineering**
"Rosensteingasse",
main focus: technical chemistry and environment

List of Publications

1. Weiss VU, Bilek G, Pickl-Herk A, Blaas D, Kenndler E: **Mimicking virus attachment to host cells employing liposomes: Analysis by chip electrophoresis.** *Electrophoresis* 2009, **30**:2123-2128.
2. Kremser L, Bilek G, Kenndler E: **Effect of detergent on electromigration of proteins: CE of very low density lipoprotein receptor modules and viral proteins.** *Electrophoresis* 2007, **28**:3684-3690.
3. Kremser L, Bilek G, Blaas D, Kenndler E: **Capillary electrophoresis of viruses, subviral particles and virus complexes.** *J Sep Sci* 2007, **30**:1704-1713.
4. Bilek G, Kremser L, Wruss J, Blaas D, Kenndler E: **Mimicking early events of virus infection: capillary electrophoretic analysis of virus attachment to receptor-decorated liposomes.** *Anal Chem* 2007, **79**:1620-1625.
5. Bilek G, Kremser L, Blaas D, Kenndler E: **Analysis of liposomes by capillary electrophoresis and their use as carrier in electrokinetic chromatography.** *J Chromatogr B Analyt Technol Biomed Life Sci* 2006, **841**:38-51.
6. Bilek G, Kremser L, Blaas D, Kenndler E: **Capillary electrophoresis of liposomes functionalized for protein binding.** *Electrophoresis* 2006, **27**:3999-4007.

International Symposia

Linz Winter Workshop 2009	XI. annual Linz winter workshop Advances in Single-Molecule Research for Biology & Nanoscience Johannes Kepler university Linz (Austria), February 2009 poster: "Uncoating of the Minor Group Human Rhinovirus"
ITP 2008	15 th international symposium on Capillary Electrophoresis Techniques Catania (Italy); August 2008 presentation: "Investigation of virus attachment to model membranes via chip electrophoresis" poster: „Resolution of the Early Infection Pathway of Human Rhinovirus to Discrete Infection Steps by Artificial Membrane Vesicles in Chip Electrophoresis and Transmission Electron Microscopy"
PhD Symposium 08	4 th PhD-symposium medical university of Vienna (Austria), May 2008
CECE 2007	4 th international interdisciplinary meeting on bioanalysis Institute of Analytical Chemistry, Brno (Czech Republic), November 2007
ITP 2006	15 th international symposium on Capillary Electrophoresis Techniques , Paris (France), August 2006 poster: "Capillary electrophoresis of liposomes functionalized for protein binding" "Affinity capillary electrophoresis for subviral 80S particles of human rhinovirus with monoclonal antibody 2G2"
CECE 2006	3 rd international interdisciplinary meeting on bioanalysis institute of analytical chemistry, Brno (Czech Republic), November 2006
CECE 2005	2 nd international interdisciplinary meeting on bioanalysis institute of analytical chemistry, Brno (Czech Republic), November 2005

Additional Skills

Technical specialization:



- Analytical chemistry, biochemistry, capillary electrophoresis of viral proteins,
- Affinity capillary electrophoresis of cell receptors and liposomes,
- Liposome preparation;

Languages:



- "Writing Scientific Texts in English – B1",
- Italian: low advanced („Corso di lingua italiana"; Rome, Italy),
- Soft skill courses: rhetoric, communication, speed reading;

Information technology:



- Advanced knowledge in Linux, Macintosh, Windows;
- OriginPro, Endnote, SigmaPlot, ChemStation, CloneManager, Peakmaster, Simul, BioEdit;

16. August 2009